VOLCANOLOGY OF TUFF RINGS AT KELLYVILLE, ONEWHERO AND BOMBAY, SOUTH AUCKLAND VOLCANIC FIELD

A thesis
submitted in partial fulfilment
of the requirements for the degree
of
Master of Science in Earth Sciences
at
The University of Waikato
by

APRIL CHRISTINA GIBSON

THE UNIVERSITY OF
WAIKATO
Te Whare Wānanga o Waikato

The University of Waikato
2011

Abstract

The South Auckland volcanic field hosts 82 volcanic centres over an area of approximately 300 km^2 in the Pukekohe, Bombay, Tuakau, Pukekawa and Onewhero regions. The intraplate, monogenetic basaltic volcanic field was active between 1.59 and 0.51 Ma, and produced scoria cones, basaltic lava flows, tuff rings and maars.

Three volcanic centres have been studied for the purpose of this thesis: the Kellyville volcanic complex, the Onewhero tuff ring and the Bombay volcanic complex. Each centre hosts a tuff ring and varying levels of associated magmatic activity, and has been studied through stratigraphic logs, facies analysis and componentry studies to illustrate the styles of eruptions and their controlling factors.

The Kellyville volcanic complex hosts a breached tuff ring and two intra-tuff ring scoria cones. The tuff ring facies identified include a lithic-rich block and bomb facies with a massive fine lapilli to block and bomb facies, and a cross bedded coarse and fine ash facies with a laminated alternating coarse and fine ash facies, dominant in the early and late stages of the eruption, respectively. The aquifer for the tuff ring eruption was the Mercer Sandstone of the Waitemata Group. Both fall and surge processes occurred, with surges becoming dominant towards the end of the tuff ring eruption. Grainsize decreased through the eruption due to an increase in water/magma ratio and a decrease in magma ascent rate and eruption energy.

The Onewhero tuff ring is the largest in the South Auckland volcanic field, and hosts a tuff ring with a separate lava flow on its outer flanks. The tuff ring facies identified include a well sorted, cross bedded alternating fine and coarse ash facies dominant in both the early and late stages of the eruption, and a poorly to very well sorted, fine ash to block and bomb facies present in discrete pulses. The aquifer for the tuff ring eruption was the ancestral Waipa/Waikato River and its alluvial sediments. Both fallout and surge processes occurred, with surges becoming dominant towards end of the tuff ring eruption. Grainsize was constant through the eruption due to a steady water/magma ratio and a stable interaction between magma and water.

The Bombay volcanic complex hosts at least one tuff ring, a tuff cone, numerous scoria and spatter cones and at least two large deposits of ponded basalt lava. The tuff ring facies identified include a well sorted coarse ash to fine lapilli facies dominant in both the early and late stages of the eruption, and a poorly sorted coarse lapilli facies which occurs intermittently throughout the eruption. The aquifer for the tuff ring eruption was the Mercer Sandstone of the Waitemata Group. Fallout from steady eruption column was dominant in the tuff ring eruption. Grainsize decreased through the eruption due to a highly efficient water/magma ratio and an increase in ascent rate and eruption fragmentation.

The eruption style of volcanism in the South Auckland volcanic field is largely controlled by the distribution of faults, as well as the interaction of differing magma supplies and ascent rates with water-bearing sedimentary rocks and surface water of the ancestral Waipa/Waikato River.

Acknowledgements

I would like to thank the two best thesis supervisors in the world, Associate Professor Roger Briggs and Doctor Adrian Pittari for their constant support and advice.

Thank you to all the amazing teachers and staff in the Earth and Ocean Sciences department at the University of Waikato who have made my time at university an exciting, inspiring experience that I will never forget.

Special thanks goes to: Steve Hood (Indie) for always being there, Rochelle Hansen for help with the identification of foraminifera, Renat Radosinsky for lab assistance and all the great advice, and Helen Turner for support with the SEM. I would like to sincerely thank diatom expert Vivienne Cassie Cooper for lending me her immense wealth of knowledge for a day.

I am grateful for funding received from the Geological Society of New Zealand's Hastie Scholarship, the AUSIMM Postgraduate Research Scholarship, and the Broad Memorial Fund.

Thank you to all the friendly farm-owners for allowing me to traipse all over their land, including Terry Glass, Richard and Jenny Andrews and the Poole family. Thank you to both James Boyce and Keith Miller for access to the Holcim Quarry at Bombay, as well as the Holcim office in Auckland.

To all my friends at university, especially Mar, Jam and Ram – thank you for all the office chats, arguments, discussions, lunches, scrapbooking sessions, birthday parties (and cakes), and breathtaking fieldtrips. You are all amazing.

To my family, thank you for always believing in me and giving me the confidence and support to accomplish whatever I set out to do in life.

And to Ryan – for your support, friendship, companionship and love, I will be forever grateful. I love you.

Table of Contents

Abstract i
Acknowledgements iii
List of Figures vii
List of Tables xi
Chapter One: Introduction 1
1.1 Introduction 1
1.2 Objectives of the study 1
1.3 Location of the study area 1
1.4 Field work 2
1.5 Laboratory analysis 3
1.6 Chapter outlines 4
Chapter Two: Setting 7
2.1 Introduction 7
2.2 South Auckland volcanology 10
2.3 Previous work at Kellyville 14
2.4 Previous work at Onewhero 15
2.5 Previous work at Bombay Quarry 15
Chapter Three: Kellyville Volcanic Complex 17
3.1 Introduction 17
3.2 Country rock geology 17
3.3 Kellyville volcanic complex 21
3.4 Scoria cones 23
3.5 Diatomite 25
3.6 Facies and stratigraphy 30
3.6.1 Kellyville tuff ring 31
3.6.2 Tuff ring facies 31
3.6.3 Tuff ring facies stratigraphy 37
3.6.4 Scoria cone facies 38
3.6.5 Basalt geochemistry 41
3.7 Componentry 44
3.7.1 Tuff ring deposits 44

3.7.2 Scoria cone deposits 47
3.8 Stratigraphic variation 49
3.9 Discussion 50
3.9.1 Is Kellyville a tuff ring or a maar? 50
3.9.2 Emplacement processes 54
3.9.3 Eruption history 57
Chapter Four: Onewhero Tuff Ring 63
4.1 Introduction 63
4.2 Country rock geology 63
4.3 Onewhero tuff ring 66
4.4 Sample localities 67
4.5 Facies and stratigraphy 73
4.5.1 Onewhero tuff ring 73
4.5.2 Tuff ring facies 73
4.5.3 Tuff ring facies stratigraphy 76
4.5.4 Lava flow facies 77
4.5.5 Basalt geochemistry 78
4.6 Tuff ring componentry 81
4.7 Stratigraphic variation 84
4.8 Discussion 85
4.8.1 Emplacement processes 85
4.8.2 Eruption history 87
Chapter Five: Bombay Volcanic Complex 91
5.1 Introduction 91
5.2 Country rock geology 91
5.3 Bombay volcanic complex 92
5.4 Quarry history 93
5.5 Facies and stratigraphy 99
5.5.1 Bombay Quarry tuff ring 99
5.5.2 Tuff ring facies 101
5.5.3 Tuff ring facies stratigraphy 103
5.5.4 Basalt flow, scoria and spatter facies 103
5.5.5 Basalt geochemistry 106
5.6 Componentry 109

5.6.1 Tuff ring 109
5.6.2 Dense basalt 110
5.6.3 Scoria and spatter 111
5.7 Stratigraphic variation 111
5.8 Discussion 112
5.8.1 Emplacement processes 112
5.8.2 Eruption history 114
Chapter Six: Discussion 119
6.1 Introduction 119
6.2 Eruption styles and processes 119
6.3 Summary 123
References 127
Appendices 133
Appendix One 133
Appendix Two 141
Appendix Three 171

List of Figures

Chapter 2: Setting Page

Figure 2.1: New Zealand active plate boundary. 8

Figure 2.2: North Island intraplate volcanism. 9

Figure 2.3: Distribution of volcanic centres in the SAVF. 12

Chapter 3: Kellyville volcanic complex

Figure 3.1: The Mercer Sandstone at the northern tuff ring rim breach. 18

Figure 3.2: The Mercer Sandstone in thin section. 18

Figure 3.3: SEM photos of planktic and unknown benthic foraminifera. 19

Figure 3.4: Koheroa Siltstone in outcrop from southern rim breach. 20

Figure 3.5: Koheroa Siltstone in thin section. 20

Figure 3.6: Mercer Township and Kellyville tuff ring breach. 21

Figure 3.7: Map of Kellyville volcanic complex. 22

Figure 3.8: Glass Hill scoria cone. 23

Figure 3.9: Scoria outcrop and mine on Glass Hill. 24

Figure 3.10: School Hill scoria cone. 25

Figure 3.11: Diatomite in outcrop. 26

Figure 3.12: Fossil leaf impressions in diatomite deposit. 27

Figure 3.13: Diatomite species in the Kellyville volcanic complex. 28

Figure 3.14: Combined stratigraphy of the Kellyville tuff ring. 29

Figure 3.15: Facies A deposits. 32

Figure 3.16: Facies A basalt ballistic. 33

Figure 3.17: Facies B in outcrop. 34

Figure 3.18: Facies B deposits. 34

Figure 3.19: Facies C in outcrop. 35

Figure 3.20: Alternating fine and coarse ash fall and surge beds. 36

Figure 3.21: Fine and coarse ash fall and surge beds and flow direction. 37

Figure 3.22: Stratigraphic log of exposed scoria outcrop, School Hill. 39

Figure 3.23: Changes in vesicularity with height within School Hill. 40

Figure 3.24: Inner textures of vesicles in scoria. 41

Figure 3.25: $Na_2O + K_2O$ wt% against SiO_2 wt%. 43

Figure 3.26: Zr/Nb ratio against Nb (ppm). 43

Figure 3.27: Tuff deposits viewed in thin section. 44

Figure 3.28: Dense porphyritic olivine basalt with olivine phenocrysts. 45

Figure 3.29: Scoria palagonite and tachylite clasts within tuff deposits. 46

Figure 3.30: Large, zoned, embayed plagioclase crystal. 46

Figure 3.31: Koheroa Siltstone lithic lapilli and block samples. 47

Figure 3.32: Scoria from School Hill scoria cone with infilled vesicles. 48

Figure 3.33: Basalt flow from School Hill scoria cone. 48

Figure 3.34: Stratigraphic variation throughout the exposed tuff ring. 51

Figure 3.35: Kellyville tuff ring eruption progression. 61

Figure 3.36: Failure of the tuff ring rim. 62

Chapter 4: Onewhero tuff ring

Figure 4.1: Geological map of the Onewhero tuff ring. 64

Figure 4.2: Carter Siltstone in outcrop at Maoa's waterfall. 65

Figure 4.3: Carter Siltstone hand specimens. 66

Figure 4.4: Locality 1 showing facies A. 68

Figure 4.5: Locality 2, northeastern tuff ring rim. 69

Figure 4.6: Locality 3 containing both facies A and B. 69

Figure 4.7: Maoa's Waterfall flowing over a basalt lava flow. 70

Figure 4.8: Combined stratigraphy of the Onewhero tuff ring. 71

Figure 4.9: Lower tuff. 75

Figure 4.10: Sample of Facies A. 75

Figure 4.11: Sample of facies B. 76

Figure 4.12: Highly crystalline olivine basalt. 78

Figure 4.13: $Na_2O + K_2O$ wt% against SiO_2 wt%. 80

Figure 4.14: Zr/Nb ratio against Nb (ppm). 80

Figure 4.15: Vesicular brown scoria clast with olivine phenocrysts. 81

Figure 4.16: Non-vesicular, crystalline basalt with olivine phenocrysts. 82

Figure 4.17: Embayed olivine crystal within tuff deposits. 83

Figure 4.18: Te Akatea Formation and Aotea Formation within tuff. 84

Figure 4.19: Stratigraphic variation throughout the exposed tuff ring. 86

Chapter 5: Bombay volcanic complex

Figure 5.1: Alluvial sediments underlying tephra from the TVZ. 92

Figure 5.2: Geological map of Bombay volcanic complex. 94

Figure 5.3: 50 m high tuff cliff exposed, Bombay Quarry. 95

Figure 5.4: History of the excavation of Bombay Quarry. 98

Figure 5.5: Jones Block Quarry after partial excavation of overburden. 99

Figure 5.6: Facies stratigraphy of the exposed 50 m tuff ring cliff. 100

Figure 5.7: Base of tuff cliff showing alluvial deposits and tephra. 102

Figure 5.8: Panoramic photo and sketch of Bombay Quarry. 103

Figure 5.9: Scoria and spatter cones within basalt flows. 104

Figure 5.10: Columnar basalt from inner quarry. 105

Figure 5.11: Sheeted basalt from inner quarry. 105

Figure 5.12: Elongated spatter lens from a spatter cone. 106

Figure 5.13: $Na_2O + K_2O$ wt% against SiO_2 wt%. 108

Figure 5.14: Zr/Nb ratio against Nb (ppm). 108

Figure 5.15: Hypocrystalline olivine basalt. 109

Figure 5.16: Broken olivine phenocryst with altered iddingsite rims. 111

Figure 5.17: Stratigraphic variation throughout the exposed tuff ring. 112

Figure 5.18: Spatter cone underneath alluvial deposits and tephra. 115

Chapter 6: Discussion

Figure 6.1: Water/magma ratios versus explosive energy. 124

List of Tables

Table 3.1: Mean vesicularity and density of Glass Hill and School Hill. 40

Table 3.2: XRF geochemical data of basalt from Kellyville tuff ring. 42

Table 4.1: XRF geochemical data of basalt from Onewhero tuff ring. 79

Table 5.1: XRF geochemical data of basalt from the Bombay Quarry. 107

Chapter One: Introduction

1.1 Introduction

The South Auckland volcanic field in New Zealand represents the complete history of a basaltic monogenetic volcanic field. The field was active 1.59 – 0.51 Million years ago (Briggs *et al.* 1994), and is young enough that erosion has not removed it from the geological record. Many of the 82 centres are easily accessible. Study of these volcanic centres can offer insight into our understanding of controls on, and eruption histories of tuff rings, maars, scoria cones and effusive centres in the South Auckland volcanic field.

1.2 Objectives of the study

Studies into the volcanism of the South Auckland volcanic field (SAVF) can improve the understanding of the full life of a monogenetic volcanic field, what controlled its character and progression, and hence by association what may control other similar monogenetic fields, such as the nearby active Auckland volcanic field. The main purpose of this thesis is to study three volcanic centres with tuff rings and varying levels of associated magmatic activity, using stratigraphic data, facies analysis and componentry data to illustrate the styles of eruptions as well as their controlling factors.

1.3 Location of the study area

The SAVF covers the Pukekohe, Bombay, Tuakau, Pukekawa and Onewhero regions (Briggs *et al.* 1994) over an area of approximately 300 km^2 (Schofield 1958; Rafferty 1977; Rafferty & Heming 1979; Weaver & Smith 1989). The field hosts 82 volcanic centres and a wide range of volcanic activity, with 38 tuff rings and maars, and 57 scoria cones and lava flows.

Three study areas have been chosen for this thesis. The Kellyville volcanic complex is situated in the southern end of the SAVF, 11.2 km south of Bombay and 150 m east of Mercer township. The complex consists of a breached tuff ring and two intra-tuff ring scoria cones. The Onewhero tuff ring is situated in the southern end of the SAVF, 17 km south of Bombay and 5 km south of the Waikato River. It is the largest tuff ring in the SAVF. A lava flow is present on the outskirts of the tuff ring. The Bombay Quarry volcanic complex is situated on the eastern side of the SAVF, 3.4 km southwest of Bombay. The complex consists of at least one tuff ring, a tuff cone, numerous scoria and spatter cones and at least two large deposits of ponded basalt lava.

1.4 Field work

Field work was undertaken over six weeks in the three study areas. Stratigraphic logs were constructed of all exposed outcrops accessible in each area.. This was limited at the Bombay Quarry, where access was limited due to safety rules. Samples were collected from significant layers and occurrences in outcrop, and photographs were taken of each outcrop and sample location. Topographical maps and GPS co-ordinates were used to determine sample and outcrop locations. Sample data is available from Appendix One.

Four stratigraphic logs were constructed of exposed tuff ring outcrops at Kellyville, as well as one of the two scoria cones. Samples were taken from the above sections, as well as the second scoria cone, a diatomite deposit, and two sections of the underlying sedimentary country rock units. Three stratigraphic logs were constructed of exposed tuff ring outcrops at Onewhero, and samples were collected from these, an outer lava flow, and the underlying sedimentary country rock units. One large stratigraphic log was measured of exposed tuff ring outcrops at Bombay Quarry, and samples were taken from this outcrop as well as those of surrounding spatter and lava deposits that were accessible. Stratigraphic logs are available from Appendix Two. Samples were also collected of alluvial and tephra deposits at the base of the tuff ring deposits. Access to Kellyville land was granted by Terry Glass and local farm workers. Access to Onewhero land was granted by

Richard and Jenny Andrews and the Poole family. Access to Holcim Quarry at Bombay was granted by James Boyce and Keith Miller.

1.5 Laboratory analysis

102 thin sections from the three field areas were made from samples representative of stratigraphic and facies changes and analysed for petrography. 62 thin sections were made from deposits associated with the Kellyville volcanic complex, including tuff (25), juvenile clasts (7), lithics (20), scoria (8) and diatomite (2). 19 thin sections were made from the Onewhero tuff ring and associated lava flow deposits, including tuff (14), lithics (3) and basalt lava (2). 22 thin sections were made from deposits associated with the Bombay Quarry volcanic complex, including tuff (9), lithics (7), basalt lava (4) and spatter (2).

An X-ray Fluorescence (XRF) spectrometer from the University of Waikato was used on fresh basalt samples in order to determine their major and trace element compositions. Only three samples (Onewhero- 1, Bombay Quarry- 2) were able to be analysed due to the degree of alteration in most basalts sampled. Major element geochemistry was analysed using fused glass disks. Samples were powdered with a tungsten carbide mill, and 0.33 – 0.35 g of powder was added with 2.50 – 2.55 g of 1.2: 2.2 flux in platinum crucibles and stirred. Crucibles were step-heated every 15 minutes in a Bradway Fusion Furnace at temperatures of 700°C, 800°C, and 1040°C with the furnace shaker mixing the contents. A pinch of ammonium iodide was added at the end of the step-heating process to prevent the contents of the crucible from sticking. The contents were then poured onto a graphite disk and flattened with a press. Once the disk had cooled, it was set on heated plates to allow the glass to anneal. The fused disks are then analysed with XRF. Trace element compositions were analysed using pressed powder pellets. 5 g of the powdered samples were mixed with 13 – 15 drops of PVA binder and put into an aluminium cup to be compressed with a hydraulic press loaded to 90 bars. The pressed sample was then put into an oven for 2 hours to evaporate the PVA binder, and then analysed by XRF. Loss On Ignition was determined by heating 2 g of powdered sample in silica crucibles in a

Bradway Fusion Furnace at 1100°C for about an hour, and measuring difference in weight after heating.

A Hitachi S-4100 Field Emission Scanning Electron Microscope with X-ray analyser (SEM) was used from the University of Waikato to assist with species identification of diatoms from Kellyville volcanic complex diatomite and microfossil material from all three study areas.

Microfossils were analysed using foraminiferal picking of sedimentary samples from all three areas in order to identify age determinant species.

Vesicularity and density were measured using vesicular basalt, scoria and spatter samples from all three study areas. 10 basaltic clasts of size 4 phi deposits were used for each sample, and maximum, minimum and average vesicularity and density measurements were determined. Vesicularity and density data are available from Appendix Three.

1.6 Chapter outlines

The outline of the thesis is as follows: Chapter 2 outlines the setting of the study area. New Zealand tectonic setting and intraplate volcanism in the North Island are discussed, specifically of the Auckland Province. Previous studies of South Auckland volcanology are discussed, as well as the volcanology of three volcanic centres that are the basis of this thesis.

Chapter 3 focuses on the Kellyville volcanic complex and presents the results of a field study on its geology, facies variations and stratigraphy, as well as laboratory studies of the componentry of both a tuff ring and two intra-tuff ring scoria cones. Stratigraphic relationships and facies analysis are used to define emplacement processes and the eruption history. The distinction of whether Kellyville is a tuff ring or a maar is discussed.

Chapter 4 focuses on the Onewhero tuff ring, outlining its geology, facies and stratigraphy as well as the componentry of a tuff ring and a nearby lava flow. Stratigraphic relationships and facies analysis are used to define emplacement processes and the eruption history.

Chapter 5 focuses on the Bombay volcanic complex, presenting the geology of the quarry and the surveying history of the basalt deposits to be mined. Facies and stratigraphic analyses are discussed as well as componentry of both the tuff ring and effusive products. Stratigraphic changes are used to define the emplacement processes and eruption history of the volcanic complex.

Chapter 6 summarises the eruption histories of all three field areas. The characteristics of the deposits are described and the main controls in eruption styles and mechanisms are interpreted.

Chapter Two: Setting

2.1 Introduction

New Zealand lies along the boundary between the Pacific and Indo-Australian plates, where both subduction and strike-slip movement occur (Barnes *et al.* 2010). The only active intraplate volcanism in the North Island occurs in Northland and Auckland, entirely in the Indo-Australian plate (Fig. 2.1) (Johnson & Wellman 1989). The intraplate volcanoes in New Zealand are generally separate from the active plate boundary zone, in areas of relative quiescence (Johnson & Wellman 1989) and have no apparent tectonic relationship with the active margin (Weaver & Smith 1989; Briggs *et al.* 1994; Cook *et al.* 2005). The Northland and Auckland areas of intraplate volcanism are about 400 km behind the active margin and are situated in an extensional environment, however only the Northland province has characteristic arc signatures (Smith *et al.* 1993; Cook *et al.* 2005).

The Northland province is 500-700 km northwest of the active margin in an area that is tectonically quiet (Weaver & Smith 1989), and the Auckland province is 350-400 km behind the present plate boundary (Weaver & Smith 1989). Northland and Auckland volcanism cover an area of approximately 2500 km^2 and 400 km^2 respectively (Weaver & Smith 1989). Both provinces can be further split up into several volcanic fields. The Northland province contains the Kaihoke-Bay of Islands and the Whangarei intraplate volcanic fields (Heming 1980; Weaver & Smith 1989; Smith *et al.* 1993; Cook *et al.* 2005). The Auckland province contains from south to north the Okete, Ngatutura, South Auckland, and Auckland volcanic fields (Cook *et al.* 2005). The North Island intraplate volcanic activity has occurred from the Miocene to recent times (Johnson & Wellman 1989; Cook *et al.* 2005) and the Auckland province shows an age trend of progressive younging (Briggs *et al.* 1994) northwards through this period (Fig. 2.2). Volcanic products of the North Island intraplate volcanism are mainly basaltic and include maars, scoria cones and lava flows - all with small volumes (Heming 1980; Kear 1996).

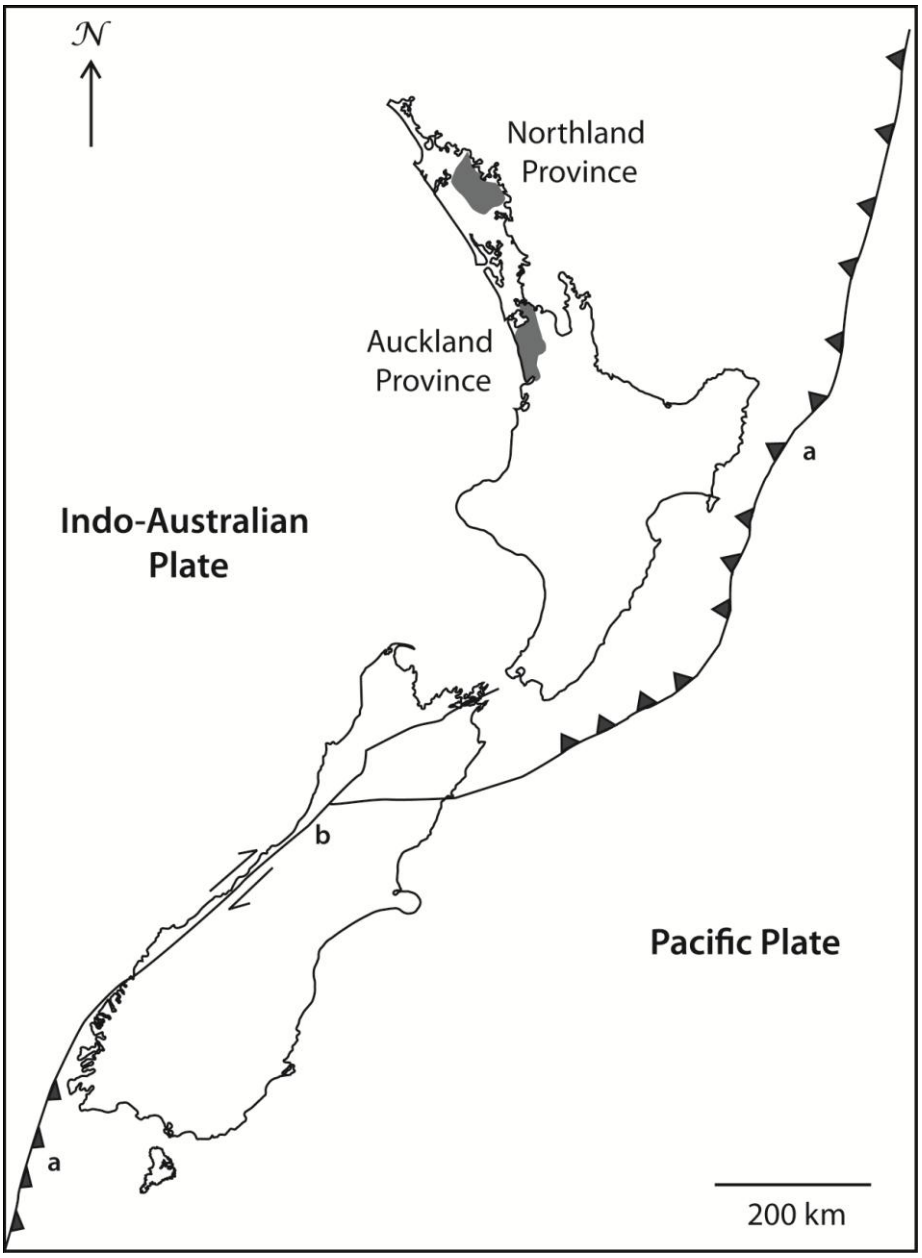

Figure 2.1: New Zealand active plate boundary, showing (a) subduction and (b) strike-slip boundaries and North Island's two active intraplate volcanic provinces (Figure adapted from Cook *et al*. 2005).

Cook *et al*. (2005) noted that the subducting Pacific Plate beneath the North Island can only be tracked to 250 km deep, and cannot be tracked to underneath the South Auckland volcanic field. Cook et al. (2005) summarise that the volcanism is caused by decompressional melting in the extensional environment of western and northern North Island.

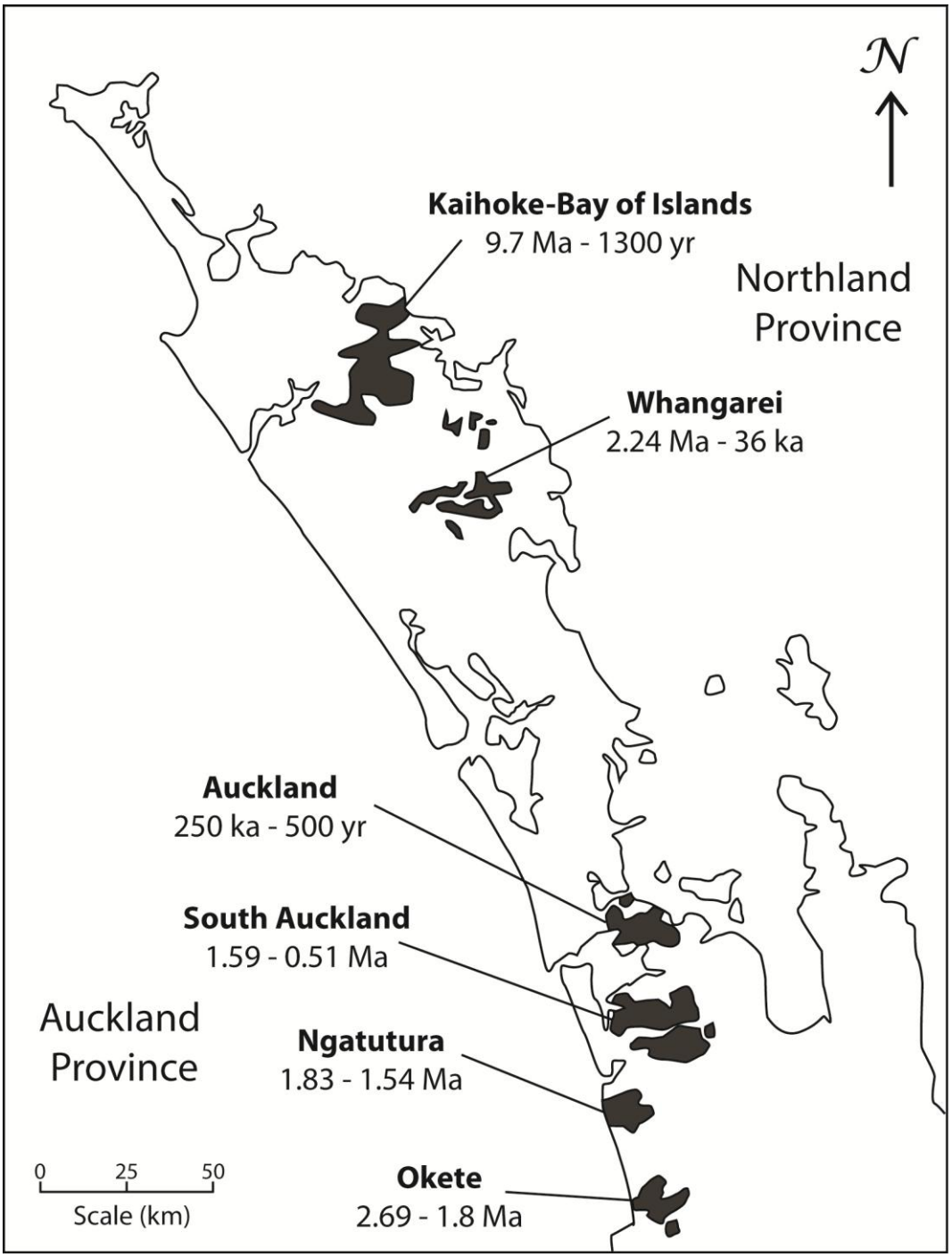

Figure 2.2: North Island intraplate volcanism, showing the two provinces and their associated fields: Northland Province, containing Kaihoke-Bay of Islands and Whangarei, and Auckland Province, containing Auckland, South Auckland, Ngatutura and Okete. Note the progressive younging northward in the Auckland Province fields (Figure adapted from Weaver & Smith 1989; Briggs et al. 1994; Cook et al. 2005 and age data from Smith *et al.* 1993; Briggs *et al.* 1994).

2.2 South Auckland volcanology

The South Auckland volcanic field (SAVF) (Fig. 2.3) covers the Pukekohe, Bombay, Tuakau, Pukekawa and Onewhero regions (Briggs *et al.* 1994) over an area of approximately 300 km^2 (Schofield 1958; Rafferty 1977; Rafferty & Heming 1979; Weaver & Smith 1989). The field is comprised of scoria cones, basaltic flows, tuff rings and tuff cones (Rosenberg 1991). The monogenetic volcanic activity has resulted in 15 to 20 km^3 of deposits (Rafferty 1977; Rafferty & Heming 1979).

The number of volcanic centres recorded for the SAVF has changed over time. An early estimate of over 70 centres (Schofield 1958; Rafferty 1977; Rafferty & Heming 1979; Heming 1980; Weaver & Smith 1989), was superseded by 97 volcanic centres (Briggs *et al.* 1994; Cook *et al.* 2005).

Recently, using a combination of mapped locations and the use of volcanic ages from Briggs *et al.* (1994) the number of tuff rings, scoria cones and effusive deposits has been recounted as 38 and 13 and 39 respectively. However the number of tuff ring centres and effusive (scoria cone and effusive) centres are 30 and 52 respectively. The reason for this is that volcanoes that were either overlapping one another or had very small distances between them were grouped as one centre. Their genetic relationship was further established using available age data. Volcanoes in the same centre were either all of one style of volcanism or a combination of tuff rings, scoria cones and effusive volcanism. This method brings the total number of volcanic centres within the SAVF to 82. Further research and understanding of each volcano and their age data would allow the above number of centres for the SAVF to be confirmed.

The SAVF was active between 1.59 and 0.51 Ma (Briggs *et al.* 1994) and is separated from the younger Auckland Volcanic Field 30 km further north by about 250 ka (Cook *et al.* 2005). The age range of the field has been obtained by 43 K-Ar dates by Briggs *et al.* (1994). The youngest age obtained was 0.56 ± 0.05 Ma at Pukekohe Cone, and the oldest was 2.24 ± 0.37 at Drury Hills cone (Briggs *et al.* 1994). A younger K-Ar date of 0.51 Ma was previously obtained by Stipp (1968) for Pukekohe Hill.

Much of the SAVF is situated in a down-faulted area of Mesozoic greywackes, sandstones and argillites (Rafferty 1977) that form the basement. The Te Kuiti Group unconformably overlies the Mesozoic basement and the Waitemata Group unconformably overlies the Te Kuiti Group (Rafferty 1977; Edbrooke 2001). The Kaawa Formation unconformably overlies the Waitemata and Te Kuiti Groups, as do pumice fall deposits from nearby eruptions in Coromandel and Taupo (Rafferty & Heming 1979; Edbrooke 2001). The Tauranga Group is the uppermost stratigraphic group in the area and is mostly exposed north of the Waikato Fault, as the Puketoka Formation and the Taupo Pumice Alluvium (Edbrooke 2001). A block of Mesozoic basement has been uplifted in the northeast part of the SAVF, and is known as the Hunua Block, which has not prevented volcanism from occurring in this region.

There is a close relationship between the tuff rings and cones in this volcanic field (Rafferty 1977). The tuff rings are commonly in clusters or nested, and range from 0.5 to 2.5 km in diameter (Rafferty & Heming 1979; Weaver & Smith 1989). Several tuff rings in the field have formed nested scoria cones where strombolian activity occurred after phreatomagmatic eruptions (Rafferty 1977; Rafferty & Heming 1979; Weaver & Smith 1989). Scoria cones in this field are commonly small and steep-sided (Rafferty 1977).

Rafferty (1977) compared the SAVF to the Auckland volcanic field, which has fewer centres, about 50 (Cassidy *et al.* 2007). Nested scoria cones are common in both the Auckland and South Auckland volcanic fields (Rafferty 1977; Weaver & Smith 1989).

Rafferty (1977) suggested that the processes that formed the South Auckland volcanism were also the cause of the Pleistocene displacement of the major faults in the area, including the Drury, Pokeno, Wairoa and Waikato faults. Approximately half of the volcanic centres are either directly on, or very close to, faults in the volcanic field. This suggests that the volcanism is largely fault controlled (Briggs *et al.* 1994; Briggs *et al.* 2010). It is also possible that faults pre-dating the volcanism are present but covered in the extensive lavas that largely cover the field (Briggs *et al.* 1994). Therefore the level of fault control of the volcanism may be larger than what is apparent.

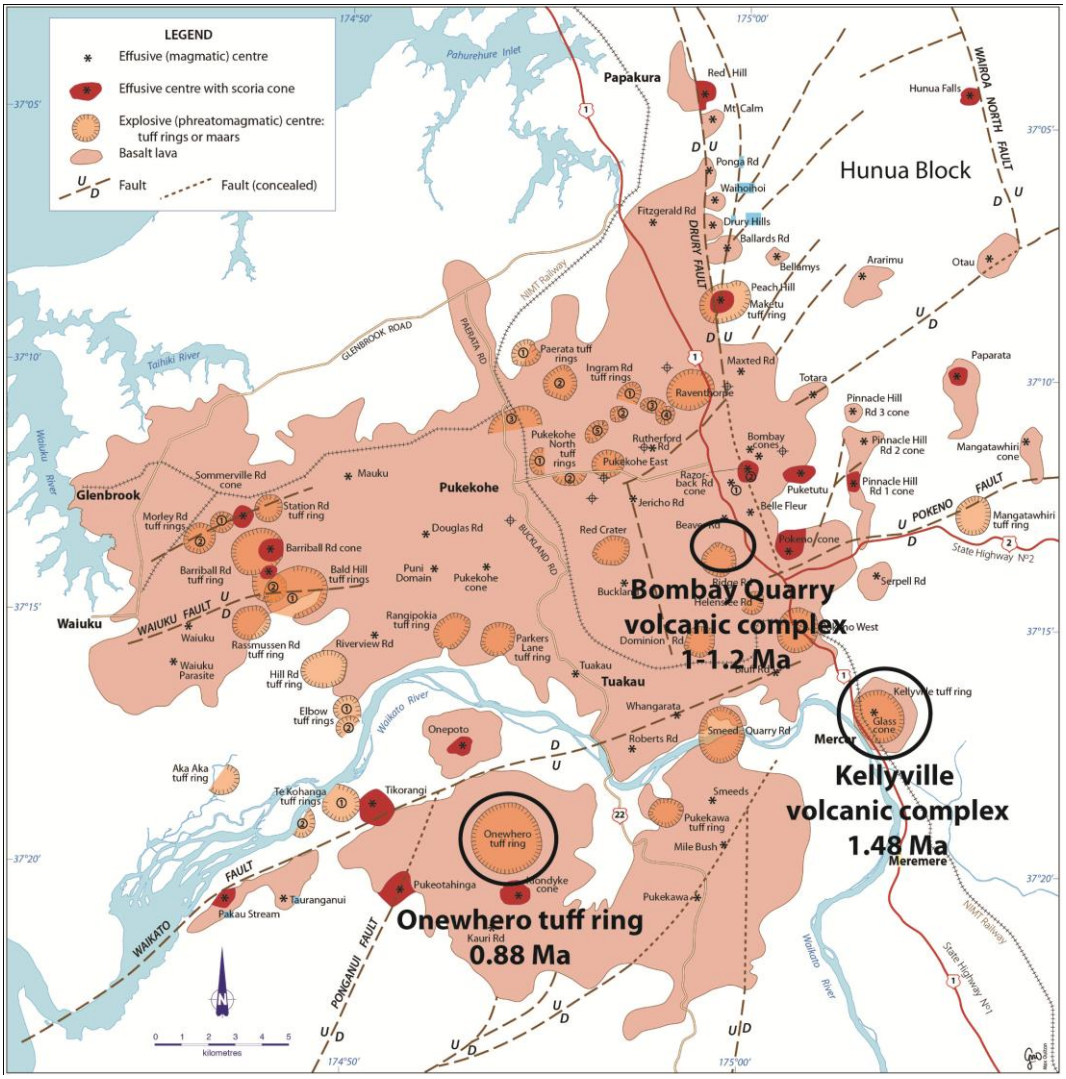

Figure 2.3: Distribution of volcanic centres in the SAVF. Two main faults are shown: Drury Fault and Waikato Fault. The three main areas of study, Kellyville volcanic complex, Onewhero tuff ring and Bombay Quarry volcanic complex are shown (Briggs *et al*. in prep. 2010).

Cook *et al.* (2005) gave the opinion that it is unlikely that the South Auckland volcanism occurred from magma chambers, but is characterised by comparatively short-lived eruptions derived from small batches of magma sourced directly from the mantle, typical of monogenetic basaltic fields elsewhere in the world (Connor & Conway 2000).

Greig (1989) studied the aquifer potential of the Kaawa Formation in the Manukau lowlands area, finding a large variation in aquifer transmissivities of 30

to 500 m^2/day. Hadfield (1988) studied the hydrogeology of the Kaawa Formation in the Pukekohe/Tuakau area, and found similar aquifer transmissivities (50 – 500 m^2/day), as well as producing geological cross-sections across the South Auckland volcanic field.

Rafferty (1977) and Rafferty & Heming (1979) suggest that the Waikato River may have had a large role in the level of phreatomagmatism in the SAVF, as several tuff rings are aligned along the Waikato River where surface water is abundant.

Early work on the "Franklin County" was undertaken by Schofield (1958), who studied basalts in South Auckland and suggested that they were between early to mid Pleistocene in age. Schofield (1958) reported the Franklin Basalts to consist of basalt flows and basaltic tuffs commonly containing Waitemata Group lithics. The lavas are all basaltic and all contain olivine, augite, plagioclase and opaques (Rafferty 1977). Schofield (1958) originally divided the South Auckland basalts into two groups: Franklin basalts and Bombay basalts, based on cone morphology and degree of weathering. Briggs *et al*. (1994), Cook (2002) and Cook *et al*. (2005) concluded that there was no basis for this subdivision. Rafferty (1977) and Rafferty and Heming (1979) decided that this would limit further classification using geochemical characteristics, and so divided the basaltic products of the SAVF into two different groups; a hypersthene-rich subalkaline group and a nepheline-rich alkaline group. Cook (2002) studied the geochemistry of a characteristic group of volcanic samples from the SAVF in a Ph.D. thesis. Cook et al. (2005) further analysed the differences between these two distinct groups of basalt, calling them Group A and Group B (respectively), using a greater range of samples taken by Cook (2002).

The petrography, physical volcanology, mechanisms of eruptions and hazard implications of one scoria cone (Onepoto volcano) and five tuff rings (Barriball Road maar, Maketu tuff ring, Raventhorpe maar, Aka Aka tuff ring, Smeed Quarry Road tuff ring) were studied in the SAVF by Rosenberg (1991), who concluded that the styles of volcanism were mainly controlled by the hydrology and lithology of the underlying country rocks. Jukic (1995) conducted a geological and geophysical subsurface investigation of Onewhero Crater and

Pukekohe Hill as part of a MSc thesis, and concluded that there are no signs of a feeder system still present. A recent study by Ilanko (2010) further summarised the facies, petrography, geochemistry, eruption and emplacement processes of the Barriball Road tuff ring.

2.3 Previous work at Kellyville

Kellyville was first described by Battey (1949) as "a crater with a breached rim and a central plug of lava and agglomerate lies just east of Mercer". Colchester (1968) completed a BSc. Hons. study describing the geology of the Kellyville tuff ring. A geological map of New Zealand (Schofield 1967) shows Kellyville as a "crescent shaped patch of Franklin basalt". The name Kellyville was first used in a table summarising the stratigraphy of the Ngaruawahia subdivision (Kear & Schofield 1978). Kermode (1992) lists Kellyville tuff ring as one of the Quaternary volcanoes in South Auckland, with an age of 1.48 My (Briggs *et al.* 1994).

Kear & Schofield (1978) list a maximum tuff ring rim height of 111 m, and a surrounding alluvial plain height of 4.5 m. Kear & Schofield (1978) also describe the breach in the crater rim and its terraces within. They point out a "small but prominent cone-shaped hill" in the centre that is composed of basaltic tuff and agglomerate, and that the surrounding tuff ring is comprised of evenly bedded basaltic material with lithics presumed to be mainly Koheroa Siltstone (Kear & Schofield 1978).

Rafferty (1977) reported that the lavas that formed the strombolian scoria cone are the same as the ones within the tuff ring deposits. Rafferty (1977) suggested that the changes in eruptive style can therefore be inferred to be caused by magma-water interaction. The diatomite deposit at Kellyville has been described by Waterhouse (1980).

The Waitemata Group was first named by Hochstetter in 1864 for the "interbedded light grey siltstones and sandstones" exposed around Waitemata harbour (Kear & Schofield 1978). Colchester (1968) reports that the Waitemata Group underlies the Kellyville Tuff Ring, and two formations of this group,

Mercer Sandstone and Koheroa Siltstone, outcrop on the northern and southern ends (respectively) of the breach in the crater. Kear (1961) described Otaian Mercer beds as calcareous siltstones and loose brown sandstones. The contacts within this group are poorly defined as they are rarely visible (Kear & Schofield 1978). The Waitemata Group extends as far south as Mercer (Kear 1961; Edbrooke 2001).

2.4 Previous work at Onewhero

Kermode (1992) lists Onewhero as the largest of the Quaternary volcanoes in South Auckland. The Onewhero tuff ring is 0.88 My (Briggs *et al.* 1994). Waterhouse (1978) produced a map detailing the geology and volcanic deposits of the Onewhero area.

Rafferty (1977) theorised that Onewhero must have blasted through the original lava flows of nearby Onewhero cone, as they are preserved in the northern outlet of the tuff ring. Rafferty (1977) noted that Onewhero has no plug, and that boreholes have failed to detect any basalt to depths of 100 m. Rafferty (1977) speculates that the lack of detected basalt could be due to the tuff ring having no magma chamber, or if the tuff ring floor had collapsed following the eruption due to withdrawal of the magma source.

Te Kuiti Group has been described around the South Auckland area by Kear (1961). Carter Siltstone has been described and given a Waitakian age (Waterhouse & White 1994). Jukic (1995) reported that the Waitemata Group is 40-60 m underneath the volcanic deposits (however this was not seen in the field, and the Te Kuiti Group outcrops at approximately 90m a.s.l.).

2.5 Previous work at Bombay Quarry

Bombay Quarry is operated by Holcims Aggregates, who have hired several companies to provide geotechnical surveys and report on the area and any factors that influence either the quality of the basalt or their ability to mine it.

According to a report made for Milburn NZ Ltd (Holcims Quarry) by John O'Brien Associates *et al.* (1994), the basalt deposit that is available to be mined occurs within gently rolling land comprised of tuff, volcanic ash and basalt. The underlying sedimentary geology is comprised of the Waitemata Group, which is present at depths of 30 to 70 m below the mineable basalt, as well as on the surrounding lower valleys and plains (John O'Brien Associates *et al.* 1994).

Ormiston Associates Ltd (1999) have reported on the basalt resource at Bombay Quarry using drilling, geological studies and resource modelling. They have concluded that the economically viable basalt resource is smaller than what was first estimated before quarrying began (first estimated at 4 million m^3, now 2.45 million m^3) (they estimated a quarry life of 13 years in 1999). "The revised geological model generally indicates that the basalt deposit comprises a high quality central core of basalt surrounded by shells of successively decreasing rock quality. This is further complicated by an explosion crater which has replaced part of the southern corner of the high quality basalt with low quality scoria and volcanic debris" (Ormiston Associates Ltd 1999)

Alloway *et al.* (2004) has provided a date for a tephra layer that appears at the base of an upper tuff succession in the quarry. The tephra layer AT-71 was dated using ITPFT (isothermal plateau fission track dating) at 1-1.2 Ma. It is correlated with a post-Ongatiti tephra layer (AT-47) from Schnapper Rock at Beachlands, and has been proved to be from the Taupo Volcanic Zone (Alloway *et al.* 2004).

Chapter Three: Kellyville Volcanic Complex

3.1 Introduction

The Kellyville volcanic complex (KVC) is situated at the southern end of the South Auckland volcanic field (SAVF) near Mercer (Fig. 2.3).

An early phreatomagmatic phase 1.48 Ma produced a tuff ring, followed by a later magmatic phase that produced two scoria cones within the tuff ring. The tuff ring was infilled with a lake that deposited diatomite.

This chapter will cover the underlying geology of the Kellyville tuff ring. Several lithologic facies and their stratigraphy have been identified of the tuff ring and scoria cones. The componentry of the tuff and scoria deposits will be discussed as well as its stratigraphic variation. A discussion of the classification, emplacement processes, and eruption history of the KVC is presented at the end of the chapter.

3.2 Country rock geology

The Kellyville tuff ring is underlain by the Mercer Sandstone and Koheroa Siltstone which are formations within the Waitemata Group (Edbrooke 2001).

Mercer Sandstone

The type section of the Mercer Sandstone (Fig. 3.1) is exposed on the northern rim breach of the Kellyville tuff ring (Kear & Schofield 1978) (locality 8). The unit is a massive to thick bedded, weakly indurated, poorly sorted, calcareous to non-calcareous, buff-coloured to brown sandstone with interbedded light grey, sandy mudstone (Kear & Schofield 1978; Edbrooke 2001). It is 26 m thick at Mercer but occurs up to 600 m thick elsewhere (Edbrooke 2001). The Mercer Sandstone dips gently north (3°) according to Colchester (1968) and is never fully exposed in outcrop, however Kear & Schofield (1978) and Edbrooke (2001) suggest that the lower contact with the Koheroa Siltstone is conformable.

Figure 3.1: The Mercer Sandstone at the northern tuff ring rim breach, locality 8. Geological hammer is 33 cm long.

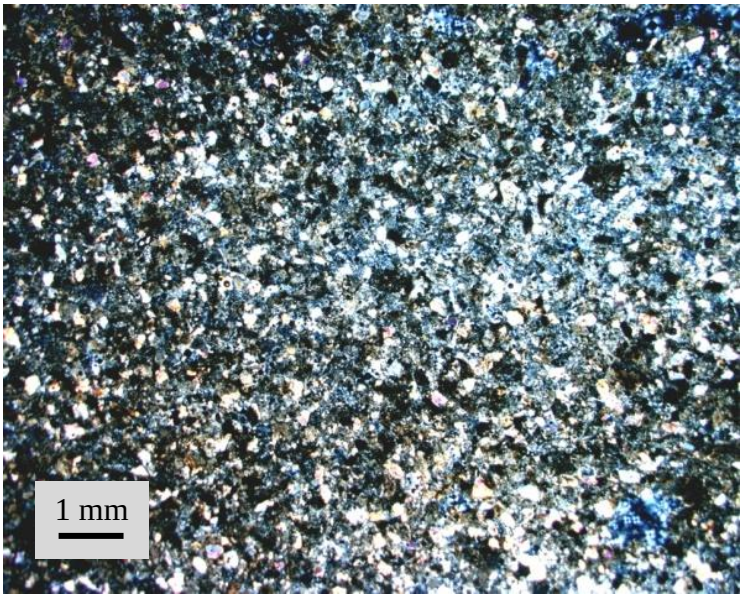

Figure 3.2: The Mercer Sandstone in thin section, under cross polarised light (XPL) showing a calcareous matrix with small quartz grains (sample W2011543).

In thin section Mercer Sandstone (Fig. 3.2) appears as a very well sorted fine calcareous sand with common quartz crystals, some glauconite, and pyrite staining. The Mercer Sandstone is Otaian in age (Kear & Schofield 1978). Sieved samples of the sandstone were picked for fossil material (Fig. 3.3). The fossils found included *Astrononion sp*. of the Rotaliina family, bivalve fragments, echinoid spines, *Gynindina sp*. benthic foraminifera, unidentified spiral benthic foraminifera (Fig. 3.3), and *Globigerina bulloides* (pers. comm. B. Hayward).

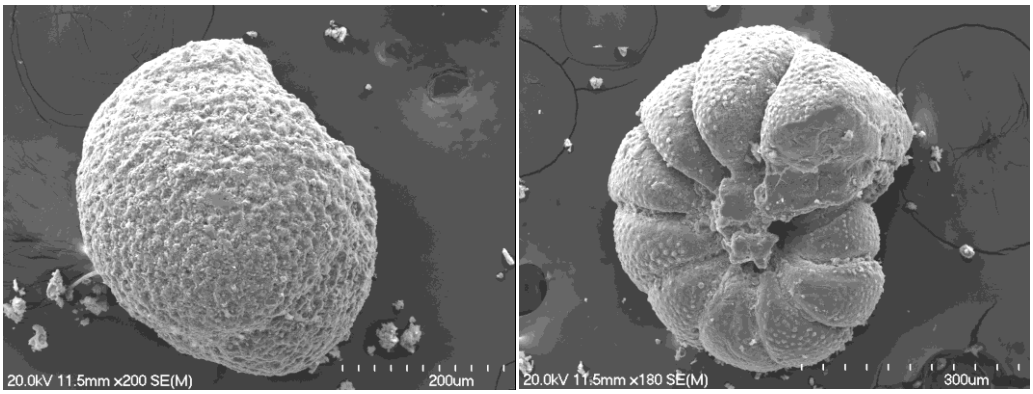

Figure 3.3: SEM photos of planktic foraminifera (left) and unknown benthic (?) foraminifera from the Mercer Sandstone (sample W2011543).

Koheroa Siltstone

The type section of the Koheroa Siltstone (Fig. 3.4) is exposed on a railway cutting on the southern rim breach of the Kellyville tuff ring, and along Koheroa Road to Mercer School (Kear & Schofield 1978) (locality 9). It is a calcareous, massive to well bedded, light grey to blue-grey sandy siltstone with interbedded calcareous sandstone (Kear & Schofield 1978; Edbrooke 2001). The Koheroa Siltstone is 27 m thick at Mercer but occurs up to 75 m thick elsewhere (Edbrooke 2001) and dips gently north (4°) according to Colchester (1968). The underlying contact with the Waikawau Sandstone is not exposed.

Figure 3.4: Koheroa Siltstone in outcrop from southern tuff ring rim breach, locality 9 (pen is 13 cm long).

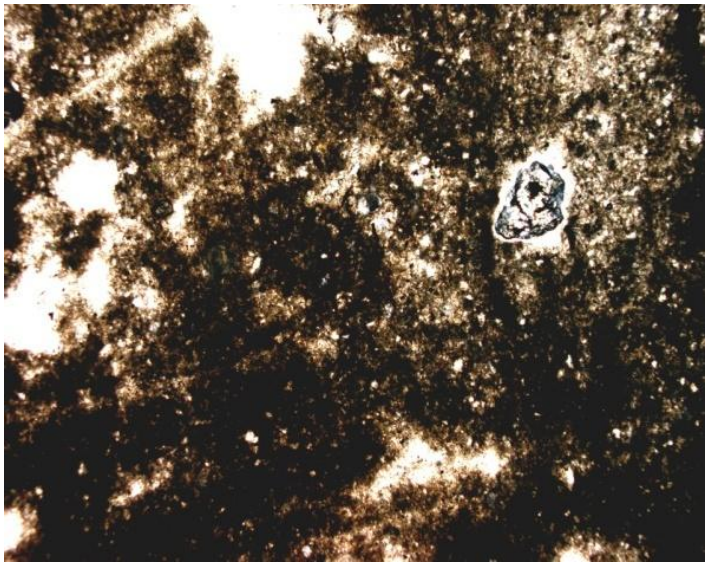

Figure 3.5: Koheroa Siltstone in thin section, plane polarised light (PPL) (sample W2011544).

The Koheroa Siltstone is a very well sorted fine calcareous silt with small quartz and plagioclase crystals, and some pyrite staining (Fig. 3.5). It is Otaian in age (Kear & Schofield 1978). Sieved samples of the siltstone were picked for fossil material. The fossils found included *Globigerina sp.*, *Globigerinoides sp.*, and *Hoegludina elegans* benthic foraminifera. The *Globigerinoides sp*. foraminifera are representative of the late-mid Miocene. The *Hoegludina elegans* foraminifera are representative of deep water (pers. comm B. Hayward).

3.3 Kellyville volcanic complex

The Kellyville volcanic complex was active 1.48 Ma (Briggs *et al.* 1994). The KVC is situated at the southern end of the South Auckland volcanic field, 11.2 km south of Bombay, 4.6 km south of Pokeno and 150 m east of Mercer township. The KVC consists of a breached tuff ring (Fig. 3.6) and two intra-tuff ring scoria cones. It is accessible from Great South Road (State Highway 1), which runs along its western side. Kellyville is one of the larger tuff rings in the SAVF, with a diameter of 1.8 km. The highest point of elevation on the tuff ring rim is 111 m. The maximum thickness of the tuff itself is 92 m, measured from the stratigraphic base. The inner base of the tuff ring ranges from 10 to 12 m a.s.l. The width of the tuff ring rim ranges from approximately 200 to 600 m based on modern day topography. The inner geomorphic slope angles of the tuff ring are approximately 10°. The outer geomorphic slope angles range from 7° to 9°. The tuff ring has been breached on its western side. The breach is 0.9 km wide, and would have allowed the lake within the tuff ring to be drained.

Figure 3.6: Mercer Township and Kellyville tuff ring breach as viewed from the northern crater rim.

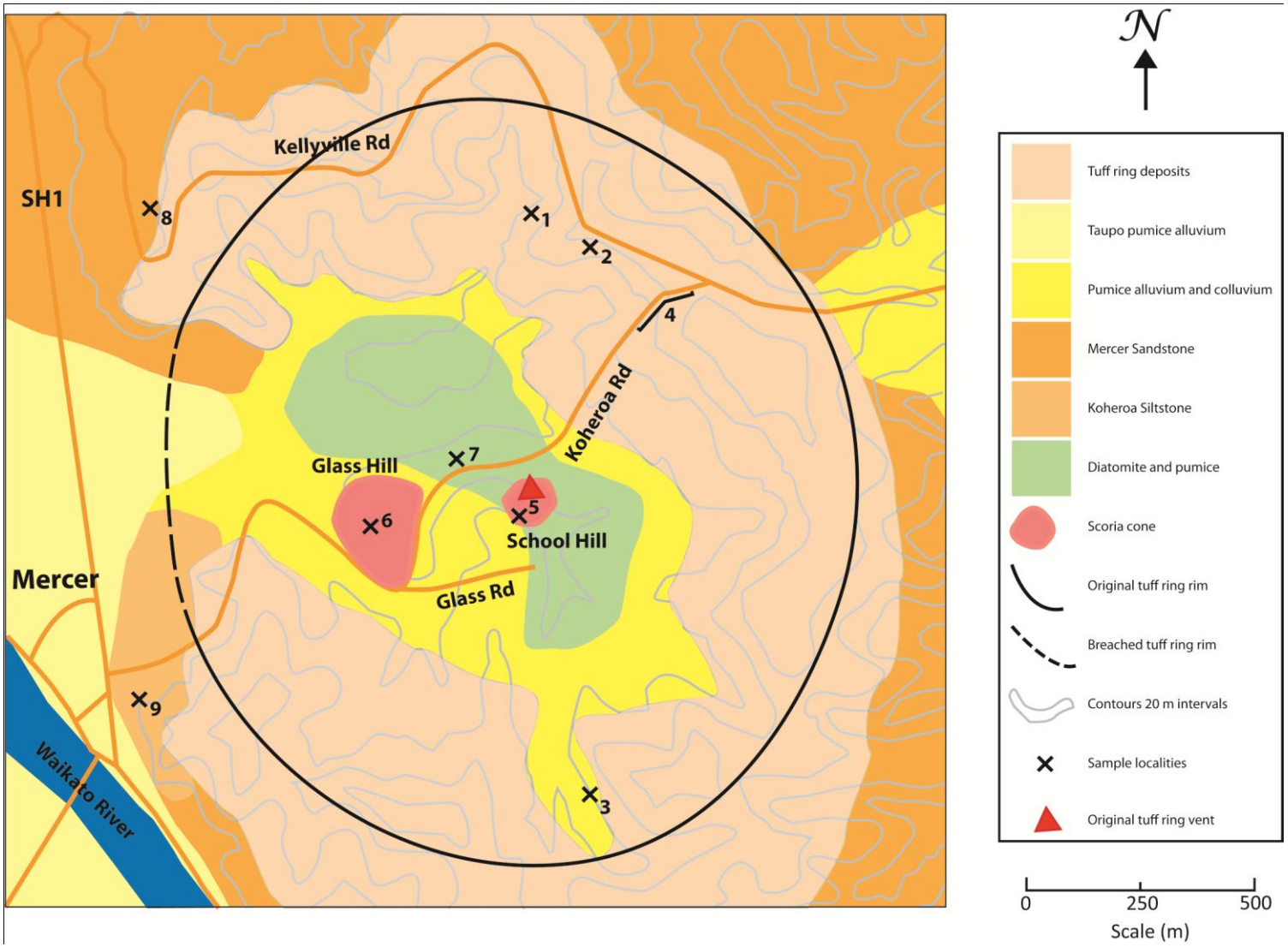

Figure 3.7: Map of Kellyville volcanic complex (Waterhouse 1980; Edbrooke 2001).

There are several roads that run through the tuff ring. Koheroa Road runs through the middle of the tuff ring from opposite the Mercer Township to the east. It provides access to Glass Hill (locality 6), the largest outcrop of diatomite (locality 7), and the largest exposed section through the tuff ring (locality 4, Fig. 3.7). It joins up with Kellyville Road, which runs along the northern tuff ring rim and joins with Great South Road. Glass Road begins from Koheroa Road near Glass Hill and runs to the previously un-named scoria cone. It provides access to Mercer School and Kellyville Cemetery. The intra-tuff ring scoria cones are located in the middle of the tuff ring. The larger scoria cone is Glass Hill, which is 45 m high and has slope angles of 20°. The smaller scoria cone which is 20 m high with geomorphic slope angles of 24°, has not been identified previously and has been named in this study as School Hill scoria cone.

Several terraces have formed while a lake existed inside the tuff ring. The terraces were formed as the pre-existing lake levels fluctuated over time. The terraces can be seen even today, and occur at 55 m, 33 m, and 8 m above sea level (Colchester 1968; Waterhouse 1980). Small streams have drained the tuff ring over time, eroding and transporting the underlying tuff as well as any recent sedimentation (diatomite) into the Waikato River.

3.4 Scoria cones

Figure 3.8: Glass Hill scoria cone and the southern crater rim behind.

Glass Hill (locality 6, Fig. 3.8, 3.9a-c) is asymmetrical: it is steeper on its south-western side and has a more gradual slope on its northern and eastern sides. The scoria cone was once quarried for scoria, most likely for railway ballast for the nearby railway line. Old mining tracks and scrap metal can be found on the southern side of the cone. An old underground mine (Fig. 3.9b,c), is still present in the southwest side of the cone, and can be accessed via a small opening in what is most likely to be a cave-in of the original tunnel entrance. The tunnel is very regular in size and shape, with a flat floor and domed, elongated roof 1.9 m high. It is 2 m wide and 28 m long from the opening to the other side, which has been caved in - possibly on purpose to prevent entry.

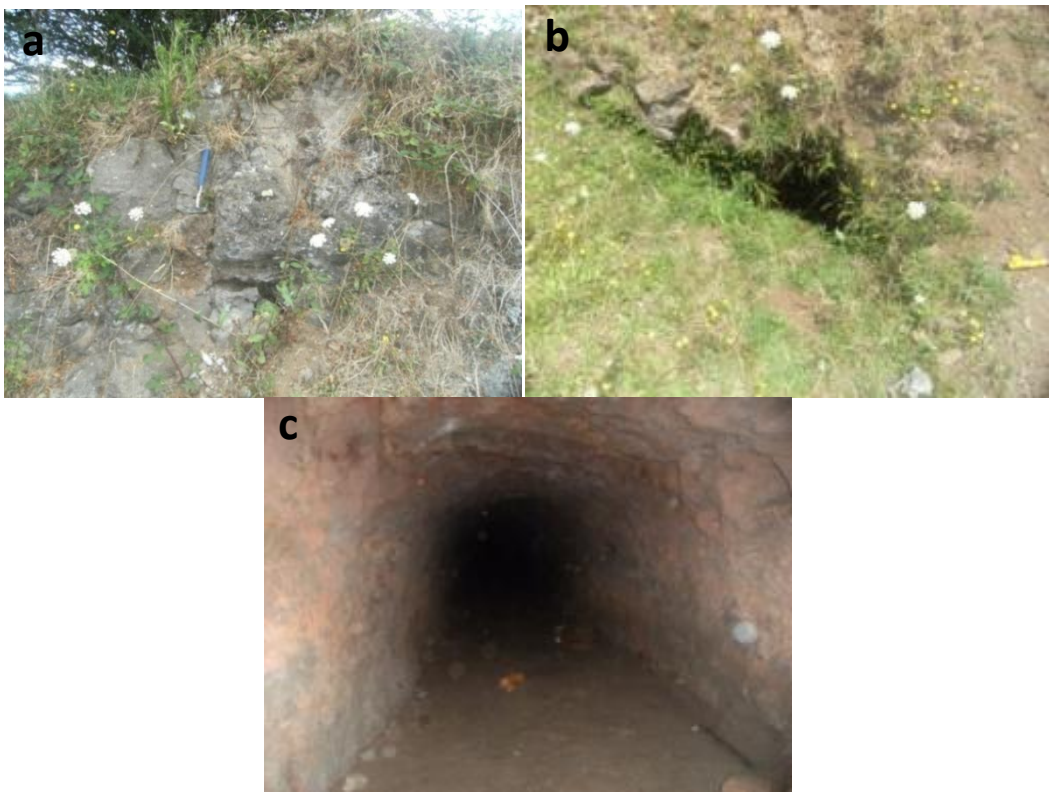

Figure 3.9: (a) Scoria outcrop on Glass Hill (geological hammer is 33 cm long); (b) Mine entrance; (c) Inside of mine.

School Hill scoria cone (locality 5) has a short basalt lava flow that has begun to flow out from the scoria cone (Fig. 3.10a,b). School Hill scoria cone (Fig 3.10c,d) has been erupted 470 m to the east of Glass Hill. Glass Hill occurs southeast of the southern mapped limit of the Drury Fault, and School Hill branches off at approximately 90° from Glass Hill.

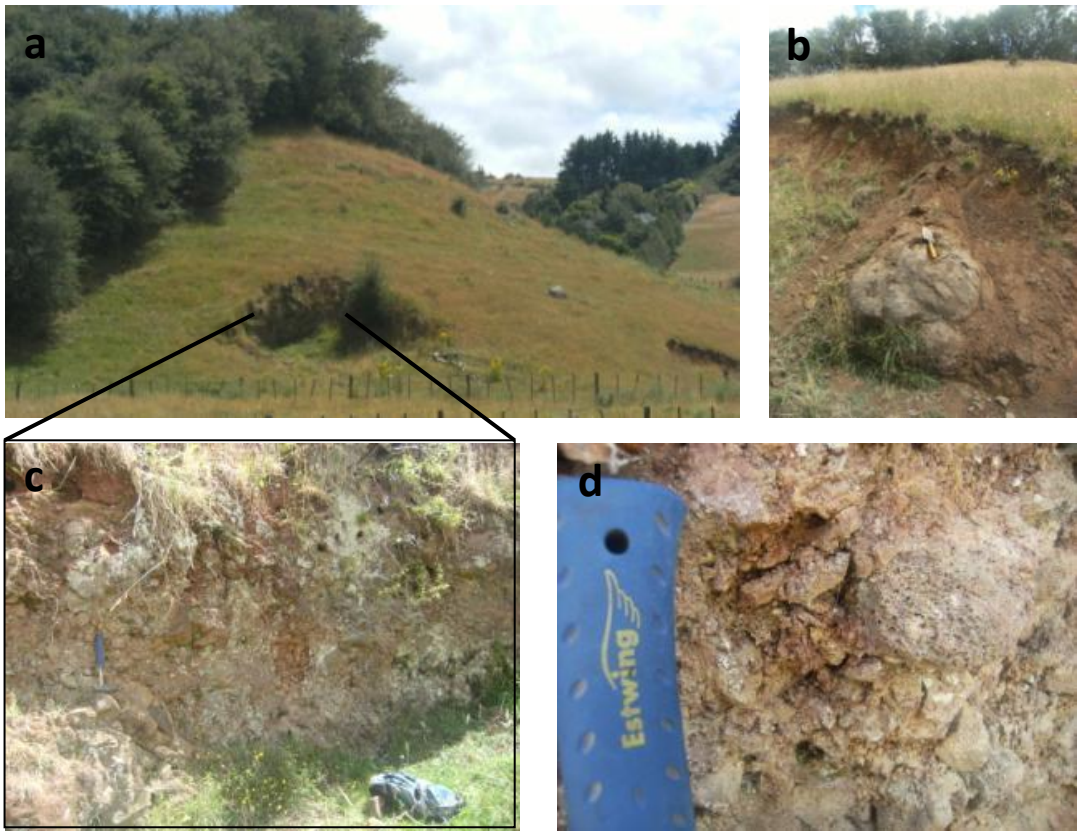

Figure 3.10: (a) School Hill scoria cone (locality 5); (b) basalt lava flow at base of scoria cones; (c) exposed scoria outcrop, hammer is 33 cm long; (d) Closer view of scoria outcrop, hammer handle as scale.

3.5 Diatomite

The diatomite in Kellyville tuff ring was first identified in 1967, and Winstone Aggregates later studied the deposit in detail in 1972 using drill logs (Waterhouse 1980). Winstone Aggregates drilled more than 30 holes up to 21 m deep (Waterhouse 1980) both north and south of Koheroa Road, and 27 of these drilled into diatomite.

Figure 3.11: (a) Diatomite in outcrop; (b) Variations in colour and layering, darker layers are rich in sediment and organic matter (sample W2011536).

Winstone Aggregates was later asked to carry out a study of the Mercer diatomite deposit (Fig. 3.11a,b) as part of the New Zealand Geological Survey, as DSIR was attempting to map the occurrences of diatomite in and around Auckland (Waterhouse 1980). This was to be used in cement if the diatomite deposit was large enough to be economically viable, and contained greater than 90% SiO_2. Three holes 10-12 m deep were drilled as well as 25 holes approximately 1m deep. All holes intersected interbedded diatomite and pumiceous material, underlain by sandstones and siltstones (Waterhouse 1980), possibly of the underlying Waitemata Group. North of Koheroa Road was an average of 8.45 m thickness of this deposit. South of the road was an average of 8 m of the deposit. Bulk deposits were taken to analyse the chemistry of the diatomite, which was found to be no more than 80% SiO_2 in composition. According to a study of the tuff ring by Colchester (1968) the diatomite here is intercalated with pumice deposits. According to Waterhouse (1980) pumice and ash deposits were deposited by the lake within the tuff ring or by the Waikato River through the rim breach. Due to these interbedded pumiceous deposits, any quarrying of this diatomite deposit would have to include sorting and separation of the pumice from the diatomite. This would be a difficult and lengthy process and was ultimately decided by Winstone Aggregates not to be viable for quarrying.

In this study, diatomite was found exposed along Koheroa Road along a 155 m long section (locality 7, Fig. 3.7). At its eastern end approximately 3.5 m is exposed, further west the deposit is exposed for 2 m, and at its western end closest to the Glass Hill scoria cone, 3 m is exposed. Diatomite was also seen just southeast of School Hill, suggesting its widespread occurrence; however the diatomite has largely been eroded out of the base of the tuff ring due to the breach in its rim. Diatomite samples showed very thin laminated layers of mixed sediments. Fossil leaf and seed imprints were also found between some of the diatomite layers (Fig. 3.12). Diatomite in thin section shows carbonaceous sediment as well as rounded grains of quartz.

Figure 3.12: Fossil leaf impressions in diatomite deposit from locality 7 (sample W2011537).

Scanning Electron Microscopy was used on diatomite samples in order to assist with diatom species identification. The diatom species *Stephanodiscus novae zealandiae* and *Cyclotella stelligera* found are shown below in Fig. 3.13. The freshwater diatoms have age ranges from the Cretaceous to Recent and are therefore not age determinate. Both *Stephanodiscus* and *Cyclotella stelligera*

species were also observed by Waterhouse (1980) in the diatomite deposit at Kellyville.

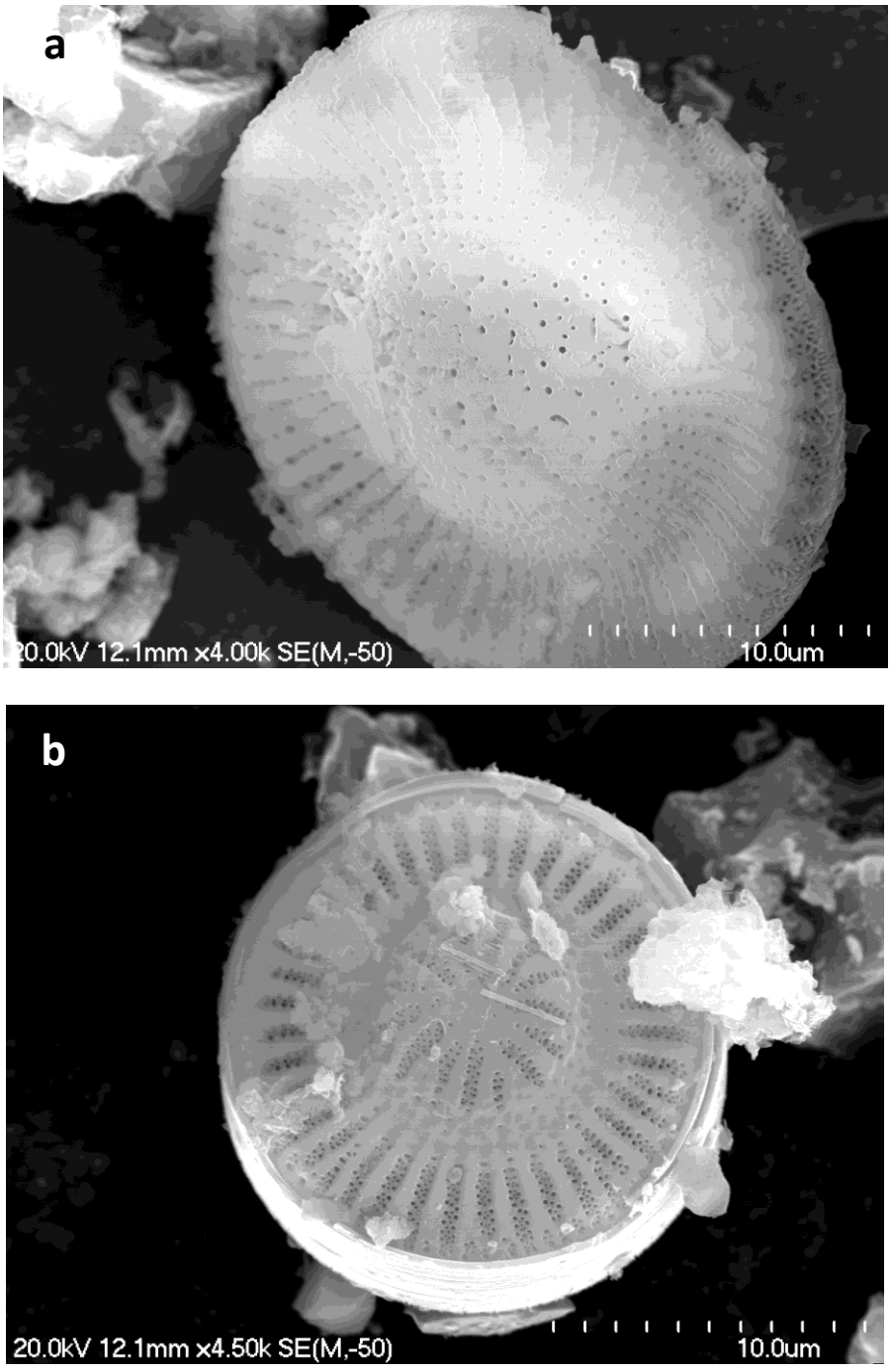

Figure 3.13: Diatomite species observed in the KVC: (a) *Stephanodiscus novae zealandiae*; (b) *Cyclotella stelligera* (pers. comm. Cooper, V. C.).

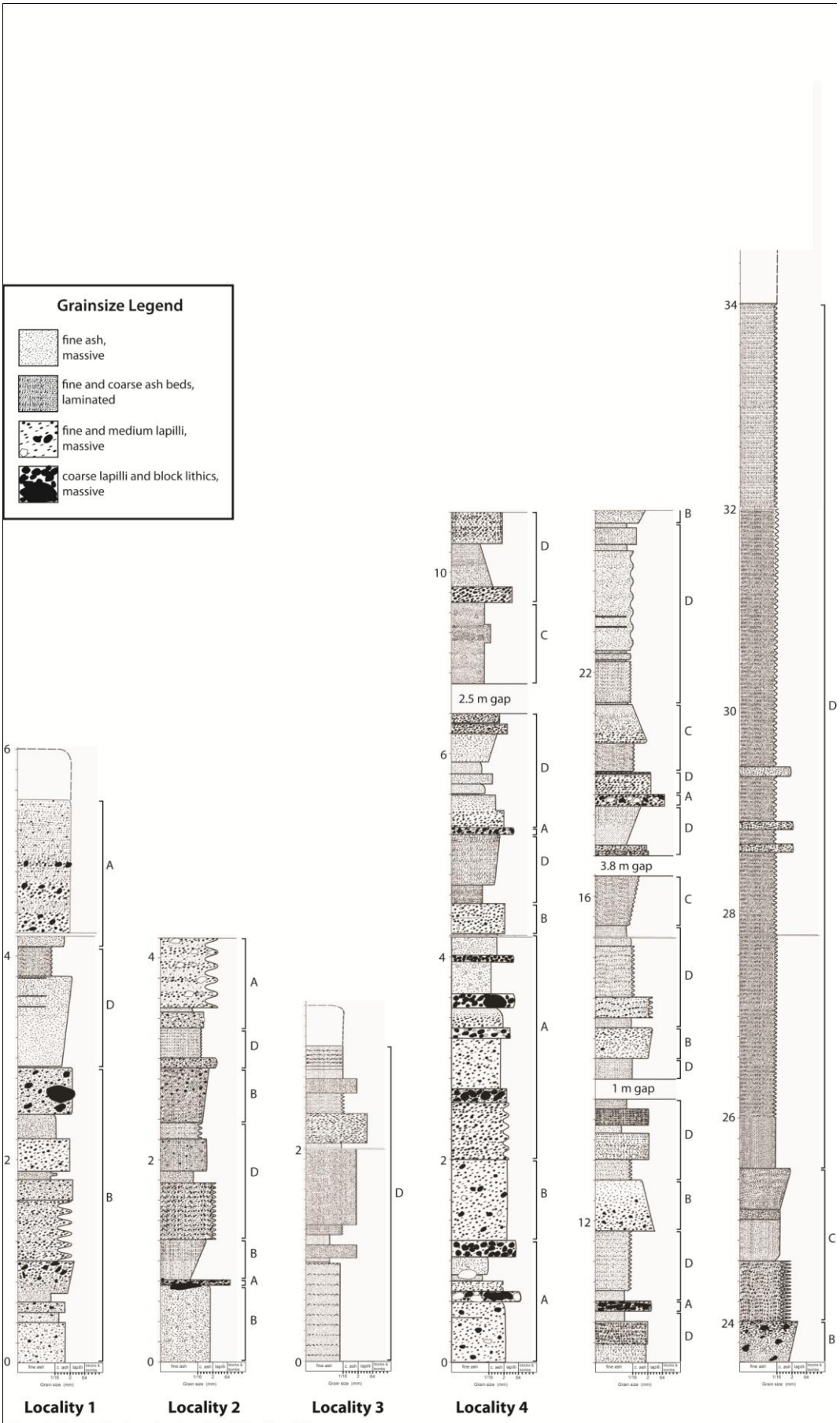

Figure 3.14: Combined stratigraphy of the Kellyville tuff ring.

3.6 Facies and stratigraphy

3.6.1 Kellyville tuff ring

The stratigraphy of the Kellyville tuff ring (Fig. 3.14) is grouped into facies. Four facies types have been recognised using field and petrological descriptions in a 60 m thick tuff ring succession (approximately 32 m is not exposed of the 92 m of tuff ring deposits). The earliest 27 m of tuff deposits alternates between a poorly to well sorted, massive to weakly bedded, lithic-rich block and bomb facies (facies A), a poorly sorted, massive, fine lapilli to block and bomb facies, present in discrete layers 30-80 cm thick (facies B), and a very well sorted, planar laminated, coarse to fine ash (facies D). From 27 m to 44 m, the tuff alternates between facies A, B, and D and a well sorted, cross-laminated, coarse to fine ash present in layers 60-150 cm thick (facies C). From 44 m to 56 m, the tuff is comprised entirely of facies D.

3.6.2 Tuff ring facies

Facies A - poorly to well sorted, massive to weakly bedded, lithic-rich blocks and bombs

Facies A (Fig. 3.15) is generally a coarse block and bomb facies. It hosts a wide range of grain sizes from fine ash to blocks and bombs and is generally weakly medium bedded with very few wavy beds, poorly to well sorted, and alternates between coarse and fine layers. Blocks and bombs occur with fine to very coarse lapilli in clast supported layers. These coarse layers (up to 20 cm thick) also occasionally consist of coarse to fine lapilli with 15% vesicular to dense sub-rounded to rounded basalt clasts (maximum clast size (Mc): 180 mm), and white lithics that show cracking and zoning (maximum lithic size (Ml): 74 mm). Scoria clasts range from coarse ash to coarse lapilli. Solitary blocks and bombs also occur within finer layers of predominantly coarse ash to fine lapilli with 2-4 cm thick bedding and fine lapilli scoria clasts, in packages up to 60 cm thick, alternating with well sorted coarse to fine lapilli, both scoria and lithics, with medium bedding, and one fine ash layer. The blocks and bombs commonly

have impacted into underlying layers, and some show features where the path of subsequent surge transported material has been blocked by the impacted ballistic block or bomb (Fig. 3.18). Blocks consist of both vesicular and dense basalt (Mc: 85 mm). Sedimentary lithics are sandstone and siltstone (Ml: 330 mm), and range in grain size from coarse lapilli (Ml: 21 mm) to very coarse lapilli (Ml: 63 mm). The sedimentary lithic blocks are commonly sub-rounded to rounded. A singular light grey-brown thinly bedded fine ash layer is intercalated with coarse ash and contains coarse ash scoria fragments. Facies A exhibits a basalt bomb within lapilli showing ballistic direction, which can be seen in Fig. 3.16 below. The feature is surrounded by fine ash fall layers.

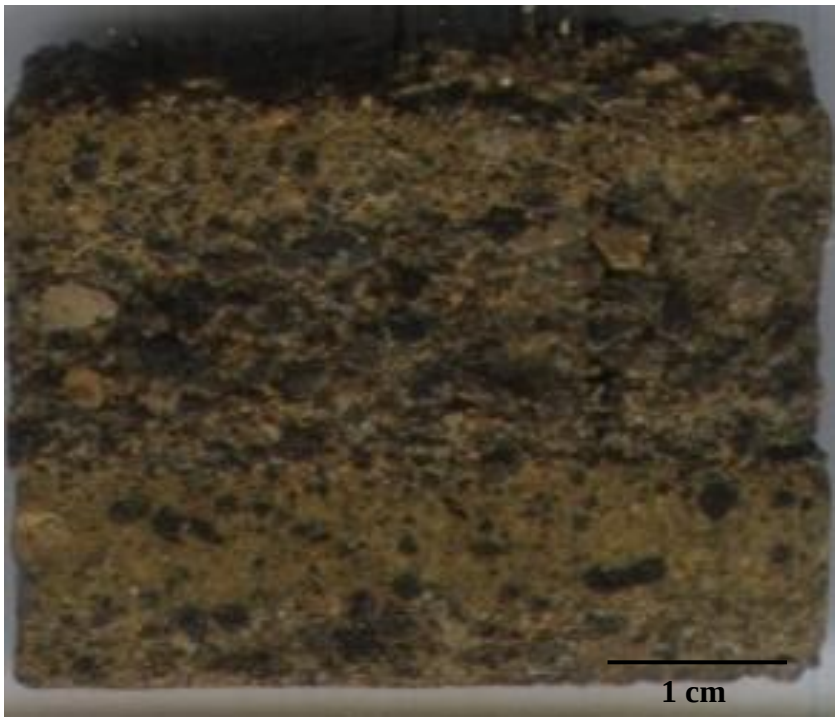

Figure 3.15: Sample of facies A deposits with fine lapilli clasts and lithics and coarse ash (sample W2011508).

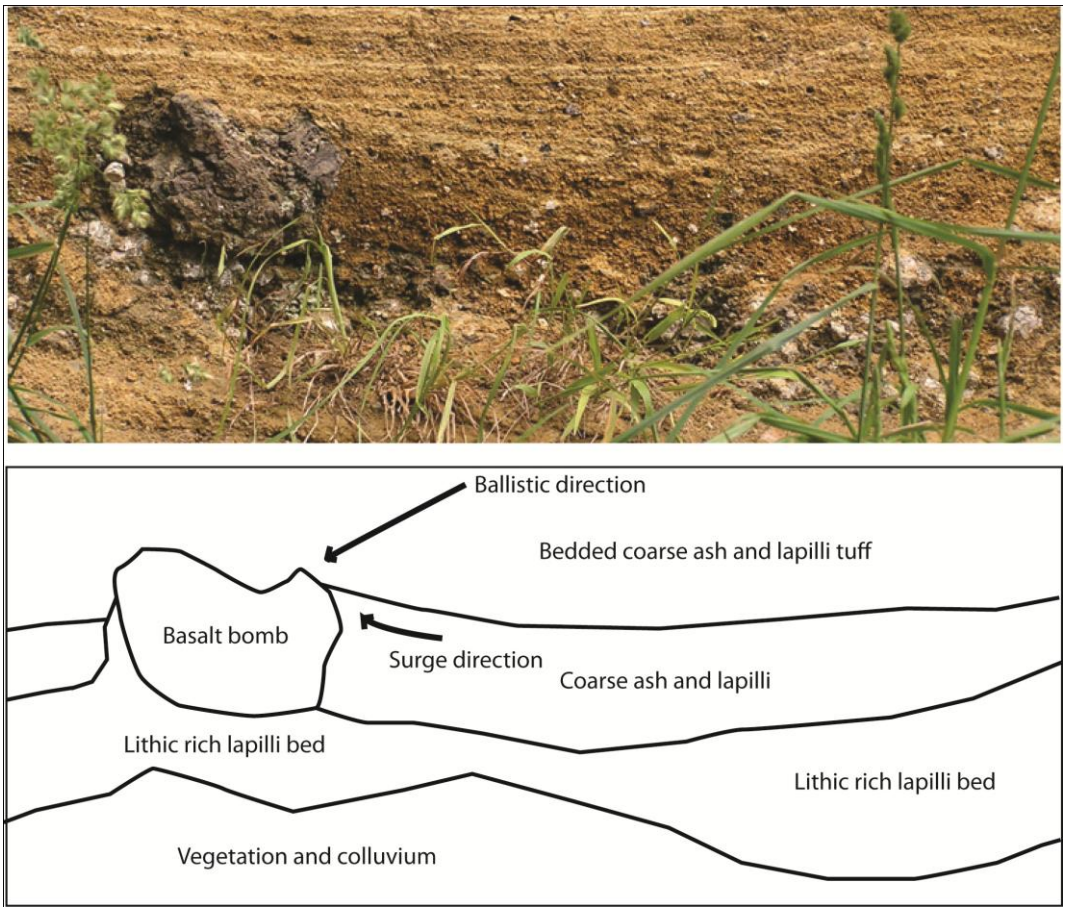

Figure 3.16: Basalt bomb in facies A showing ballistic direction.

Facies B- poorly sorted, massive, fine lapilli to blocks and bombs

Facies B (Fig. 3.17, 3.18) is a massive to diffusely bedded, poorly sorted fine to medium lapilli to block and bomb scoria facies. The facies forms medium to thick beds (10 – 80 cm). Some coarse lapilli occur as both siltstone and sandstone lithics (Ml: 46 mm) and basalt clasts (Mc: 23 mm). Sub-angular to rounded siltstone and sandstone lithics (Ml: 90 mm) and vesicular and dense angular basalt clasts (Mc: 43 mm) also occur within the finer lapilli. Normal grading occurs in diffuse beds ranging from fine lapilli to fine ash. Reverse grading occurs as diffusely bedded coarse ash coarsening upwards to fine and medium lapilli, with an abrupt upper contact. The exceptions in this facies are occasional well sorted, very fine ash to coarse ash layers.

Figure 3.17: Facies B in outcrop showing fine to coarse lapilli clasts and lithics and coarse ash, locality 2. Geological hammer handle is 3.2 cm across.

Figure 3.18: Facies B sample showing ash and lapilli layers with common juvenile clasts (sample W2011582).

Facies C- well sorted, cross-laminated, coarse to fine ash

Facies C is a cross bedded, fine to coarse ash to fine lapilli facies (Fig. 3.19). It is characterised by thin to laminated low angle cross beds and wavy lensoidal beds that pinch out, in 60 - 150 mm thick packages. This facies is generally well sorted and normally graded. Cross bedded, coarse ash beds commonly contain fine scoria and dark grey, dense (slightly vesicular) basalt lapilli clasts (Mc: 47.2 mm) and occasional coarse lapilli. Ash beds are up to 10 mm thick and coarsen upwards to coarse ash cross beds 7- 25 mm thick that pinch out. Beds of very fine cemented lapilli grade upwards to laminated, slightly cross bedded, fine to coarse ash.

Figure 3.19: Facies C in outcrop showing cross-beds and direction of transport, at locality 4.

Facies D- very well sorted, planar laminated, coarse to fine ash

Facies D is responsible for the thickest amount of deposit in the exposed sections of the Kellyville tuff ring. Facies D is mostly comprised of very well sorted, fine and coarse ash layer couples 7 – 10 cm thick, with occasional fine to medium scoria rich lapilli beds (Fig. 3.20, 3.21). These coarser beds can

occasionally be planar laminated, very fine lapilli with very thin to thin bedding, and also occasionally show reverse grading from very fine lapilli to fine lapilli. In general, the facies is thinly to very thinly bedded to laminated, with some wavy laminated beds. The fine ash beds are light brown to white, very finely laminated to massive and approximately 10-15 mm thick. The coarse ash beds show thin and sometimes wavy bedding, with occasional reverse grading, in thicker (40-70 cm) layers. Solitary coarse lapilli to blocks or bombs occur within the coarse and fine ash beds, some with sag or build-up features into the underlying layers.

Figure 3.20: Alternating fine and coarse ash fall and surge beds, some show low angle cross bedding and others are continuous. The vent is to the right, scraper is 28 cm long.

Figure 3.21: Alternating fine and coarse ash fall and surge beds, some show low angle cross bedding and others are continuous. Direction of flow is shown by arrow. Photo is looking south and the vent is to the right. Scraper is 28 cm long.

3.6.3 Tuff ring facies stratigraphy

Three sections through the Kellyville tuff ring have enabled a composite stratigraphy to be constructed (Fig. 3.14). These sections are all to the east of where the vent would have been during the phreatomagmatic eruption.

There is one exposed section through the southern part of the Kellyville tuff ring (locality 3) that is at a similar elevation to that of the other exposed sections present, and indicates some of the lateral changes in facies architecture of the tuff ring (Fig. 3.14). The exposed section is to the south of where the vent would have been during the phreatomagmatic eruption (Fig. 3.7). Locality 3 is entirely facies D, and appears very similar to the stratigraphic section observed at locality 4.

3.6.4 Scoria cone facies

Facies E – Scoria cones

Kellyville facies E consists of highly vesicular scoria lapilli, agglutinated at its base. School Hill scoria cone (locality 5) provided the only representative section, about 2.6 m high (Fig. 3.22). Samples were taken from both scoria cones and these are discussed below. At the base of School Hill scoria cone, up to 0.9 m, the scoria was vesicular (up to 3 mm) red-brown and clasts were strongly welded together, so that their outlines were hard to identify. The scoria was mainly massive to diffusely bedded. Mid-way up the section, from 0.9 to 1.95 m, the scoria was light to medium grey and red-brown, with angular clasts of fine and medium lapilli (Mc: 5.4 mm) to coarsest lapilli (Mc: 43 mm) and angular scoria blocks (Mc: 117 mm). At the top of the exposed scoria section, from 1.95 to 2.4 m, the scoria was red-brown and clasts were predominantly fine lapilli size, with few coarse lapilli (Mc: 43 mm) and few blocks (Mc: 118mm). The upper 20 cm was covered in soil.

School Hill scoria cone shows a lower vesicularity and higher density closer to the top of the exposed section, and a higher vesicularity and lower density towards the base (Fig. 3.23). Vesicularity and density of samples from Glass Hill scoria cone and School Hill scoria cone are listed in the below Table 3.1.

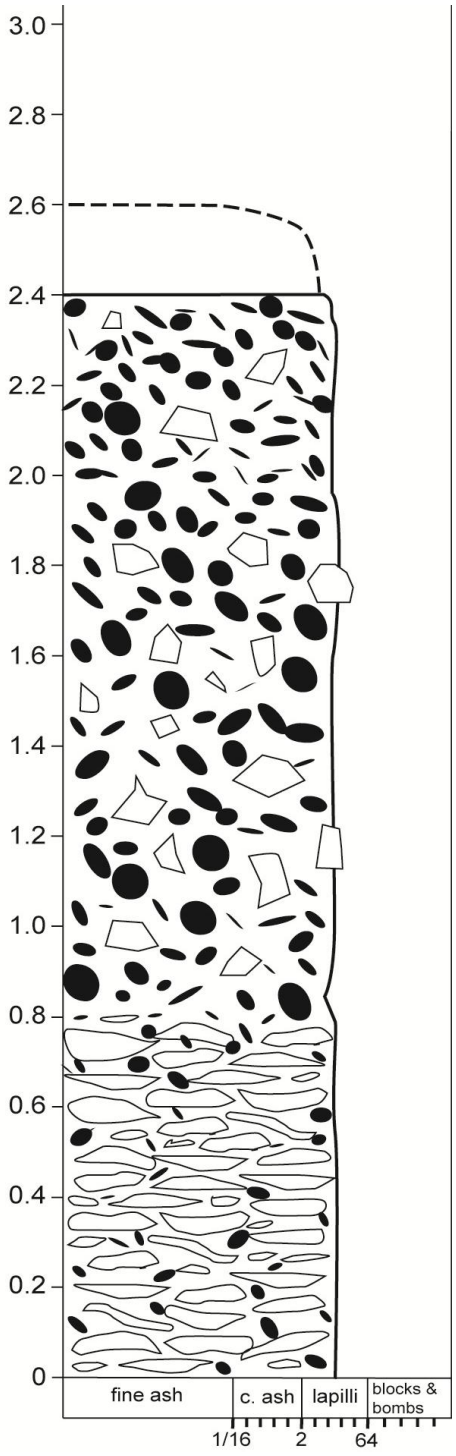

Figure 3.22: Stratigraphic log of exposed scoria outcrop from School Hill scoria cone. Exposed outcrop is 2.6 m high.

Table 3.1: Mean vesicularity and density of Glass Hill (locality 6) and School Hill (locality 5) scoria cones with height.

Scoria cone height	Mean vesicularity %	Mean density g cm^{-3}
Glass Hill scoria cone		
Top	34.18	1.97
Middle	55.57	1.33
Base	39.64	1.81
School Hill scoria cone		
Top	73.30	0.80
Middle	64.68	1.06
Base	63.55	1.09
Flow	34.23	1.97

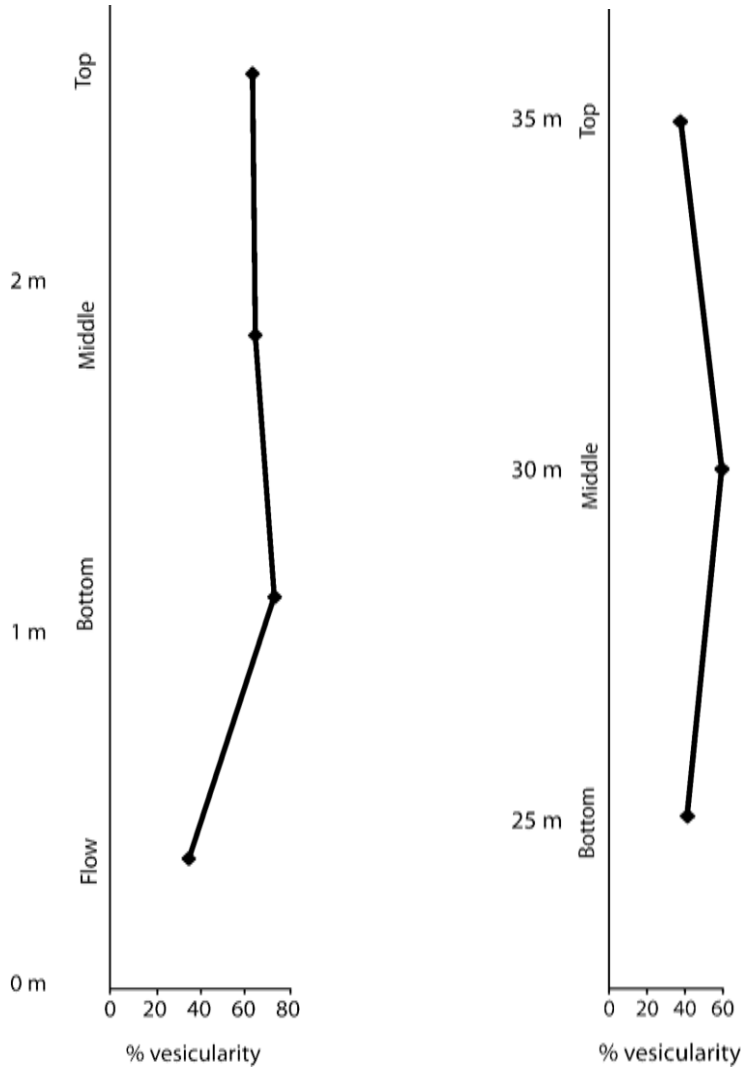

Figure 3.23: Changes in vesicularity with height within School Hill (left) and Glass Hill (right) scoria cones.

Scanning electron microscopy was used on small scoria samples in order to examine the vesicle size and structures. Vapour-phase altered vesicle textures and crystal formations were also observed during this analysis (Fig. 3.24).

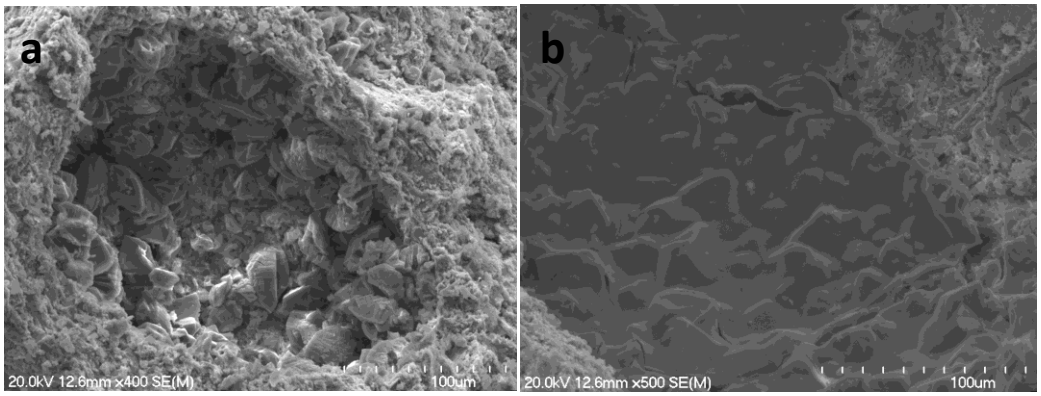

Figure 3.24: Inner textures of vesicles in scoria, showing a: crystal formation and b: vapour phase alteration.

3.6.5 Basalt geochemistry

The geochemistry of basalt from the Kellyville volcanic complex has been summarised in the table below (Table 3.2), and compared with the geochemistry of the two other study areas. Unaltered basalt samples were not available for XRF analysis; therefore data from Cook (2002) has been used. The $Na_2O + K_2O$ wt% have been compared to SiO_2 wt% in order to distinguish between group A and group B basalt types. In Fig. 3.25 representative data for Kellyville and Bombay tuff rings were identified as group B, however Onewhero tuff ring was not distinguished by this comparison. Fig. 3.26 compares Zr/Nb ratios with Nb (ppm), and allows data from the Onewhero tuff ring to be distinguished as group A.

Group A represents a transitional basalt to tholeiite group, and is derived from the shallow upper mantle (Cook 2002). Group B represents a basanite to hawaiite group, and is derived from the upper mantle (Cook 2002). The data below suggests that magma sources from the Kellyville and Bombay tuff rings were generated at larger depths than the magma source from the Onewhero tuff ring.

Table 3.2: XRF geochemical data of basalt from Kellyville tuff ring, with comparative data from Onewhero tuff ring and Bombay Quarry tuff ring. *KTR*: Kellyville tuff ring sample from Glass Hill quarry, *OTR*: Onewhero tuff ring sample from Kaipo Flats Road, boulder from tuff, *BQTR*: Bombay Quarry juvenile clast from tuff ring. Sample geochemistry data with labels in italics are from Cook (2002).

Sample	***KTR***	***OTR***	***BQTR***
	ne-hawaiite	alkali ol-basalt	alkali-ol basalt
Major elements			
SiO_2	43.84	46.24	48.19
TiO_2	2.68	2.25	2.29
Al_2O_3	12.66	13.73	15.32
Fe_2O_3	15.49	14.96	13.15
MnO	0.21	0.18	0.19
MgO	7.56	10.05	6.36
CaO	9.41	9.47	7.98
Na_2O	3.31	3.14	3.91
K_2O	1.43	0.73	2.03
P_2O_5	1.19	0.35	0.79
Total	97.78	101.10	100.21
LOI	1.93	-0.94	0.90
Trace elements			
Sc	17	24	16
V	189	227	177
Cr	128	278	159
Ni	110	181	90
Cu	54	65	58
Zn	148	100	129
Ga	23	23	27
As	2.1	1.3	-
Rb	17	12	33
Sr	1171	387	1300
Y	34	21	32
Zr	315	130	410
Nb	60	18	65
Ba	328	120	548
La	76	15	52
Pb	6.9	2.5	5.5
Ce	160	46	94
Th	6.5	1.3	6.8
U	1.4	0.1	4.4
Group	**B**	**A**	**B**

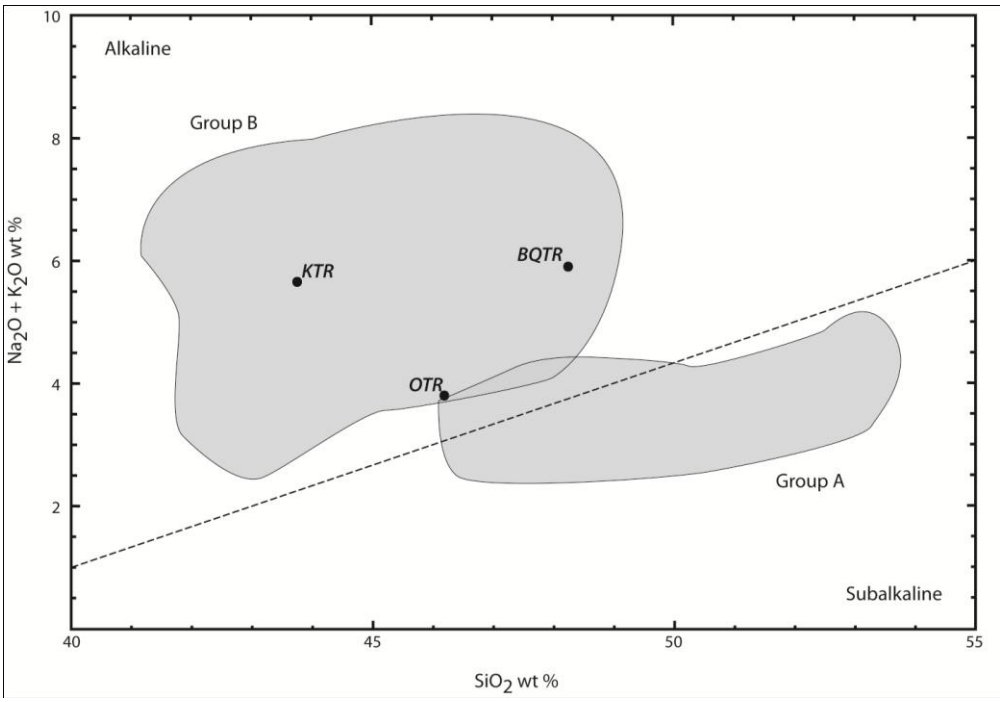

Figure 3.25: $Na_2O + K_2O$ wt% against SiO_2 wt%, with typical boundaries of Group A and B basalt from the SAVF (Cook 2002). Labels in italics are from Cook (2002).

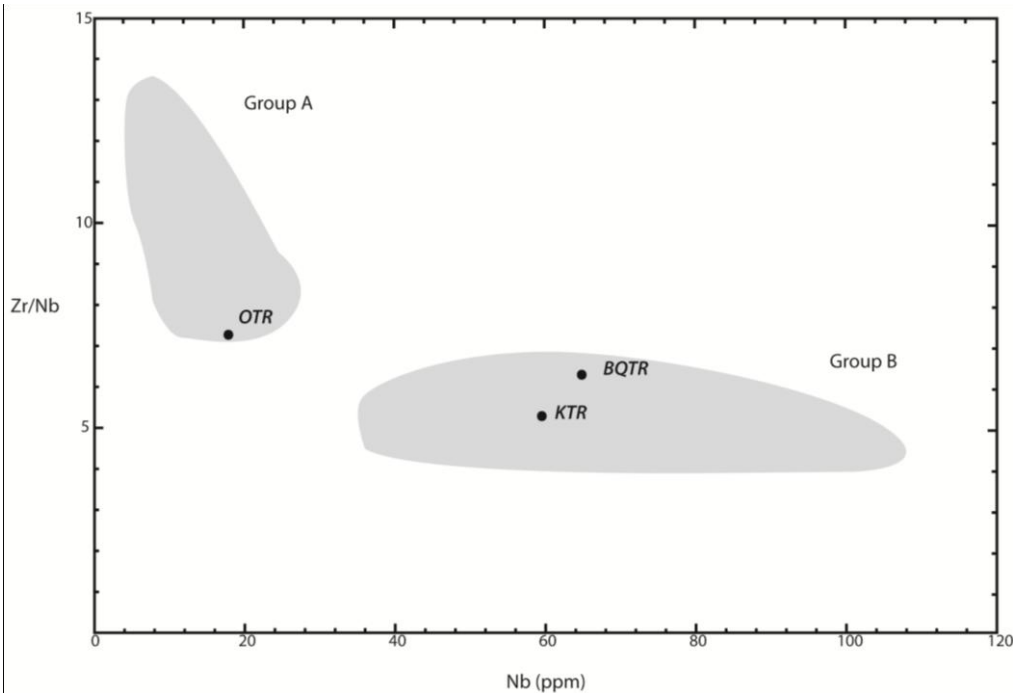

Figure 3.26: Zr/Nb ratio against Nb (ppm), with typical boundaries of Group A and B basalt from the SAVF (Cook 2002). Labels in italics are from Cook (2002).

3.7 Componentry

3.7.1 Tuff ring deposits

The tuff deposits that constitute the Kellyville tuff ring (Fig. 3.27) are comprised of a mixture of varied basaltic juvenile and lithic material, set in a matrix of lithic-rich ash and scoria shards.

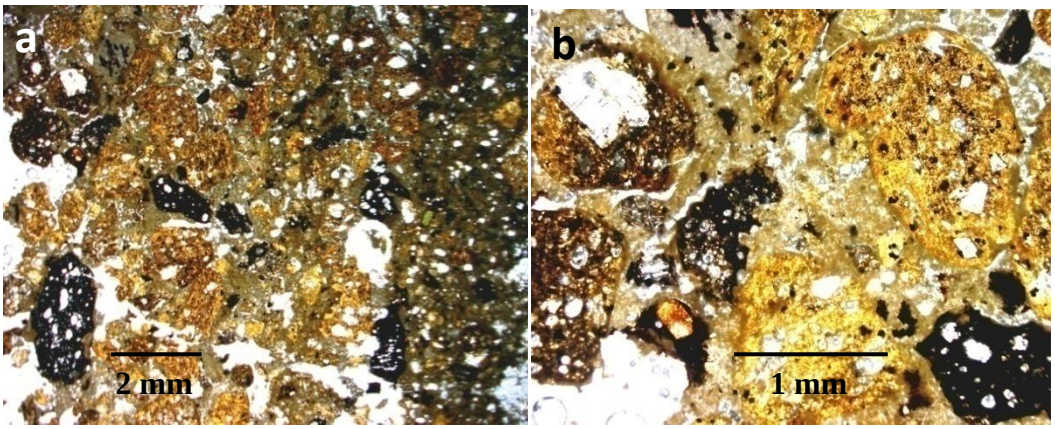

Figure 3.27: Tuff deposits viewed in thin section under PPL (a) common orange scoria clasts and vesicular basalt clasts, with lithic fragments, quartz crystals and glauconite pellets, and calcareous ash matrix; (b) orange and brown scoria clasts with olivine phenocrysts, vesicular basalt clasts, and lithic-rich ash matrix (sample W2011508).

Juvenile basalt clasts

Dense olivine basalt clasts are present throughout the Kellyville tuff deposits. In thin section, basalt clasts are sub-rounded with palagonite groundmass (Fig. 3.28). Phenocrysts include olivine and plagioclase with rare augite. The olivines are commonly altered to iddingsite and are occasionally embayed (Mc: 0.55 mm). Plagioclase is present as small phenocrysts and laths in the groundmass. Augite phenocrysts appear as purple titanaugite. Quartz lithics are occasionally present within the basalt (Mc: 0.3 mm). Some vesicles occasionally occur within the dense basalt (Mc: 0.35 mm).

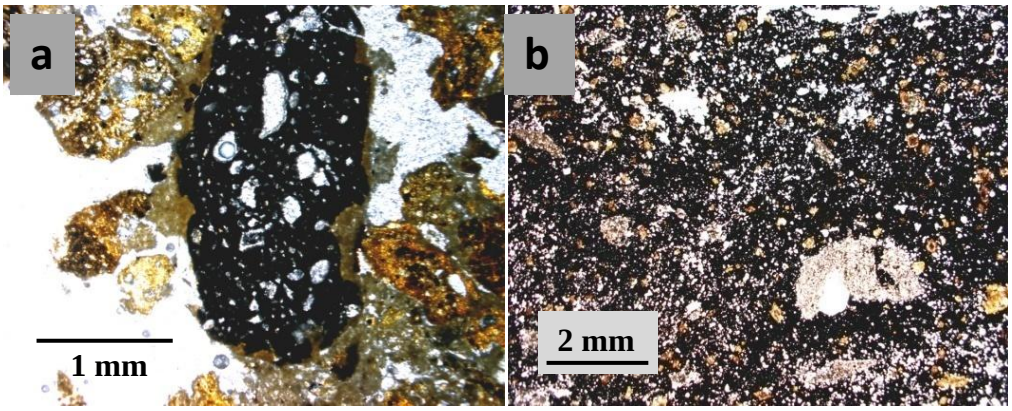

Figure 3.28: (a) Dense porphyritic olivine basalt with olivine phenocrysts (sample W2011508); (b) Olivine phenocrysts have been altered to iddingsite, and can be seen in palagonitic groundmass (sample W2011512).

Scoria

Scoria is very common, and present throughout tuff deposits from Kellyville. Two types of scoria are found in thin section, with distinguishable colour differences. Orange-yellow coloured scoria clasts are palagonite, and brown-black coloured scoria clasts are tachylite (Fig. 3.29). Some deposits are entirely composed of one type; others are mixed. Both types are rounded and mainly highly vesicular with amygdales, although vesicularity does vary. Olivine is the most common phenocryst, and is present within both types of scoria. Fresh euhedral to subhedral olivine occurs throughout the scoria, but most common are olivine variably altered to iddingsite. Some olivines have been embayed. A very large tabular olivine phenocryst was found in thin section to be 1.75 mm long. Small opaques are also present as within the groundmass, as well as small plagioclase laths. Vesicularity of scoria within the tuff deposits ranges from 30 to 55%.

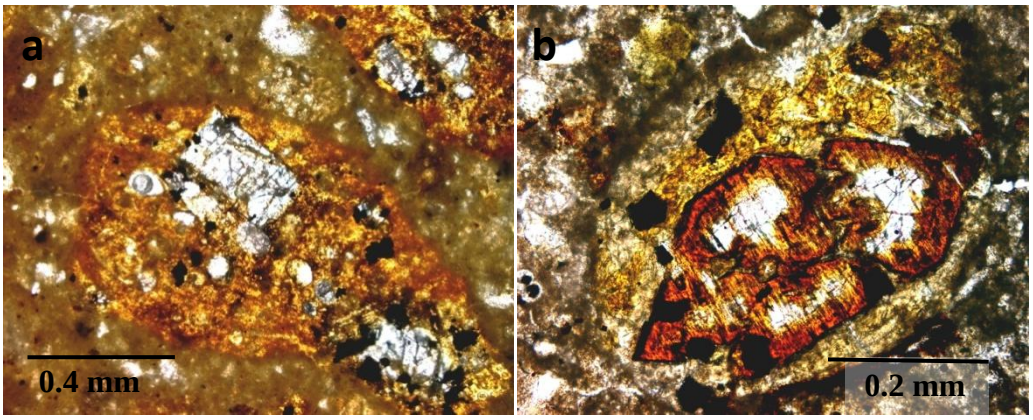

Figure 3.29: Scoria palagonite and tachylite clasts within tuff deposits (PPL): (a) hosting many large olivine phenocrysts (sample W2011505); (b) some olivine phenocrysts are partially altered to iddingsite (sample W2011529).

Crystals

Olivine is the most common crystal type present. The maximum size of olivine crystals is 0.75 mm. The olivines are very rarely fresh; most are partially or completely altered to iddingsite. Some olivines have been embayed as well as altered, giving them a slightly broken up or rounded appearance. Plagioclase crystals (Fig. 3.29) were also present in tuff deposits from Kellyville, but are much less common than olivine. The maximum size of plagioclase crystals is 0.05 mm. Most plagioclase crystals are lath-shaped. The largest plagioclase found is over 1 mm in length and had once been tabular in shape (Fig. 3.30).

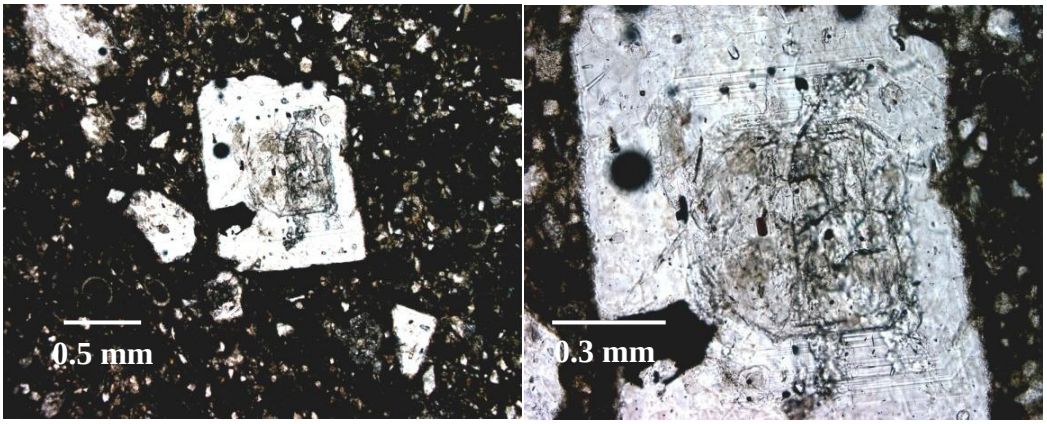

Figure 3.30: Large, zoned, embayed plagioclase crystal within tuff deposit (sample W2011517).

Lithics

Two main types of lithics were observed in tuff deposits from Kellyville. Koheroa Siltstone has a matrix of fine calcareous mud and with angular quartz and small broken calcite crystals (Fig. 3.31). Fossils were uncommon, suggesting excavation of a fossil-poor level. Uncommon *Globigerina sp*., *Globigerinoides sp*., and *Hoegludina elegans* were found. The largest lithic fragment of this type found in thin section was 11 mm long. Mercer Sandstone has a fine, calcareous mud matrix. The lithic has abundant subhedral to euhedral quartz up to 0.1 mm, plagioclase (some very large zoned crystals) and calcite crystals. Compacted *Astrononian sp*., *Gynindinia sp*. and unidentified foraminifera were found as well as echinoderm fossils. Glauconite pellets were common.

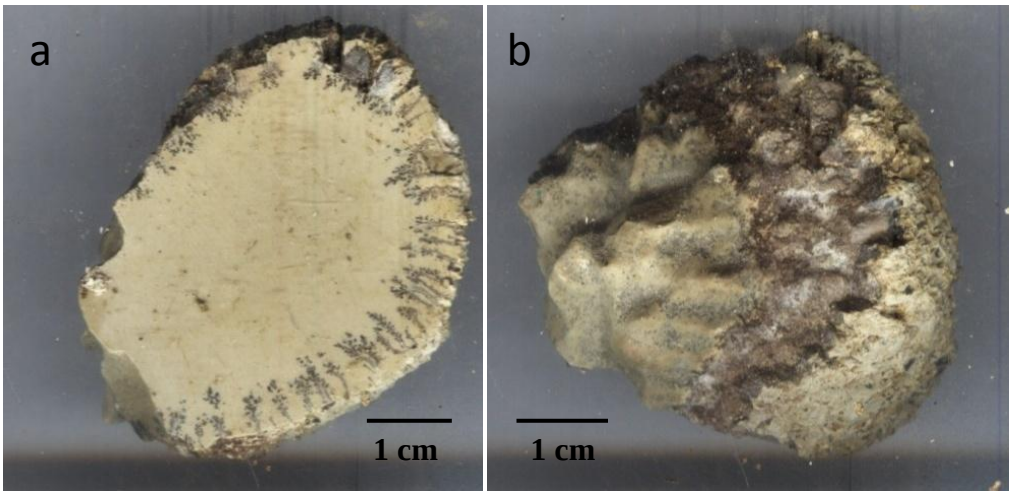

Figure 3.31: Koheroa Siltstone lithic lapilli and block samples; (a) heat penetration of the lithics; (b) heat-altered outer textures (sample W2011615).

3.7.2 Scoria cone deposits

Scoria is the only clast type in both Glass Hill and School Hill scoria cones, and phenocrysts are euhedral to subhedral altered olivines. Some have been shattered, and some have been weathered to the extent that they are wearing away and rims have turned brown. Plagioclase laths are also very common phenocrysts in juvenile scoria clasts in both scoria cones. Glass Hill groundmass is glass with small plagioclase laths. School Hill glass groundmass is highly altered and appears red. Scoria vesicles are commonly infilled with secondary material either

as inner vesicle fringes or entire vesicle infills (Fig. 3.32). The infilling material can be either clear and appear needle-like, or brown in colour. The basalt flow (Fig. 3.33) from School Hill scoria cone has many plagioclase laths and altered olivines within a highly altered glass groundmass.

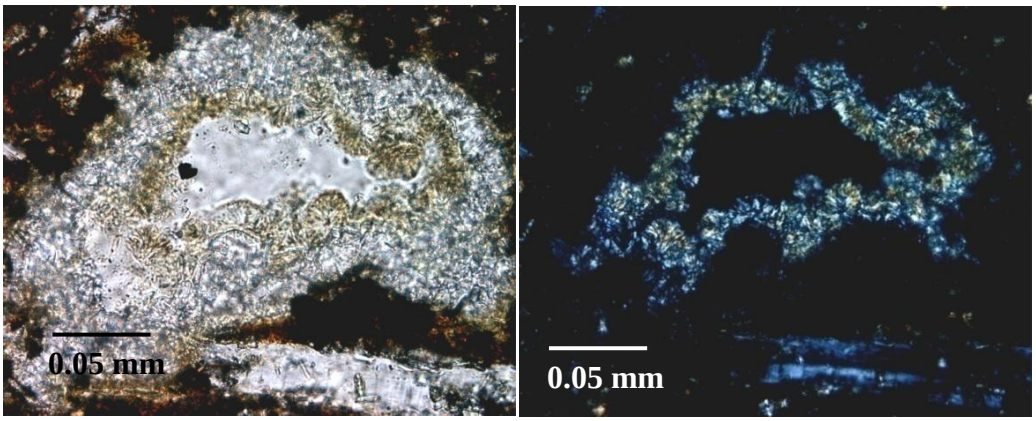

Figure 3.32: Scoria from School Hill scoria cone with infilled vesicles showing secondary minerals (PPL left, XPL right) (sample W2011622).

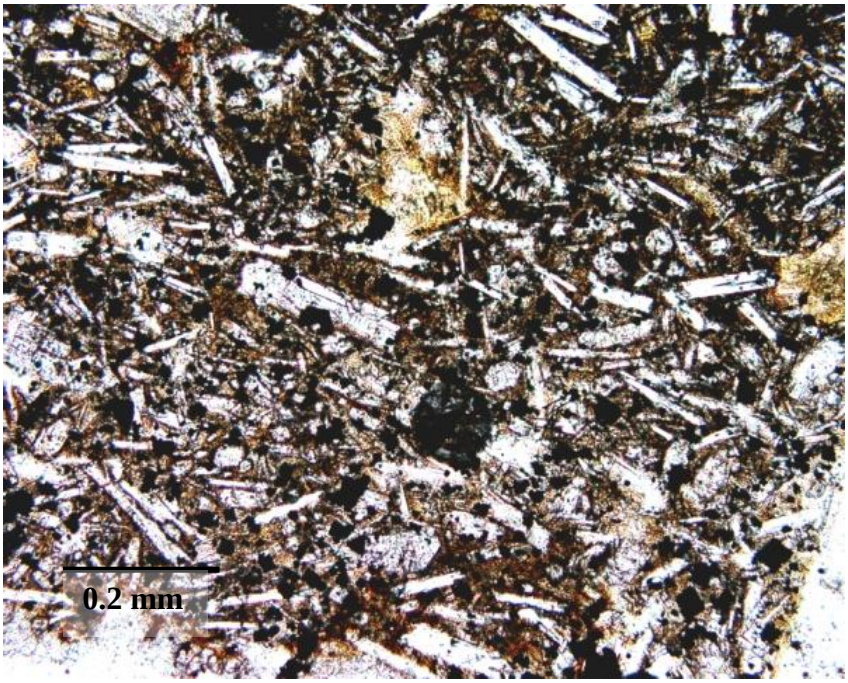

Figure 3.33: Basalt flow from School Hill scoria cone, with abundant plagioclase laths in a crystalline groundmass of plagioclase and olivine (sample W2011552).

3.8 Stratigraphic variation

The deposits of Kellyville tuff ring show many variations through their stratigraphy which reflect progressive changes in eruption. Grainsize varies a great deal throughout the tuff ring, and these variations are evident in Fig. 3.34 below. Despite the variation and gaps within the stratigraphic record, general trends are evident. Coarse material such as medium to coarse lapilli and blocks and bombs occur almost throughout the record, however these are concentrated mostly at the beginning and middle of the stratigraphic sections. Fine material such as coarse and fine ash is present throughout the entire tuff ring. A general trend can be seen where grain size appears to gradually decrease overall with stratigraphic height. Componentry of the tuff ring deposits is shown in Fig. 3.34. Juvenile material of scoria, dense basalt, and crystals are mostly dominant (over 60%) throughout the tuff ring. There are some exceptions to this where lithic material is dominant. Lithic material includes Mercer Sandstone and Koheroa Siltstone. There are sharp increases in lithic material at 30 m, 35 m and 48 m, indicating an increase in water content in the eruption (Houghton *et al.* 2000). Vesicularity of the juvenile clasts within the tuff deposits is illustrated in Fig. 3.34. Vesicularity shows a general increasing trend in the first 5 m of outcrop from 30 % to 55%. The vesicularity then generally decreases from 55% to 30%. Lithic type varies throughout the stratigraphic record of the tuff ring (Fig. 3.34). Mercer Sandstone is more porous than Koheroa Siltstone. Mercer Sandstone is therefore the expected lithic to occur within the tuff ring deposits as it should be the easiest to fragment and is a more likely source of external water. Increases in the shallow Mercer Sandstone occur throughout the exposed stratigraphic record, indicating widening of the vent. Early on in the stratigraphic record from 0–25 m, both Mercer Sandstone and Koheroa Siltstone are present in the lithic material within the tuff. Mercer Sandstone is the dominant lithic type at this stage, at 80-90%. This continues up the tuff ring exposures from 30-35 m, 36-45 m, and 46-60 m with variations in the amount of Mercer Sandstone lithic from between 60 to 100% (Koheroa Siltstone therefore varies from between 40 to 0%). Approximately half way through the exposed tuff ring section at 27 m a large fluctuation in lithic composition occurs within the deposits, where Koheroa Siltstone is entirely dominant. Mercer Sandstone then returns to being the

dominant lithic type in the deposits, at 26 m, 28-30 m, 36 and 45 m, with fluctuations between 60 to 100%. Another large fluctuation occurs close to the top of the exposed tuff ring, where the Koheroa Siltstone is dominant at 50 m. The deposits then return to being mostly dominated by Mercer Sandstone until the top of the exposed outcrop.

3.9 Discussion

3.9.1 Is Kellyville a tuff ring or a maar?

There are many similarities between tuff rings and maars and their classification can be difficult to ascertain. Tuff rings and maars are both formed by phreatomagmatic volcanic activity in the form of Surtseyan eruptions when magma interacts with some form of groundwater or surface water reservoir. These can later be followed by other magmatic-type eruptions. Both are more explosive than tuff cone eruptions, have large, circular (Francis & Oppenheimer 2004) crater diameters of similar size, that range between 750 and 1750 m in diameter (Fisher & Schmincke 1984; Francis & Oppenheimer 2004), with diameters up to 3 km (Cas & Wright 1987). In the nearby Auckland volcanic field, maars have diameters of 0.3 to 0.8 km, and tuff rings have typical diameters of 1 to 2.2 km (Cassidy *et al.* 2007). Both have a small ejecta volume in comparison to tuff cones. Tuff rings and maars are present only where there is enough water to produce a phreatomagmatic eruption in the right conditions. Erosion of the rim increases the diameter of tuff rings and maars and sedimentation in lakes decreases their depth. Both can form deposits from air fall and surges, with accretionary lapilli and bomb sags. Both can form up to 100 m thick deposits (Cas 1989).

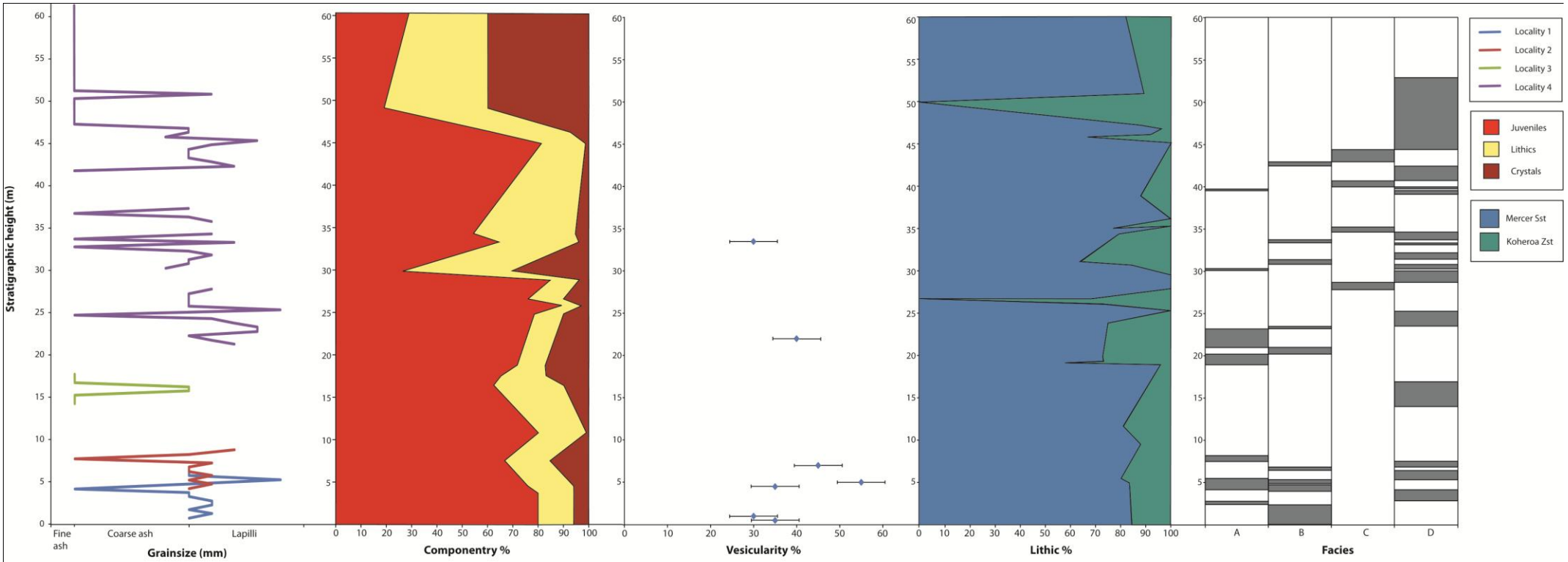

Figure 3.34 : Variation with stratigraphic height throughout the exposed tuff ring successions.
Variation from left to right includes grainsize, componentry, vesicularity of juvenile clasts within tuff deposits, lithic type and facies.

Tuff rings are generally features with positive relief and higher profiles than those of maars (Cas 1989) that have been built up above the surface. They are characteristically rich (90-100%) in magmatic material such as highly fragmented scoria and accumulations of Surtseyan tephra (Cas & Wright 1987; Francis & Oppenheimer 2004). Tuff rings have inner floor levels equal to or higher than the surrounding land elevations (Cas & Wright 1987; Manville *et al.* 2009). Tuff rings typically have steep inner and outer slopes that are approximately equal (Cas & Wright 1987). Inner dipping beds are a common occurrence of tuff rings (Cas 1989). Tuff rings can also form scoria cone complexes (Cas 1989). Tuff rings evolve through an explosive coarse stage to a stage with dominant thinly-bedded surge deposits (Wohletz & Sheridan 1983).

Despite the fact that maars are well known for their formation of lakes, tuff rings can also form lakes given the right conditions, for example Diamond Head tuff ring in Honolulu, Hawaii (Francis & Oppenheimer 2004).

Maars are generally features of negative relief and lower profiles (Cas 1989) that those of tuff rings (Francis & Oppenheimer 2004). Maar deposits are characteristically poor in magmatic material (Francis & Oppenheimer 2004) but can range from 0 to 100% (Cas & Wright 1987). The deposits are commonly rich in lithic material which can dominate the deposits. Maars have inner floors that are lower than the surrounding ground elevations (Cas 1989; Manville *et al.* 2009), and are literally holes in the ground instead of structures built up above it, due to the excavating nature of the explosions that formed them (Francis & Oppenheimer 2004). Maars can be between 10 and 500 m deep (Fisher & Schmincke 1984; Lorenz 2003; Francis & Oppenheimer 2004). They have low rims of ejected material with inner slopes that are steep enough (sometimes vertical) to expose the underlying country rock (Cas & Wright 1987; Cas 1989) when fresh, but typically quickly erode to much lesser slopes (Francis & Oppenheimer 2004). Outer slopes are typically very gentle with little to no inwards dipping beds in the deposits (Cas & Wright 1987; Lorenz 2003) Due to their negative relief, maars very commonly form lakes. Maars can also form scoria cone complexes.

Kellyville tuff ring has an inner floor that is approximately 10-12 m higher than that of the surrounding land elevation, however this difference can be accounted for by the 8 m of deposition of diatomite and carbonaceous lake sediments. This suggests that the original elevation of the inner floor of the crater was either equal to, or less than the surrounding land elevations. Kellyville tuff ring has a tuff thickness of 92 m today, which would have been the minimum of the original tuff ring thickness. Both maars and tuff rings can have rims up to 100 m thick. Kellyville also formed a lake within it, which is more common in maars but can also occur in tuff rings.

Deposits from Kellyville tuff ring have many coarse lithic-rich layers and the fine material is commonly lithic-dominated, but the majority are still juvenile (scoria)-rich. Due to the dominant nature of the juvenile clasts and the build-up of a thick ring of pyroclastic material, Kellyville is most likely to be a tuff ring.

3.9.2 Emplacement processes

Facies A represents unsteady vent-clearing stages with pulses of large lithic-rich ballistic blocks that have been ripped from the vent and deposited roughly around the crater during explosions within the country rock as the magma interacted with external water (Németh & White 2003; Nemeth *et al.* 2008). Facies A is dominated by coarse, poorly sorted lithic-rich fall deposits. Many of these poorly sorted deposits have no bedding, representing a sustained part of the eruption (Houghton *et al.* 2000). Poor sorting reflected by a mix of fine and coarse clasts can be due to wet eruptions causing the early flushing of fine material from phreatomagmatic eruption clouds, which then is deposited by rapid fallout at the same speed and time as the denser, larger material (Houghton *et al.* 2000; Németh & White 2003). This can also be caused by differing ejection angles. Some deposits have weak bedding, caused by variation in the fallout rate (Németh & White 2003). This represents very fast deposition from fallout of eruption plumes or highly concentrated base surges (Németh & White 2003) and an intermittent eruption with pulsing intensity (Houghton *et al.* 2000). Both Mercer Sandstone and Koheroa Siltstone are present suggesting unstable vent conditions (Németh & White 2003); however Mercer Sandstone is the most common lithic

type within the deposits of this facies. The fragmentation depth is therefore close to the surface. The high lithic content of this repetitive stage in the eruption represents the increased intensity of the eruption and the low stability of the sedimentary rocks that formed the vent walls, as well as the increased level of interaction between their water source and the rising magma (Németh & White 2003). Lithic blocks appear sub-rounded to rounded, due to abrasion as they were transported from their source, up through the vent. Large angular basalt blocks also occur in this facies, and originated from solid basalt perhaps originating from the lining of the pre-eruption vent, or cooled juvenile material from very early on in the eruption. Some sub-rounded basalt bombs are also present in this facies, rounded due to fluidal movement and rotation with ballistic transport. Basalt blocks and bombs commonly have impacted into underlying layers, and some show features where the path of subsequent surge transported coarse ash and lapilli have been blocked by the impacted ballistic block or bomb (Fig. 3.18). Flow direction of the surge can be ascertained as material will have been deposited on one side of the impacted ballistic and not the other. Once the coarse ash and lapilli have been deposited up to the height of the ballistic block or bomb, the surge transported material will flow over it, leaving a lower level of deposit on the other side. The coarse nature of the juvenile clasts within this facies represents a drier eruption and low efficiency of fragmentation, perhaps reflecting the energy of the eruption at this stage (cf. Houghton *et al.* 2000; Houghton & Gonnermann 2008). Occasional fine ash layers with no bedding that occur represent periods in the eruption where deposition is dominated by the fallout of finer material from the eruption column (Houghton *et al.* 2000). Occasional normally-graded beds represent a fluctuation in the energy of the eruption, or a change in the eruption column incline (Houghton *et al.* 2000).

Facies B represents varying pulses of explosive activity where lithics are being ripped from the vent walls and fragmented along with juveniles from the vent as well as the erupting magma, which is being fragmented as volatiles reach the surface and as it interacts with water-bearing sedimentary rocks. The vent is moderately stable and magmatic material is common as well as lithic material. Facies B is therefore dominated by coarse fall deposits with little sorting, comprised of a mixture of varied lithics as well as scoria and dense basalt. These

poorly sorted deposits have no bedding and represent a sustained stage in the eruption with a high water content and differing ejection angles causing the fine material to be deposited by rapid fallout at the same rate as the coarse material (Houghton *et al.* 2000; Németh & White 2003). These deposits occasionally alternate with scoria-rich ash, representing periods where deposition is primarily from fallout of the remaining eruption cloud (Houghton *et al.* 2000). Reverse grading within this facies may be caused by variations in magma-water interaction as Facies B is fall dominated, however evidence of some surges is apparent with abrupt upper contacts indicating shear zones. A sharp increase in the proportion of Koheroa Siltstone lithics occurs at 31 m, suggesting a change in vent depth caused by drawdown of the fragmentation level (cf. Houghton *et al.* 2000). Ballistic fallout of lithic blocks and juvenile basalt bombs occur.

Facies C represents steady pulses of highly fragmented material, where magma-water interaction is stable. Vent stability is reflected in the lack of very coarse and lithic-rich deposits (Nemeth *et al.* 2008). The eruption is variable at this stage, with pulsing intensity (Houghton *et al.* 2000) and is mostly dominated by juvenile material, indicating dry stages in the eruption with limited fragmentation energy (Houghton *et al.* 2000; Németh & White 2003), with the exception of 35 m, where the water content of the eruption (and the lithic proportion) increased. Facies C is dominated by cross-bedded, surge-dominated fine to coarse ash. These are mostly well sorted and very thinly bedded due to many thin surge layers. Some fine lapilli are present and the cross beds are normally graded due to gravity settling in surge layers. The cross beds pinch out and can form lenses and wavy beds. The lithic material in the deposits of this facies is dominated by the shallow Mercer Sandstone, indicating fragmentation depth is shallow. The smaller juvenile size within this facies represents a higher efficiency of fragmentation (Houghton *et al.* 2000).

Facies D represents steady pulses of highly fragmented juvenile and lithic material, where a steady rate of magma is interacting with a steady source of water. Facies D is therefore dominated by alternating, thinly bedded, very well sorted, coarse ash and fine ash couples, with occasional thin, scoria-rich fine lapilli layers. This represents alternating fall layers (finer material) and surge layers (coarser material) that pinch out and occasionally show reverse grading.

These may in part be related as surges and their overlying fall (settling) layers; however some layers are continuous enough to be individual fall layers. Some bedding may be due to changes in the fallout rate (Németh & White 2003). The vent is very stable and therefore coarser material is isolated and uncommon. The abundance of fine-grained material in this facies represents the high water content of this eruption, increasing the efficiency of phreatomagmatic fragmentation (Houghton *et al.* 2000). Two marked increases in Koheroa Siltstone occur at 26 m and 50 m, where Koheroa Siltstone is the only lithic present in the deposits, representing a downward shift in fragmentation depth (Houghton *et al.* 2000), where the vent is not being widened. A decrease in juveniles and increase in lithics also occurs within this facies towards the end of the eruption, indicating an increase in water content (Houghton *et al.* 2000).

3.9.3 Eruption history

Kellyville tuff ring is a phreatomagmatic deposit resulting from interaction of basaltic magma with a large volume of external water. The eruption that formed the Kellyville tuff ring occurred 1.48 million years ago (Briggs *et al.* 1994) and likely lasted from hours to days (Manville *et al.* 2009). The creation of the volcanic complex, including the tuff ring and both intra-tuff ring scoria cones likely lasted for weeks to years.

The eruption began as basalt magma intruded into sedimentary rocks of the Waitemata Group and towards the surface (Fig. 3.35). The rising magma reacted with both the Koheroa Siltstone and the Mercer Sandstone as the vent was first being established. At this stage the vent was unsteady and lithic blocks would have been torn away to form the vent walls as the magma reacted from the aquifer within them (Németh & White 2003; Nemeth *et al.* 2008) (Fig. 3.35). The presence of more than one type of lithic implies that the vent was unstable (Németh & White 2003). An unsteady supply rate of magma, coupled with an unsteady vent causing repetitive collapses of lithic material into the vent and therefore variations in water flow caused the explosive activity to pulsate (Houghton *et al.* 2000). This stage in the eruption is represented by facies A, B and D. Comparing juvenile and lithic proportions can provide an estimated

water/magma ratio, which can be used to estimate the efficiency of the eruption. The estimated water/magma ratio of this stage in the eruption is 0.2, suggesting that the eruption is close to being highly efficient (Wohletz & Sheridan 1983).

As the eruption progressed, the vent continued to form and excavate the surrounding country rock, causing explosive pulses to deposit lithic-rich, coarse, air-fall material around the vent. The vent passed through stages of moderate stability where juveniles from both the vent walls and magma are fragmented by water interaction and are deposited as coarse air-fall material along with the lithic material being excavated from the vent. Stages of stronger fragmentation caused finer grained material to be deposited in alternating layers of coarse ash surge and fine ash fall layers (Houghton *et al.* 2000). This may have been caused by an increase in the magma-water ratio or an increase in volatiles and explosivity. This stage in the eruption is represented by facies A, B and D. The estimated water/magma ratio of this stage is 0.3 – at which the interactions between magma and water are at the highest possible efficiency (Wohletz & Sheridan 1983).

The eruption then fluctuated between unsteady vent-clearing explosions; moderately steady pulses where both lithic and juvenile material was fragmented; stages where magma-water interaction efficiency was high; and also stages where the vent was stable and formed pulses of highly fragmented material, which were deposited by surges. This stage had many large lithic ballistics, suggesting instability in the vent (Németh & White 2003). This stage in the eruption is represented by all facies (A, B, C, and D). The estimated water/magma ratio at this stage is 1, and has a lower eruption efficiency than the earlier stages in the eruption (Wohletz & Sheridan 1983).

Towards the end of the eruption, the vent became very stable, and magma-water interaction became highly efficient. Slight pulses were represented by the alternation of surge and fall deposits within the highly fragmented material (Fig. 3.35). This last steady stage took place over perhaps a third of the time of the eruption. The majority of fine-grained material (fine and coarse ash) was lithic-rich throughout almost the entire tuff ring, due to the soft nature of the lithics as well as the water content causing fragmentation. This stage in the eruption is represented by facies D.

The cause of the end of the eruption was most likely due to a decrease in magma supply rate and a subsidence of the intruding magma body. This would have allowed the vent to fill up with surrounding sediments and erupted material, forming a diatreme. The basaltic volcanic products sampled from Kellyville tuff ring (nepheline hawaiite) can be categorised as Group B basalt (Cook 2002).

The later magmatic phase of the eruption may have occurred as a continuation of the eruption where subsurface water interaction was low enough to produce the scoria cones, either from the same vent or perhaps from a dyke that had branched off from the original vent. The magmatic phase of the eruption also may have occurred weeks to years (Houghton *et al.* 1999) after the tuff ring eruption, where a magmatic source, perhaps in the form of a dyke, intruded into the overlying sedimentary rocks and produced the two massive, highly vesicular scoria cones by Hawaiian fire fountaining. In both cases, the dyke could have originated from either a fresh magma source or the original source responsible for the phreatomagmatic eruption. As the magma type is very similar to that seen within the tuff ring basalts, the latter option is more likely. This also suggests that the time between the formation of the tuff ring and the scoria cones was small as there would have been little time for magma differentiation. The two scoria cones may have been fed from one dyke which then formed a sill and then a further dyke to form a second scoria cone 470 m away.

Vesicularity changes with height in both scoria cones are evident, and overall, scoria deposits of Glass Hill have lower vesicularity than those of School Hill. This decrease in vesicularity and associated increase in density with height suggests changes in the eruption as the cones were formed. Magma volatiles may have decreased over the phase of the eruption, decreasing the vesicularity of the scoria deposit with height. The basalt flow at the base of School Hill scoria cone has higher density and lower vesicularity than that of lowest unit in the adjacent scoria section, and may have originated from its base, as a type of clastogenic flow, or perhaps a later, less fragmented phase or lower volatiles phase towards the end of the creation of the scoria cone.

The magmatic intrusion may be controlled by a southward extension of the Drury Fault, which has been mapped out as far south as Pokeno cone, but no

further. Kellyville appears 6 km south of the mapped extent of the fault, and would intersect the fault if it does continue southward.

The location of the vent from which Kellyville tuff ring formed can be deduced from the radius of the tuff ring. School Hill scoria cone is approximately in the centre of the tuff ring, suggesting that it may represent the original vent from which the phreatomagmatic eruption occurred. This suggests that School Hill was the first scoria cone formed, followed by Glass Hill as a branch-off of the original dyke. The duration of the eruption would have been short lived (days to years) (Németh & White 2003; Nemeth *et al.* 2008).

After the tuff ring and scoria cones had been crated, a lake formed within the tuff ring and deposited 8 m of diatomite and carbonaceous lake sediments. The lake would have formed within days to months (Németh & White 2003; Nemeth *et al.* 2008), however the diatomite deposit would have formed over a much longer time. At a much later stage the tuff ring was breached on its western side by erosion caused by the Waikato River.

The highest elevation of the tuff ring rim preserved today is likely to be at least the minimum height of the original tuff ring deposit (minus the topographic height of the floor), which would have decreased over time with erosional processes. The present day tuff ring slope angles are lower than what would have been the original angles, due to erosion of the rim, as well as partial rim collapse that has occurred over time (Fig. 3.36). This is evident in the exposed section through the tuff ring rim on the eastern end of Koheroa Road, where small slump faults are visible. This suggests failure of the tuff ring rim during the eruption, or long-term failure of the rim, in towards the centre of the tuff ring. This would cause the inner slope to decrease over time. The elevation of the floor of the tuff ring will have been altered since the eruption. The original height of the floor will be at least 8 m below the height of the diatomite deposit. Sedimentation from the eroding tuff ring itself may also have contributed to the floor. As the elevation of the floor is currently approximately 10 to 12 m, this suggests that the tuff ring floor would have originally been about even with the surrounding ground level.

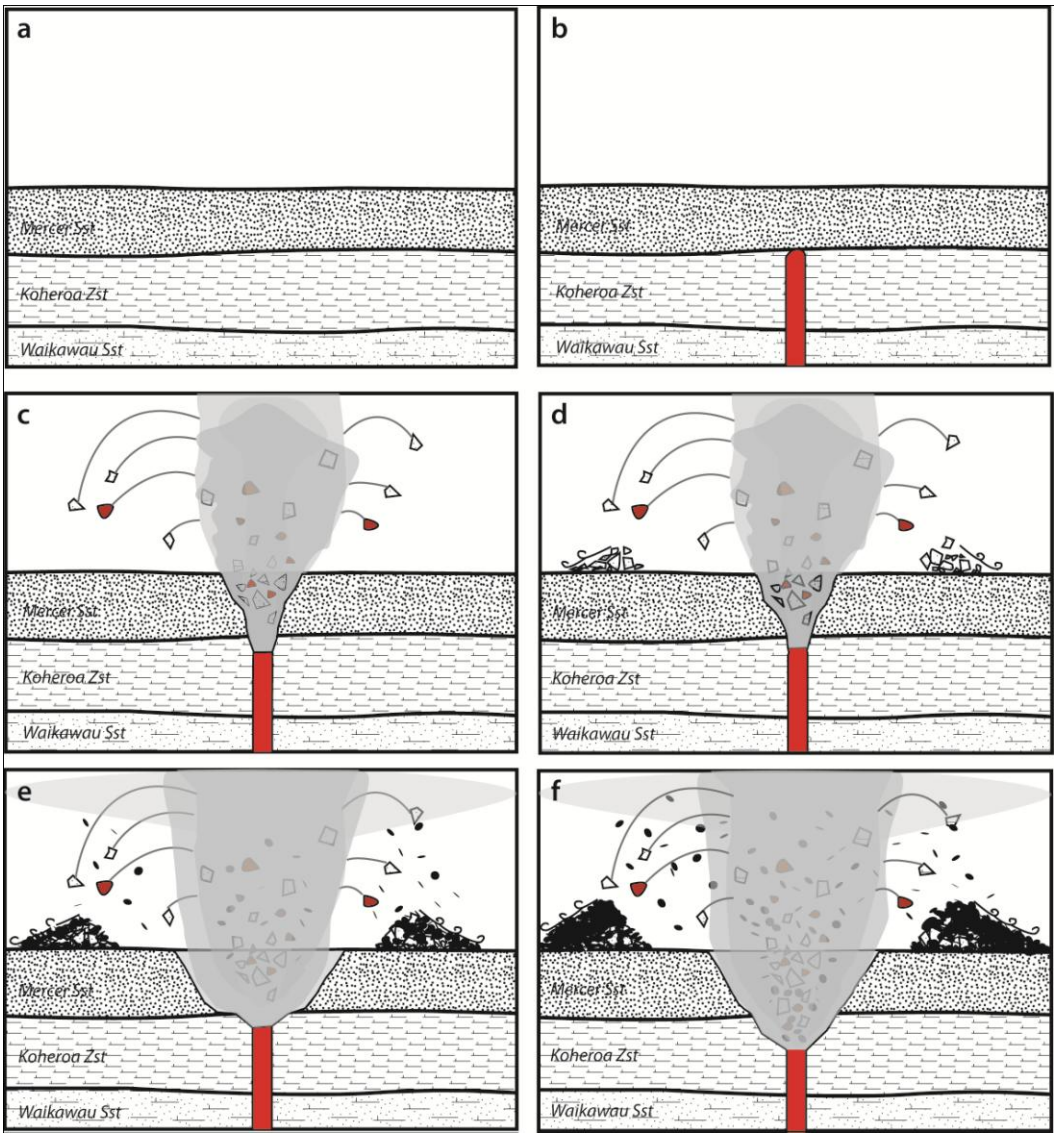

Figure 3.35: Kellyville tuff ring eruption progression (based on diagrams from Wohletz & McQueen 1984); (a) Stratigraphic layers represent from top to bottom: Mercer Sandstone, Koheroa Siltstone and Waikawau Sandstone; (b) intruding magma source was initially mostly unreactive with Koheroa Siltstone; (c) fragmentation occurred of both Mercer Sandstone and Koheroa Siltstone; (d) eruption deposited juvenile rich deposits and lithic-rich ballistics; (e) occasional stages of fragmentation dominantly in Mercer Sandstone; (f) occasional stages of fragmentation dominantly in Koheroa Siltstone (drawdown of fragmentation).

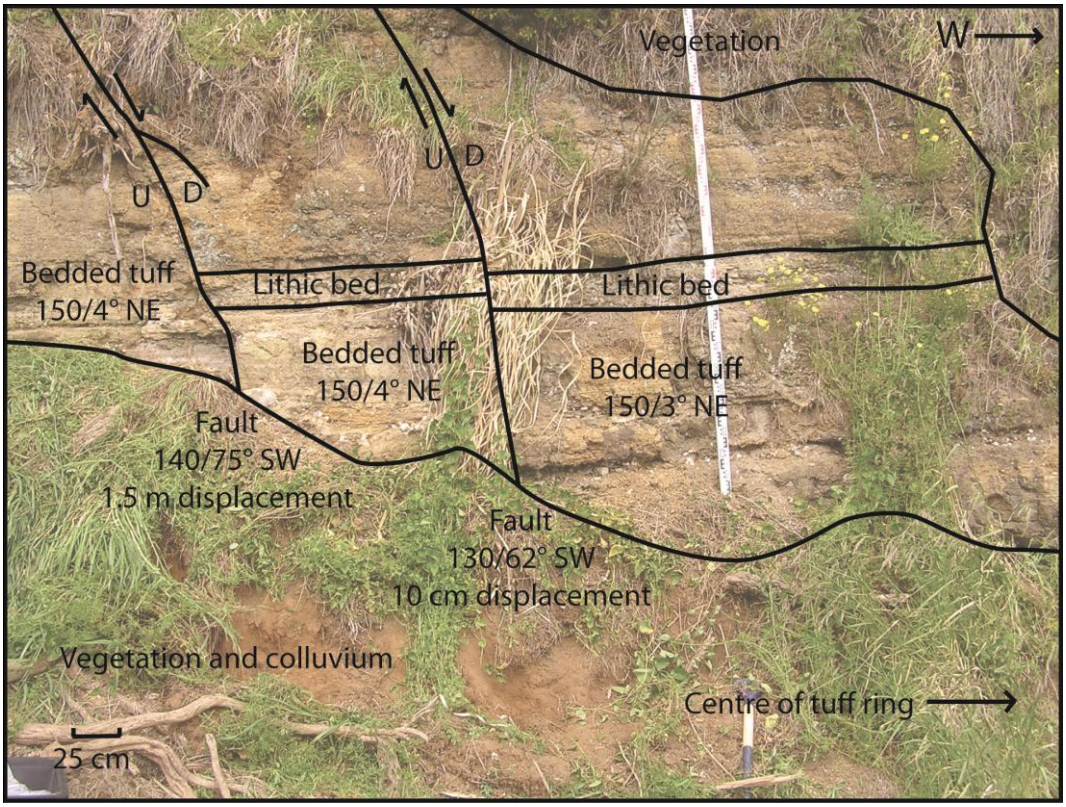

Figure 3.36: Failure of the tuff ring rim, at locality 4.

Chapter Four: Onewhero Tuff Ring

4.1 Introduction

The Onewhero tuff ring was formed 0.88 Ma (Briggs *et al.* 1994). A basalt lava flow derived from either the separate Onewhero cone or an unknown nearby effusive vent has caused a waterfall on the outer rim of the tuff ring. This chapter will cover the underlying geology of the Onewhero tuff ring. Several lithologic facies and their stratigraphy have been identified within the tuff ring. The componentry of the tuff deposit and basalt flow will be discussed as well as its stratigraphic variation. The chapter will be summarised with a discussion of emplacement processes and eruption history.

4.2 Country rock geology

The country rock units surrounding the Onewhero tuff ring belong to the Te Kuiti Group (Kear 1961). The Carter Siltstone of the Te Akatea Formation is the youngest unit of the Te Kuiti Group. Carter Siltstone outcrops on the northeast outer edge of the tuff ring underlying a basalt lava at locality 4 (Fig. 4.1) and is exposed here 4 m thick. Carter Siltstone is a friable, light grey-white highly calcareous massive or weakly bedded siltstone, with very fine small scale laminations (Fig. 4.2) (Edbrooke 2001). The siltstone has darker iron-rich zones up to 20 cm thick (Fig. 4.3a,b), fining up to finer siltstone with no visible iron zones. The exposed face is highly weathered. According to Waterhouse & White (1994), Carter Siltstone is typically between 10-90 m thick, and usually contains age dependent foraminifera (Fig. 4.3c) that indicate the deposit is Waitakian in age. The Aotea Formation underlies the Te Akatea Formation, and hosts the Waimai Limestone. The Waimai Limestone formed in the Late Oligocene and is a cross-bedded, indurated flaggy limestone that grades upward to grey, calcareous sandstone, and further into grey siltstone (Edbrooke 2001).

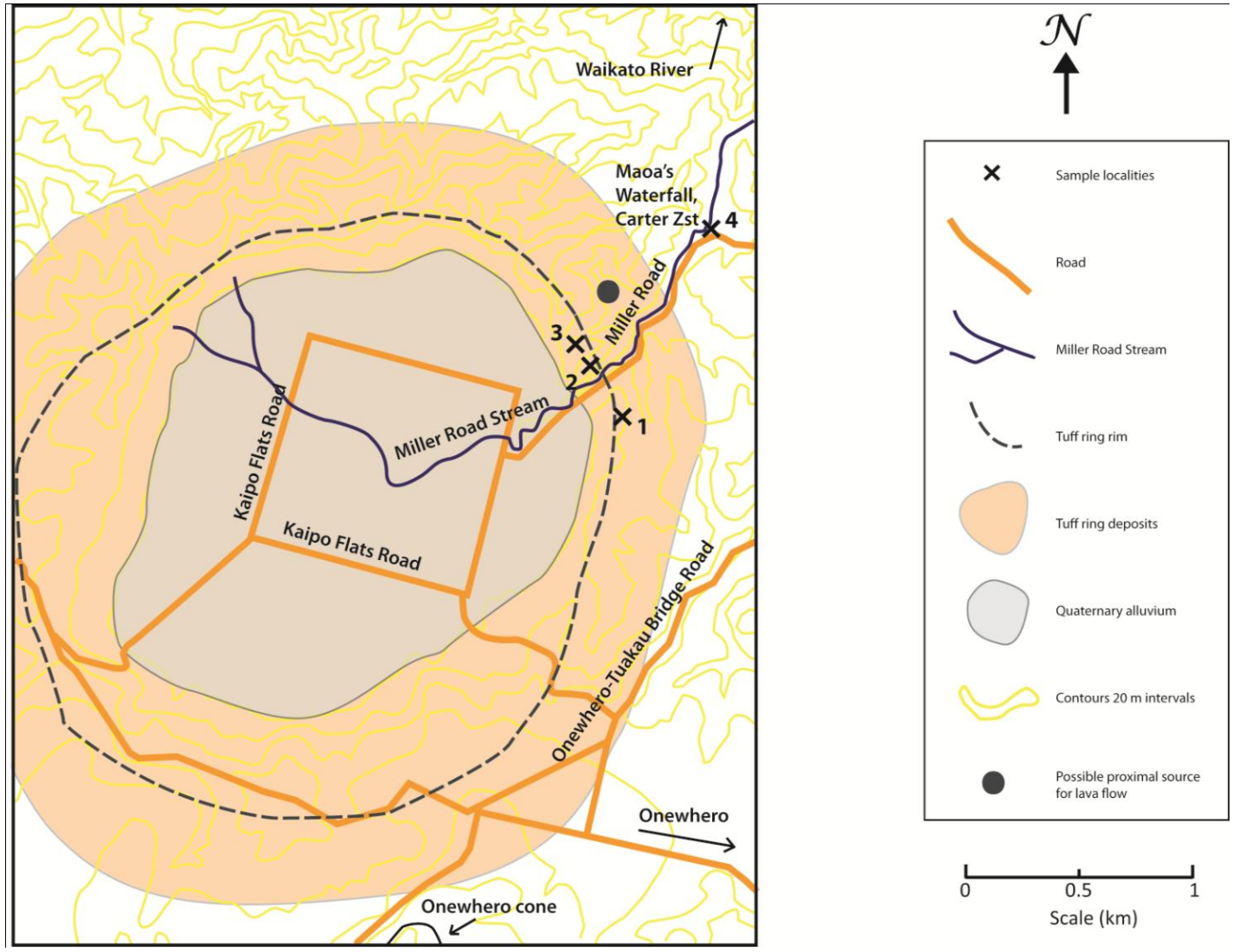

Figure 4.1: Geological map of the Onewhero tuff ring, showing field localities.

The Whaingaroa Formation underlies the Aotea Formation, and is a massive, glauconitic calcareous siltstone. Underneath this is the Glen Massey Formation: calcareous sandstone, siltstone and basal glauconitic sandy limestone. Both the Whaingaroa and Glen Massey Formations outcrop to the northeast of the Onewhero tuff ring (Edbrooke 2001).

Figure 4.2: Carter Siltstone in outcrop at Maoa's waterfall, exposed here 4 m thick with small scale laminations and 20 cm thick iron-rich layer shown.

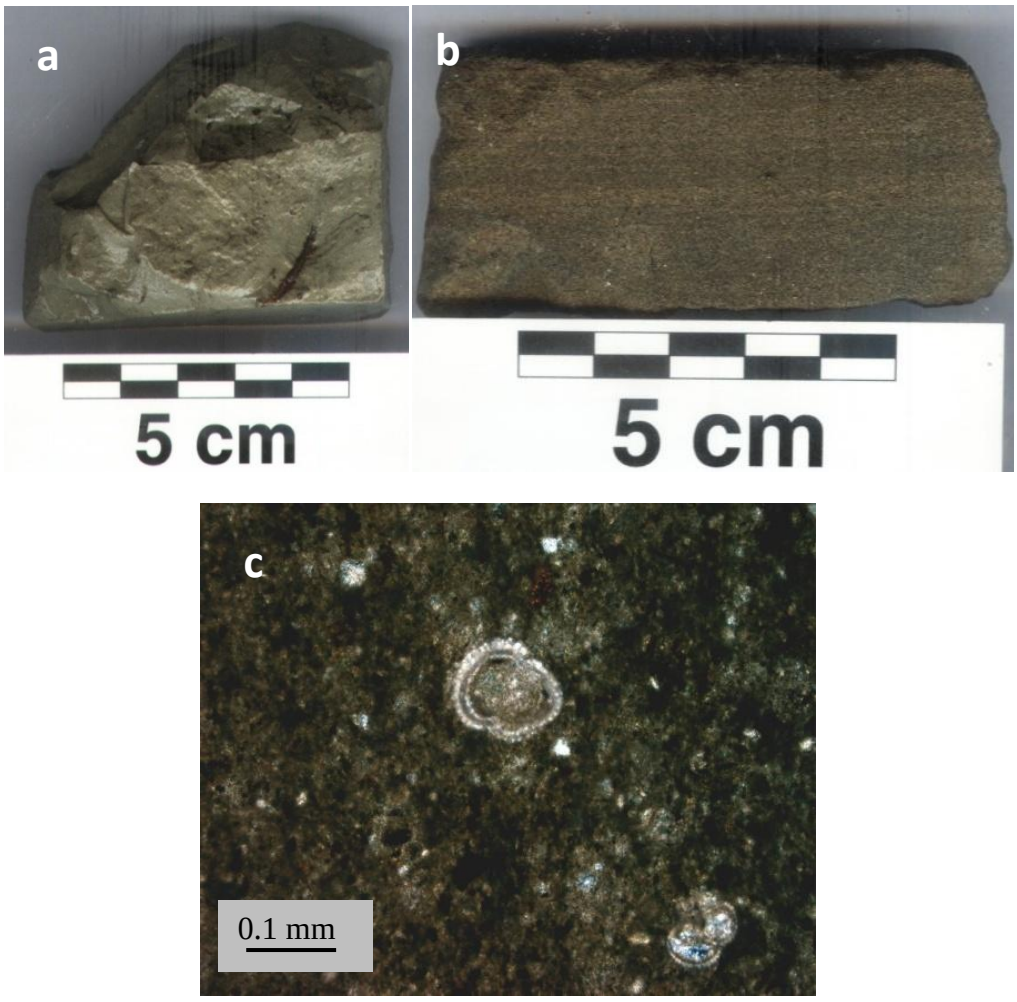

Figure 4.3: Carter Siltstone from locality 4 at Maoa's waterfall. Hand specimens of: (a) fossil plant fragment (sample W2011623); (b) darker iron-rich layer (sample W2011624); (c) photomicrograph showing *Globorotalia sp.*(?) (centre), disseminated quartz grains and calcareous mud matrix (XPL) (sample W2011623).

4.3 Onewhero tuff ring

The Onewhero tuff ring (Fig. 4.1) is situated at the southern end of the South Auckland volcanic field (SAVF), 17 km south of Bombay and 5 km south of the Waikato River (Fig. 2.3). Onewhero tuff ring is the largest tuff ring in the SAVF (Kermode 1992), with a diameter of 2.6 km at its widest point. The tuff deposit is approximately 750 m wide around the entire tuff ring. The highest point

of elevation on the tuff ring rim is 182 m a.s.l, and the maximum height above the exposed base of the tuff ring is 87 m. The floor of the tuff ring ranges from 95 m to 110 m a.s.l. The inner geomorphic slope angles of the tuff ring range from 25° to 14°. The outer geomorphic slope angles range from 6° to 7°. There are several roads that run through the tuff ring (Fig. 4.1). Onewhero-Tuakau Bridge Road provides access into the tuff ring, and Kaipo Flats Road forms a 1 km square directly in the centre. Miller Road provides access to the exposed sections and connects Kaipo Flats Road to Maoa's Waterfall. A small stream named Miller Road stream has cut through the northeast side of the tuff ring rim exposing a cross-section through the tuff ring 30 m high. The stream cutting is approximately 60 m wide.

The geomorphology of Onewhero tuff ring has been modified by erosion and partial collapse. The inner and outer tuff ring angles are very different. The sections of tuff ring that are most preserved are either side of where the stream cuts through the rim. These are also the places with the largest inner angles. The highest vantage point on the northeast rim at the top of locality 3 offers a view of the remaining rim to the west, which appears much less steep and lacks defined structure. The north, south and west sides of the tuff ring in general appear to have been eroded. The outer edge of the tuff ring has been eroded by many streams, including Miller Road stream, and has a variable surface that gradually decreases to surrounding elevations of approximately 20 m. A higher inner floor elevation than that of the surroundings is characteristic of tuff rings (Cas & Wright 1987).

4.4 Sample localities

There are very few outcrops of the tuff ring, but there is an excellent exposure on the NE side where it has been incised by the Miller Road stream. Here are three exposed sections that show stratigraphic variation. The stratigraphically lowest exposed section (locality 1), is 20-25 m thick, and outcrops on the southern side of the small stream (Fig. 4.4). The large exposed section was accessible for the lower 15.5 m. On the opposite side of the stream, approximately 200 m to the north, is a large 30 m thick cliff section (locality 2)

(Fig. 4.5). The base of the section occurs at the same elevation as that of 5 m up the exposed section of locality1, and provides approximately 20 m overlap. The cliff allowed access to the lowest 10.5 m of the exposed tuff ring. The base of a smaller outcrop (locality 3) on the same side of the stream occurs at approximately the same elevation as the top of the large cliff (Fig. 4.6). This outcrop exposes 12 m and provides the stratigraphically highest exposure of the tuff ring rim.

Figure 4.4: Locality 1 showing facies A south of the stream. Section is 4 m high.

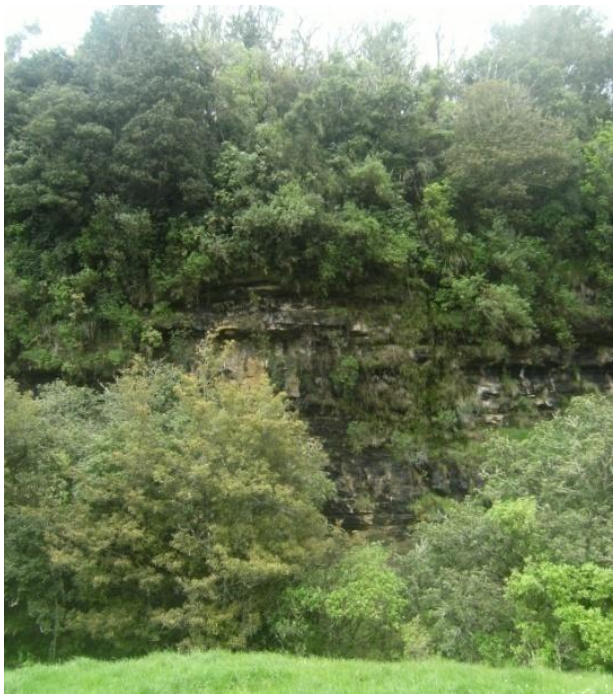

Figure 4.5: Locality 2, showing exposure of the northeastern tuff ring rim, north of the stream.

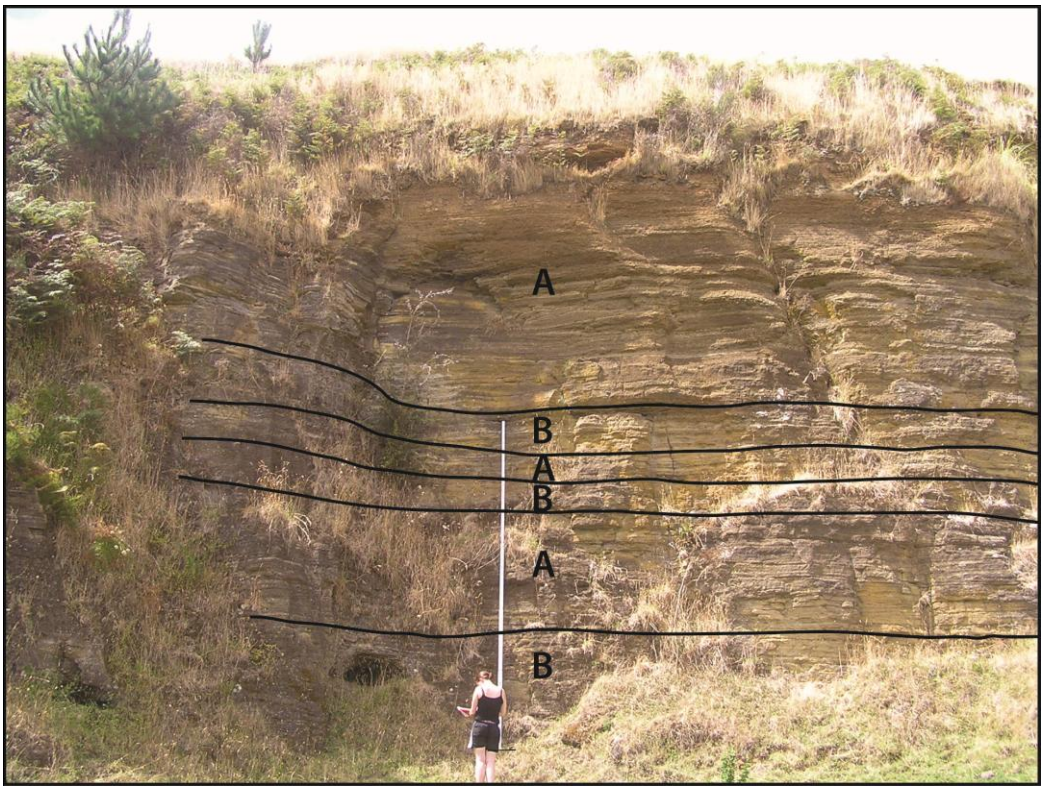

Figure 4.6: Locality 3 containing both facies A and B. Cliff is 12 m high.

Te Wai Heke o Maoa, or Maoa's Waterfall (locality 4) is located 800 m northeast of Onewhero tuff ring rim and is part of the Miller Road stream (Fig. 4.7). The waterfall drops by 32 m in elevation and the stream continues northeast to drain into the Waikato River. The waterfall flows over a basalt lava flow about 30 m thick and has originated from an early magmatic stage of the Onewhero vent or a proximal vent on the outskirts of Onewhero tuff ring. The lava flow overlies Carter Siltstone of the Te Kuiti Group. The siltstone is exposed at the base of the waterfall for 4 m and outcrops further downstream.

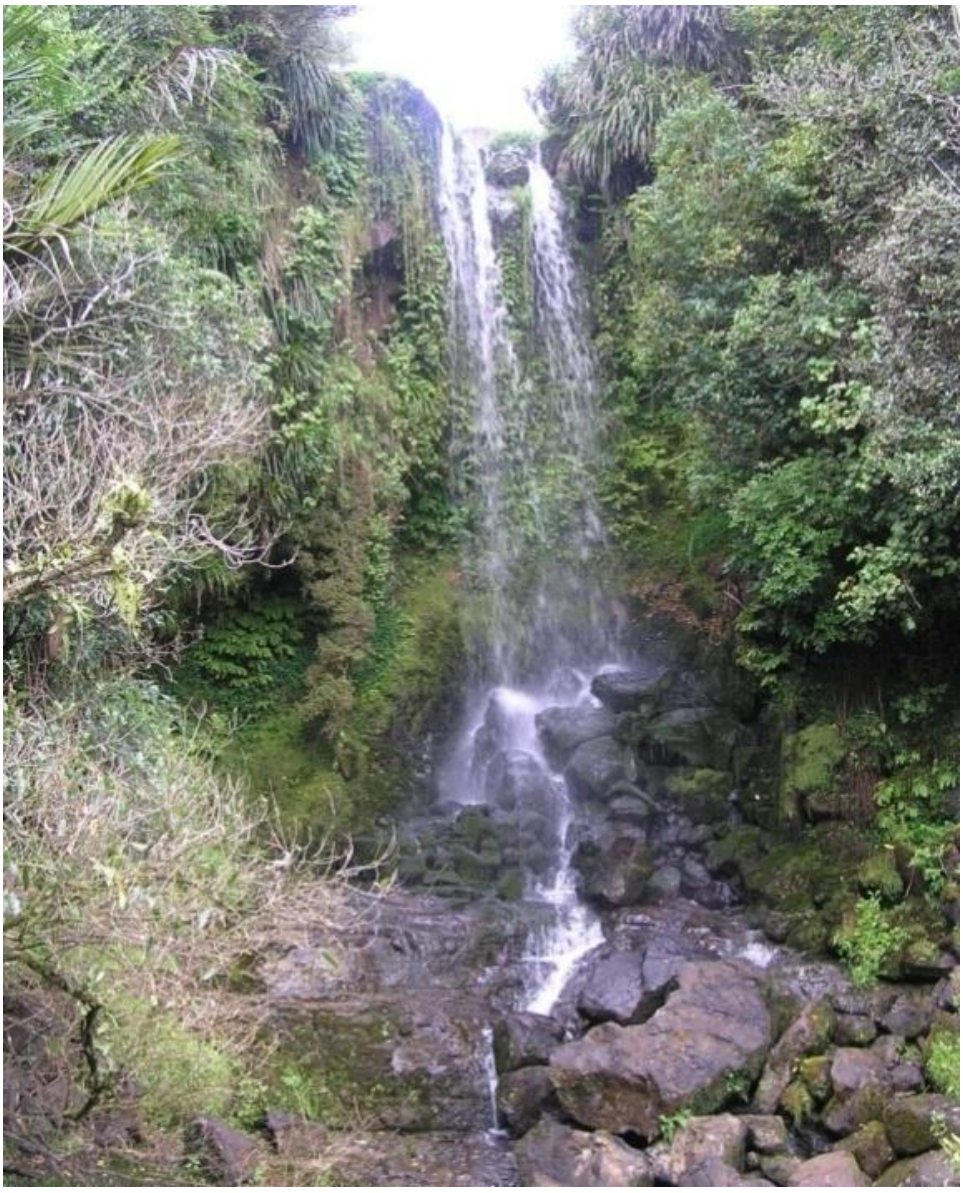

Figure 4.7: Maoa's Waterfall (locality 4), flowing over a basalt lava flow.

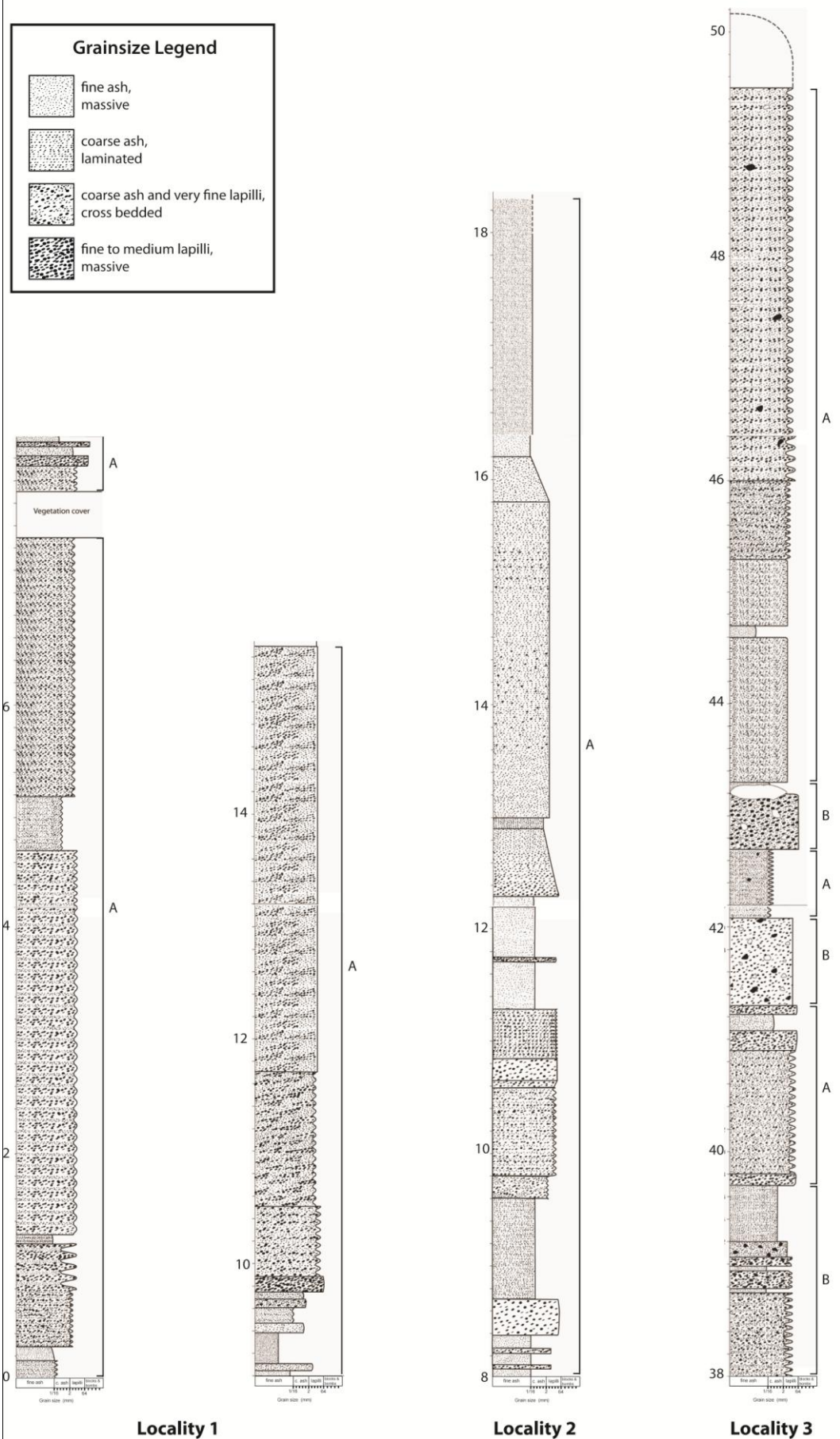

Figure 4.8: Combined stratigraphy of the Onewhero tuff ring

4.5 Facies and stratigraphy

4.5.1 Onewhero tuff ring

Stratigraphic logs from localities 1-3 of the Onewhero tuff ring can be seen in Fig. 4.8. Two facies types have been recognised using field and petrographical descriptions in 15.5 m, 10.5 m and 12 m thick tuff ring successions. The lowermost succession of 15.5 m (locality 1) consists entirely of a well sorted, wavy and cross bedded, alternating fine and coarse ash facies (facies A). The middle succession of 10.5 m (locality 2) overlaps with the lowermost succession, and is also entirely comprised of facies A. The upper succession of 12 m (locality 3) is separated from the lower successions by 19.5 m and consists of both facies A and facies B: a poorly sorted to massive, weakly bedded, fine ash to coarse lapilli facies.

4.5.2 Tuff ring facies

Facies A - well sorted, cross bedded, alternating fine and coarse ash

Facies A (Fig. 4.6) is generally a well sorted, wavy and cross bedded, alternating fine and coarse ash facies. Grain size ranges from fine ash to isolated blocks and bombs. Facies A is generally thinly to diffusely bedded with laminated, wavy and cross beds. The layers within this facies are mostly medium to well sorted. Blocks and bombs mainly appear as isolated features, impacted into finer layers. Blocks are the most common, and occur as dark, angular basalt clasts and lithics (maximum: 60 cm). Blocks and bombs occur individually within beds of alternating coarse ash and medium lapilli with fine ash layers.

Moderately to well sorted, dark, fine to medium lapilli beds, with both juvenile clasts and lithics also occur. These beds are diffusely bedded, can be rich in orange and red scoria, and often contain grey slightly vesicular basalt clasts (Mc: 10.6 mm). Fine lapilli occasionally occur as thinly bedded layers with reverse grading up to coarser fine lapilli. Fine lapilli also appear in diffusely to well bedded, normally graded layers grading up to coarse ash. These layers commonly have small scale wavy bedding. Laminated and well sorted coarse ash

frequently appears within cross-bedded layers alternating with very fine lapilli beds 5-7 cm thick. Approximately 60% well sorted coarse ash also alternates with well bedded, moderately sorted darker fine lapilli beds (40%), with occasional very well sorted fine ash beds 4-10 mm thick. Very well sorted coarse ash, with approximately 25% subangular fine lapilli clasts (Mc: 4.8 mm), fine upwards to coarse ash with very fine lapilli clasts. Normally graded single coarse ash beds also occur as medium-bedded coarse ash with alternating fine lapilli beds, fining up to weakly bedded coarse ash with some very fine lapilli, then to well sorted, massive coarse ash, grading up to well sorted, massive fine ash. Fine and coarse ash beds alternate with laminated, wavy and cross beds. Alternating fine and coarse ash occur with intermittent very fine to medium lapilli layers. Wavy bedding is low angle, with wavelengths of 1.2 m and varying amplitudes of 25-50 mm. The fine ash fraction is commonly very well sorted and massive. Alternating fine and coarse ash also host approximately 5% subrounded very fine to coarse lapilli clasts (Mc: 2.8 mm) and lithics (Ml: 4.6 mm). Laminated fine ash beds occur with 2-4 cm thick, wavy bedded very fine lapilli beds. The beds have clasts and lithics that are orange, grey and red in colour. Cross beds within the fine and coarse ash pinch out away from the vent. Facies A is the most common facies in Onewhero tuff ring.

Facies B – poorly to very well sorted, fine ash to blocks and bombs

Facies B (Fig. 4.9, 4.10) is generally a poorly to very well sorted, diffusely to well bedded to massive, fine ash to block and bomb facies. Grain size ranges from fine ash to blocks and bombs. Blocks and bombs occur as concentrated layers in this facies, as well as infrequent isolated juvenile clasts and lithics within finer layers. Moderately sorted coarse, medium and fine lapilli occur together in concentrated layers, with lithics (Ml: 13.5 mm) and juvenile clasts (Mc: 10 mm), and 4 mm of fine ash on top. Coarse lapilli also occurs in a very weakly bedded, lapilli-rich coarse ash layer with 60 to 70% coarse lapilli clasts, very few lithics, and few basalt blocks. Poorly sorted coarse ash beds occur with medium to fine lapilli (figure 4.11), consisting of sub-rounded to angular juvenile clasts (Mc: 20 mm) and rounded lithics (Ml: 27.5 mm).

Figure 4.9: Lower tuff (4m from outcrop base) at locality 1, showing facies A: low-angle wavy bedding in fine to coarse ash. Photo is looking north, vent is to the left.

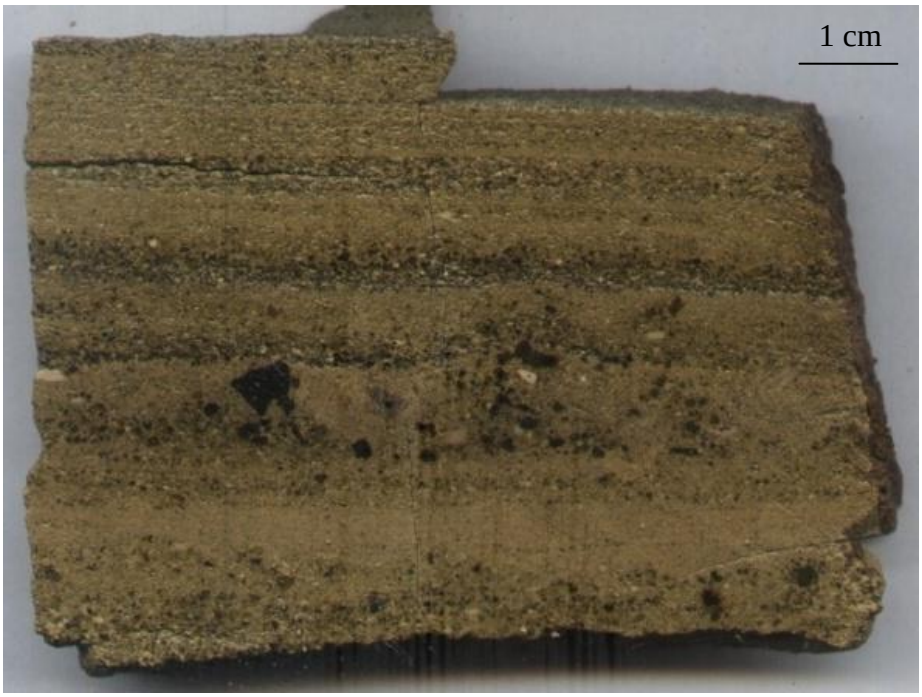

Figure 4.10: Sample of Facies A from the top (14.7 m from base) of locality 3, showing alternating coarse and fine ash with very fine lapilli beds (sample W2011628).

Poorly sorted coarse ash to fine lapilli beds also occur with large coarse block and subrounded bomb clasts and subangular lithics. Medium bedded coarse ash occurs with approximately 40% massive, light fine ash layers within beds. Light coloured, massive fine ash occurs as individual continuous beds, with one dark angular block clast approximately 60 cm long impacted into the ash.

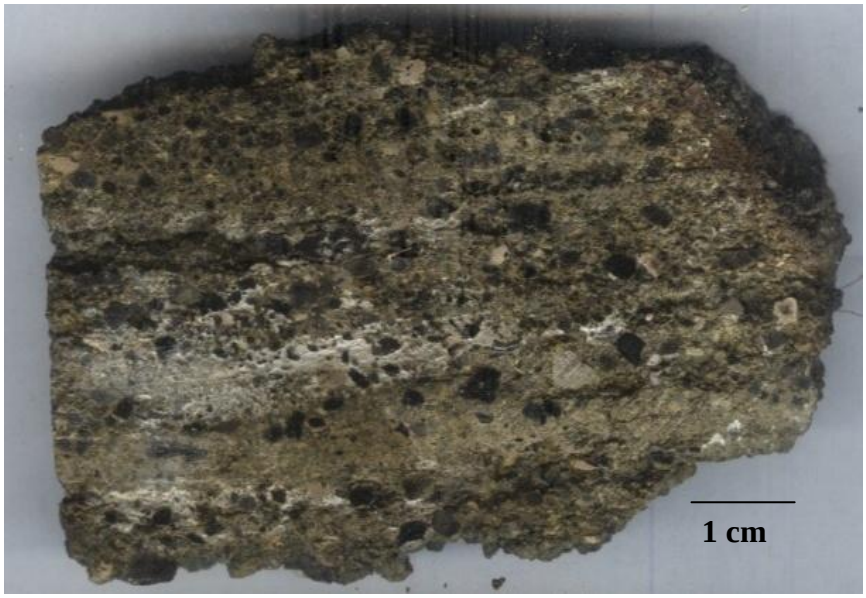

Figure 4.11: Sample of facies B from locality 2 (0.9 m from base), with coarse ash and very fine lapilli (sample W2011604).

4.5.3 Tuff ring facies stratigraphy

The three exposed sections of the Onewhero tuff ring are relatively close to one another (up to 200 m apart) and can therefore be used together to determine vertical facies variations for the tuff ring (Fig. 4.8). The lowermost tuff ring exposures (locality 1 and 2) are comprised of facies A, and the uppermost (locality 3) is comprised of both facies A and facies B. There is a 19.5 m gap in between the upper and lower exposures, however as there is little variation between them, it can be assumed that the gap consists of either primarily facies A or an alternation of facies A and B.

Horizontal facies variation can be determined using localities 1 and 2. Locality 3 is stratigraphically higher than the other outcrops and cannot be used in a comparison. Localities 1 and 2 have stratigraphic overlap of 10.5 m (0 - 10.5 m

in locality 1, and 5 - 15.5 m in locality 2, allowing horizontal changes in facies to be established. The overlap areas of both localities consist of facies A. At the base of each section of overlap, locality 1 is dominantly coarse ash, and locality 2 is dominantly fine lapilli. 5 m above the base of overlap, locality 1 is dominantly medium lapilli and locality 2 is dominantly medium to coarse lapilli. 10 m above the base of overlap, locality 1 is dominantly fine to coarse ash and locality 2 is dominantly medium to coarse lapilli. Within this area of overlap, the tuff deposits to the north of the Miller Road stream (locality 1) are finer in general than the tuff deposits to the south of the stream (locality 2), which coarsen upwards.

4.5.4 Lava flow facies

Facies C- basalt lava flow

Facies C consists of crystalline basalt (Fig. 4.12) present in the lava flow beneath the waterfall (locality 4) (Fig. 4.7). The flow is a non-vesicular, hypocrystalline, fine-grained, porphyritic olivine basalt. Its groundmass is comprised of plagioclase laths, anhedral olivine fragments, titanaugite, granular titanomagnetite and glass. Phenocrysts include common shattered euhedral to anhedral, unaltered olivine, and uncommon subhedral, purple titanaugite. The basalt is massive with no signs of flow direction.

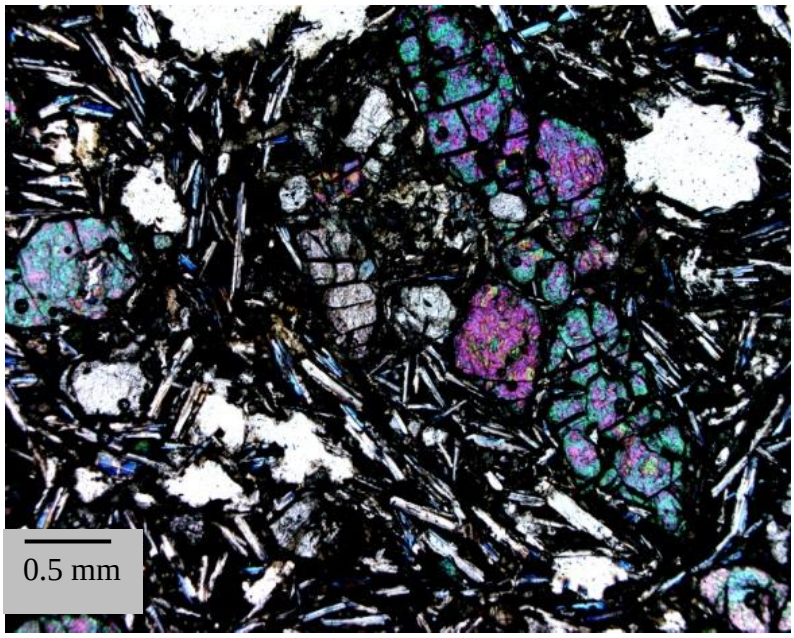

Figure 4.12: Highly crystalline olivine basalt from locality 4 in thin section, showing plagioclase and glass groundmass and olivine phenocrysts (sample W2011626).

4.5.5 Basalt geochemistry

The geochemistry of basalt from the Onewhero tuff ring has been summarised in the table below (Table 4.1), and compared with the geochemistry of the nearby lava flow and Onewhero Cone. The $Na_2O + K_2O$ wt% have been compared to SiO_2 wt% in order to distinguish between group A and group B basalt types. In Fig. 4.13 most of the representative data for the Onewhero tuff ring identified it as group A, however two samples were not distinguished by this comparison. Fig. 3.14 compares Zr/Nb ratios with Nb (ppm), and distinguished all data as group A.

Group A represents a transitional basalt to tholeiite group, and is derived from the shallow upper mantle (Cook 2002). The data below suggests that the magma source from the Onewhero tuff ring was generated at shallow depths in the upper mantle.

Table 4.1: XRF geochemical data of basalt from Onewhero tuff ring and nearby Onewhero cone and lava flow. *OTR*: Onewhero tuff ring sample from Kaipo Flats Road, boulder from tuff, *OLF*: Onewhero lava flow sample from outer tuff ring, *OC*: Onewhero cone sample from Kauri Road, OLF: Onewhero lava flow sample (sample W2011626) from outer tuff ring. Sample geochemistry data with labels in italics are from Cook (2002).

Sample	***OTR***	***OLF***	***OC***	**OLF**
	alkali ol-basalt	hawaiite	hawaiite	
Major elements				
SiO_2	46.24	47.52	46.87	46.86
TiO_2	2.25	2	2.08	2.22
Al_2O_3	13.73	14.04	13.44	13.82
Fe_2O_3	14.96	13.93	14.05	14.87
MnO	0.18	0.18	0.18	0.17
MgO	10.05	9.43	9.93	8.89
CaO	9.47	9.25	8.5	9.48
Na_2O	3.14	3.01	2.80	2.73
K_2O	0.73	0.61	0.76	0.60
P_2O_5	0.35	0.27	0.31	0.30
Total	101.10	100.24	98.92	99.95
LOI	-0.94	-0.21	0.94	0.11
Trace elements				
Sc	24	27	23	-
V	227	228	225	179
Cr	278	351	288	266
Ni	181	217	191	213
Cu	65	62	52	75
Zn	100	98	102	115
Ga	23	22	20	21
As	1.3	1.5	0.7	-
Rb	12	10	15	5.6
Sr	387	331	328	330
Y	21	25	22	21
Zr	130	130	133	125
Nb	18	16	18	17
Ba	120	117	129	112
La	15	15	17	9.4
Pb	2.5	2.1	3.8	2.1
Ce	46	42	49	27
Th	1.3	2.2	2.6	<1.5
U	0.1	0.1	1.5	2.7
Group	**A**	**A**	**A**	**A**

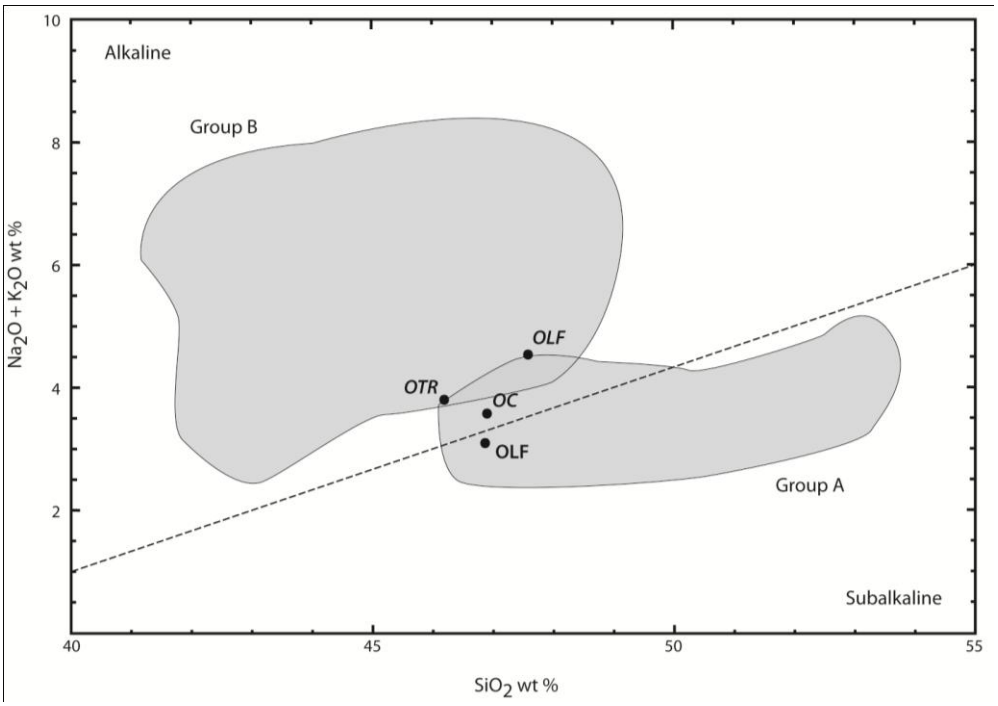

Figure 4.13: $Na_2O + K_2O$ wt% against SiO_2 wt%, with typical boundaries of Group A and B basalt from the SAVF (Cook 2002). Labels in italics are from Cook (2002).

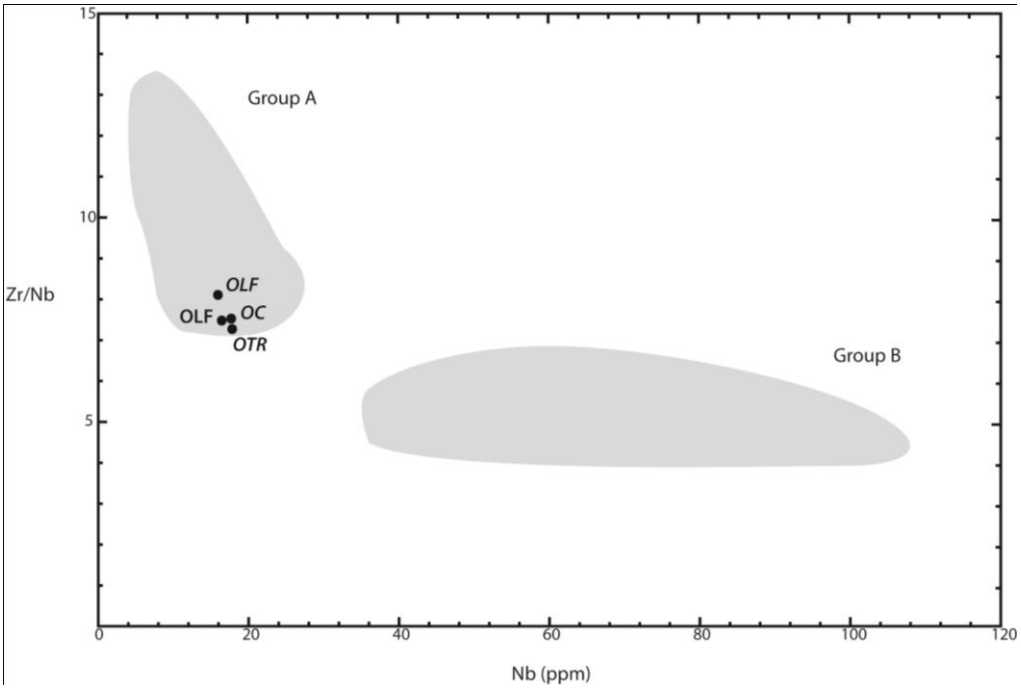

Figure 4.14: Zr/Nb ratio against Nb (ppm), with typical boundaries of Group A and B basalt from the SAVF (Cook 2002). Labels in italics are from Cook (2002).

4.6 Tuff ring componentry

The tuff deposits that constitute the Onewhero tuff ring are comprised of a mixture of varied juvenile and lithic material.

Scoria

Scoria is the dominant juvenile clast throughout the Onewhero tuff ring. Two types of scoria are found in thin section: orange-yellow palagonite and brown-black tachylite clasts (Fig. 4.15). Most tuff deposits contain both scoria types; however the orange palagonite scoria is the most common. Both scoria types are moderately vesicular (30 – 45%) with amygdales, and anhedral in shape. The most common phenocryst present within both types of scoria is olivine. Unaltered olivine phenocrysts occasionally occur within the scoria; however most olivines are partially to completely altered to iddingsite. Titanomagnetite occurs within the scoria groundmass.

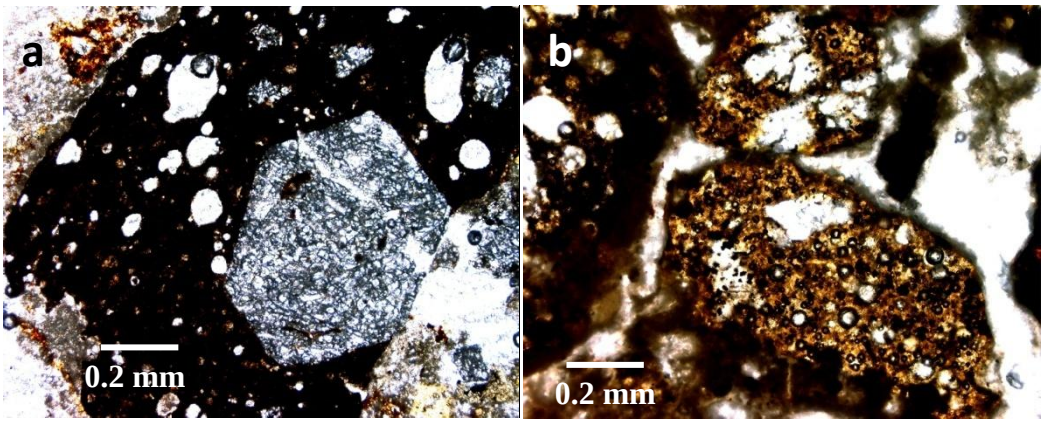

Figure 4.15: (a) Vesicular brown scoria clast with euhedral to subhedral olivine phenocrysts, within tuff deposits from locality 1 (sample W2011520); (b) Vesicular orange scoria clast with subhedral olivine phenocrysts, within tuff deposits from locality 1 (sample W2011523).

Juvenile basalt clasts

Non-vesicular, olivine basalt is present within the Onewhero tuff deposits and can be seen in thin section. In thin section basalt clasts are angular to sub-rounded, with fresh to slightly devitrified glassy groundmass. There are two main types of dense basalt within the tuff deposits: crystalline basalt with abundant plagioclase, olivine and augite phenocrysts (Fig. 4.16a); and basalt with

plagioclase laths within the hyalopilitic groundmass and olivine phenocrysts (Fig. 4.16b). Olivine phenocrysts are commonly altered to orange to red iddingsite rims. Titanaugite is occasionally present as small phenocrysts.

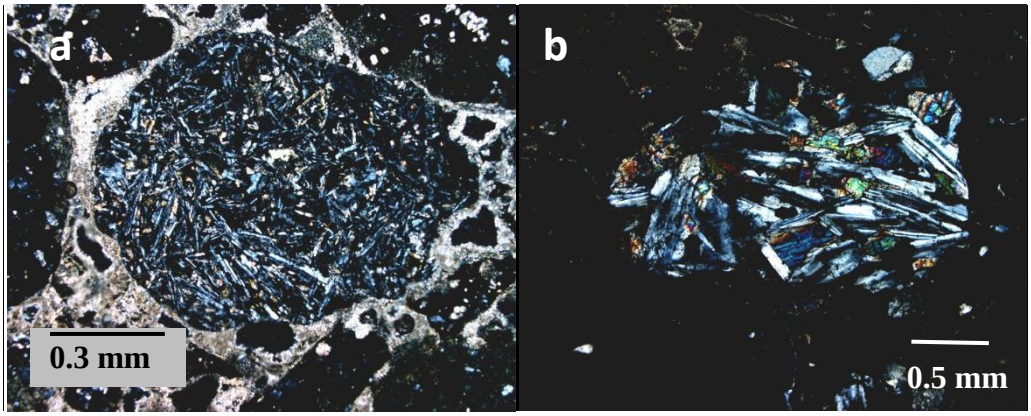

Figure 4.16: (a) Non-vesicular, crystalline basalt with olivine phenocrysts, and plagioclase laths and glass groundmass, within a calcite-rich ash matrix from tuff in locality 1 (sample W2011524); (b) Non-vesicular, crystalline basalt with plagioclase, augite and olivine phenocrysts, within a tuff deposit from locality 2 (sample W2011604).

Crystals

(a) Juvenile crystals

Crystals of olivine were present in every tuff sample taken from Onewhero. The olivines are very rarely fresh, and are often highly altered (Fig. 4.17). Others have iddingsite rims and some have been embayed. The largest olivine crystal found was 2.5 mm long. Some uncommon augite crystals were also present.

(b) Xenocrysts

Uncommon hypersthene crystals are also present, which are likely to be from Quaternary alluvium deposits. Crystals derived from lithic material include many quartz crystals, some of which may be derived from Quaternary alluvium. Plagioclase laths present may be derived from either lithic material or juvenile material, or both.

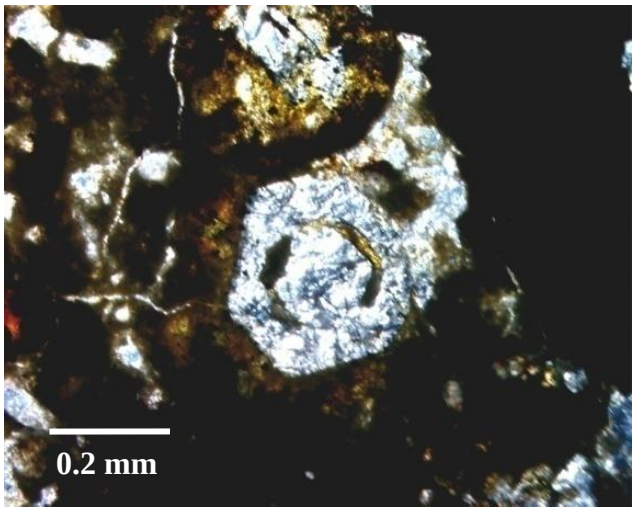

Figure 4.17: Euhedral embayed olivine crystal within tuff deposit from locality 3 (sample W2011560).

Lithics

Accessory lithic material is present within the Onewhero tuff deposits (Fig. 4.18a,b) up to a maximum 27.5 mm. Lithics occur as two main types and the formations have been deduced by fossil abundance and lithic type: (1) Te Akatea Formation lithics with a calcite-mud matrix with quartz crystals and some planktic foraminifera, and glauconite pellets, and (2) Aotea Formation lithics with a calcite-mud matrix, common quartz and appear to have little to no fossil material. The largest lithic fragment found within thin section is 7.5 mm long and 3.25 mm wide, quartz-rich calcite mud with no fossils.

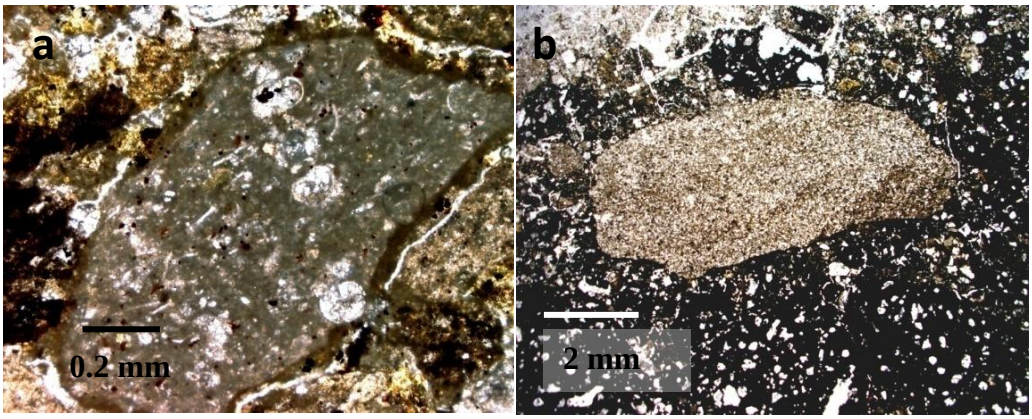

Figure 4.18: (a) Te Akatea Formation fragment within tuff from locality 1 (sample W2011520); (b) Aotea Formation xenocryst within basalt clast, within tuff deposit from locality 2 (sample W2011604).

4.7 Stratigraphic variation

The deposits of Onewhero tuff ring show many variations through their stratigraphy which reflect changes in eruption from beginning to end. Grainsize variation through the tuff ring can be seen in Fig. 4.19 below. There is a large gap in the recorded stratigraphy due to lack of accessible outcrop, however general trends can still be seen. In the lower half of the exposed section, between 104 and 120 m elevation, dominant grain size varies between fine ash to fine lapilli. In the upper half of the exposed section, dominant grain size varies between fine ash and coarse lapilli. Fig. 4.19 shows a slight trend of coarsening upwards through the tuff deposits, reflecting a change in eruptive conditions. Componentry of the tuff ring deposits can be seen in Fig. 4.19. Juvenile material is dominant throughout the tuff ring, and is very variable in the first exposed 15 m of outcrop. Juvenile material proportion decreases very slightly (approximately 10%) up the exposed outcrops. Lithic proportion also decreases (approximately 5%) very slightly up the exposed outcrops, and the proportion of free crystals (both juvenile and accessory) increases (from approximately 10 to 20%). Vesicularity of the juvenile clasts within the tuff deposits is illustrated in Fig. 19. There is little variation in vesicularity (15%) of the vesicular basalt deposits; however a general increase is evident in the lower 8 m of outcrop, followed by a general decrease to approximately 12 m. An increase in vesicularity also occurs around 40 m.

Accessory lithic type varies throughout the stratigraphic record of the tuff ring, which can be seen in Fig. 4.19. The dominant lithic type within the tuff ring deposits is the Te Akatea Formation, which is entirely dominant at 3, 11 and 40 m. The Aotea Formation occurs in the deposits in a smaller amount, and peaks of this lithic occur at 2.5, 9.5 and 42.5 m, up to 50%. Overall the peaks in the Aotea Formation become smaller up the outcrop, and the Te Akatea Formation becomes more dominant.

4.8 Discussion

4.8.1 Emplacement processes

Facies A represents a highly energetic, alternating fall- and surge-dominated phase of the eruption. Surges have created many thin cross beds within the ash-rich deposits as well as some wavy beds. Uncommon ballistic fall-out is represented by isolated lithic and juvenile clast blocks within finer deposits. Coarser beds of mainly juvenile clasts with some lithics represent a "drier" stage of the eruption with less water content, and lower fragmentation efficiency and energy of the eruption (Houghton *et al.* 2000; Németh & White 2003; Houghton & Gonnermann 2008). Lithic type is mostly the shallow Te Akatea Formation, but sharp increases at around 2 m and 8 m in the proportion of the Aotea Formation indicate a downward shift in the fragmentation depth of the eruption (Houghton *et al.* 2000). Conversely, peaks in the proportion of Te Akatea Formation such as those at 3 m and 11 m signify that fragmentation of the eruption occurred near the surface at these stages, and vent clearing would have occurred. A peak of lithic content overall around 6 m indicates an increase in the water content of the eruption and fragmentation of the sedimentary rocks that make up the walls of the conduit.

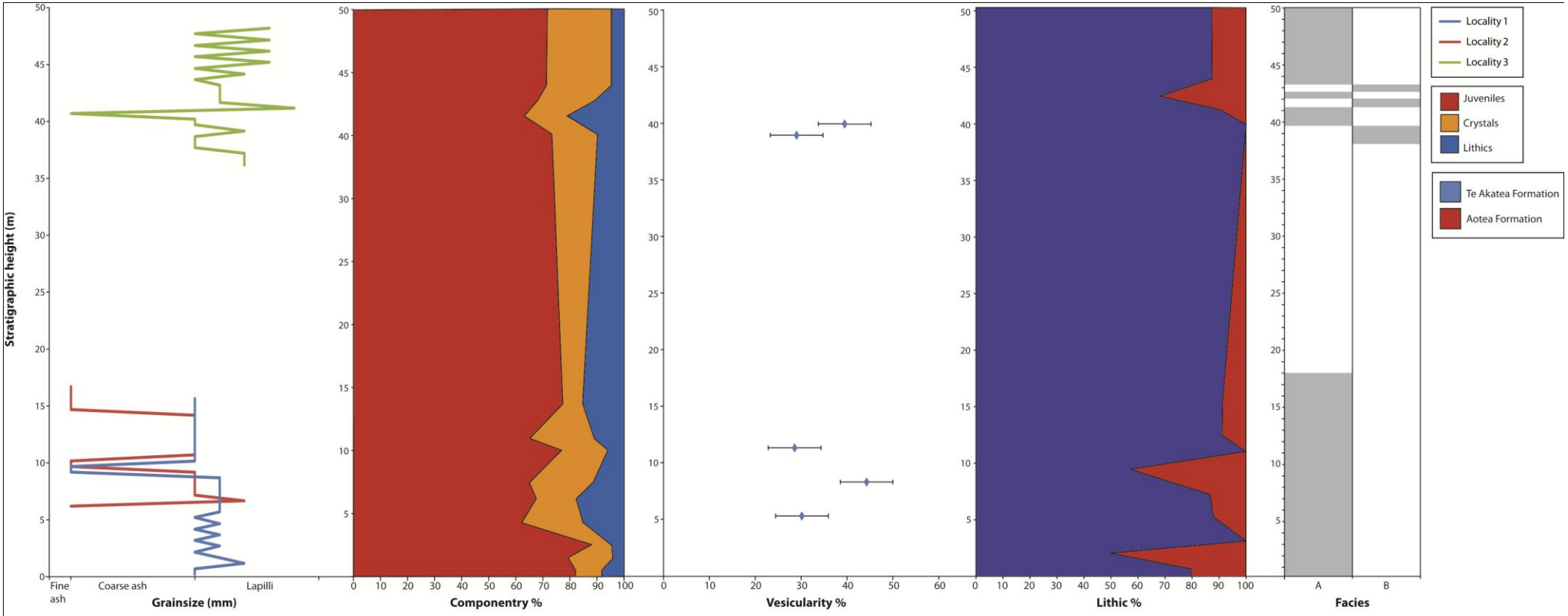

Figure 4.19: Variation with stratigraphic height throughout the exposed tuff ring successions.
Variation from left to right includes grainsize, componentry, vesicularity of juvenile clasts within tuff deposits, lithic type and facies.

Facies B represents an energetic, fall-dominated phase of the eruption. Poorly sorted deposits with weak bedding represent a sustained period of the eruption where a high level of water content and differing ejection angles causes finer material to be deposited in rapid fallout from eruption clouds at the same time as denser, coarser material (Houghton *et al.* 2000; Németh & White 2003). Poorly sorted layers of alternating fine and coarse material represent pulsing bursts caused by the fluctuating energy of the eruption and variation of the fallout rate (Németh & White 2003). Finer ash layers occur between these eruption stages, indicating periods where deposition is dominantly from fallout of the residual eruption cloud (Houghton *et al.* 2000). Isolated lithic blocks and juvenile clast blocks and bombs represent ballistic fallout and are uncommon. Coarser material, from fine to medium lapilli, both juvenile clasts and lithics, represents instability in the conduit. A peak in lithic content around 37 m indicates a peak in the water content of the eruption and fragmentation of the sedimentary rocks of the conduit. Lithic type is mainly the shallow Te Akatea Formation. A peak in the proportion of the Aotea Formation at around 38 m indicates a lowering of the fragmentation depth in the vent (Houghton *et al.* 2000)

Facies C represents a nearby, most likely separate, dry, magmatic phase suggesting that ascent rate was either very fast, or it originated from a vent that was already established (Cas 1989).

4.8.2 Eruption history

Onewhero tuff ring is a phreatomagmatic deposit resulting from the interaction of basaltic magma with a large volume of external water. The eruption that formed the tuff ring commenced 0.88 million years ago, and occurred over a brief period, typical of tuff ring eruptions (Németh *et al.* 2003; Houghton & Gonnermann 2008).

The eruption began as basalt magma intruded into water-bearing sedimentary rocks. The occurrence of both fine ash and lithic fragments is evidence of this magma water interaction (Houghton *et al.* 1999). The underlying geological unit, Carter Siltstone of the Te Kuiti Group, is not very porous and so

is unlikely to have been the aquifer responsible for the eruption. Quartz, hypersthene and plagioclase lithic crystals found in some of the tuff deposits suggest that the aquifer may have been river alluvial deposits (Briggs *et al.* 2010). As the Onewhero area has since been uplifted by 2.7 km to the west, decreasing to 0.7 km to the east by the Waikato Fault (Hochstein & Nunns 1976), it is possible that the Onewhero tuff ring erupted at the level of the ancestral Waipa/Waikato River. The rising magma would have interacted with the river water and water-bearing alluvium deposits and caused a phreatomagmatic eruption. Due to the varying lithic types present within the tuff, the eruption must have also interacted with sedimentary layers below the Quaternary alluvium – these lithic types have been assumed to be the underlying Te Akatea Formation and the Aotea Formation.

The beginning of the eruption may have had near-silent with vent-clearing pulsing jets giving out large amounts of steam (Kokelaar 1986) and pulsating ballistic fallout as the conduit was initiated, however this cannot be seen in stratigraphic section. Throughout the eruption the changing geometry (due to the soft nature of the sedimentary rocks) of the vent would have been filled with a mixture of fallout tephra from the pulsing jets and water (Kokelaar 1986). As the eruption progressed, the vent became more stable and allowed a steady interaction of magma and water supply from sedimentary rocks (facies A). Alternating surges (caused by collapse of the pulsing jets) (Kokelaar 1986) and fallout caused by frequent numerous pulsing explosions occur in this stage of the eruption, and are relatively steady and very repetitive. Later in the eruption there were larger scale surges resulting from a larger amount of water interacting with the magma, causing many pulsating explosions due to higher energy (facies B). Coarser and finer material was deposited together within high-energy surges and subsequent fallout (Wohletz & Sheridan 1983). This increase in energy may have been due to a decrease in mass ratio between magma and water or a decrease in stability in the vent, causing material to coarsen.

The Onewhero tuff ring has the largest diameter of all tuff rings in the SAVF, and is also relatively high (87 m from floor). The extent of these deposits suggests that the volume of magma was large - perhaps the largest of all the tuff rings. Due to the steady nature of the deposits (grainsize, juvenile proportion), a

steady supply of water must have been readily available for interaction with the magma. As mentioned above, the most likely aquifer source for the eruption is the ancestral Waipa/Waikato River and its associated alluvial deposits, which have very high porosity, permeability and transmissivity, providing a large, constant source of external water for the eruption. Comparing juvenile and lithic proportions can provide an estimated water/magma ratio, which can be used to estimate the efficiency of the eruption. The estimated water/magma ratio of the Onewhero tuff ring eruption is 0.2, suggesting that the eruption was efficient (close to the ideal ratio of 0.3) (Wohletz & Sheridan 1983). The absence of an associated magmatic phase from the Onewhero tuff ring vent also suggests that the interaction between the magma and water was continuous and that the ascending magma ceased before the water supply. All basaltic volcanic products sampled from Onewhero tuff ring (alkali olivine-basalts), Onewhero cone and the nearby lava flow (hawaiites) can be categorised as Group A basalts (Cook 2002).

The basalt lava flow that underlies the waterfall on Miller Road stream could be from a distal source, such as a vent surrounding Onewhero, or from an early magmatic stage of the Onewhero vent. If the lava flowed over the same area before the tuff ring eruption, there would be a large amount of basalt blocks when the phreatomagmatic eruption broke through the lava flow, however this does not appear to be the case within the visible tuff deposits. The flow could also be from a proximal source, such as a vent on the outskirts of the Onewhero tuff ring. This would explain the lack of large basalt material in the tuff deposits. The thickness of the basalt at Maoa's waterfall could mean that the basalt reached a pre-existing valley that provided a place to pond the basalt. The basalt could also be an intrusive body that has been exposed and eroded.

Chapter Five: Bombay Volcanic Complex

5.1 Introduction

The Bombay volcanic complex (BVC) was formed 1.0 – 1.2 million years ago (Alloway *et al.* 2004), as dated from a tephra layer at the base of one of the tuff rings present in the quarry (Fig. 5.1). The volcanic complex is the product of many eruptions and consists of at least one tuff ring, a tuff cone, numerous scoria and spatter cones, and at least two large deposits of ponded basalt lava (Fig. 5.2). A second source of basalt lava has been found to the north of the first. This chapter will cover the geology of the area and the history of the quarry. Several lithologic facies and their stratigraphy have been identified within an exposed tuff ring. The componentry of the basaltic tuff deposits will be discussed as well as the stratigraphic variation. The chapter will be summarised with a discussion of emplacement processes and eruption history.

5.2 Country rock geology

The Tauranga Group formed in the Late Miocene to Pleistocene, and unconformably overlies the Waitemata Group (Edbrooke 2001). The Tauranga Group rocks consist of alluvial sediments rich in Taupo pumice deposits (Edbrooke 2001). Valleys have eroded the volcanic material in the area to expose both Tauranga and Waitemata Group (Fig. 5.2) rocks (GCNZ Consultants 1990; John O'Brien Associates *et al.* 1994). Drill hole data have identified the underlying contacts with the quarry basalt deposit to be Tauranga Group in some places, and Waitemata Group in others (John O'Brien Associates *et al.* 1994).

The Otaian Mercer Sandstone of the Waitemata Group outcrops in the BVC area. Alluvial deposits deposited on the Waikato River floodplain underlie the basalt in this area (Edbrooke 2001). A large cliff has been cut within Bombay Quarry that exposes 50 m of tuff ring rim. At the base of the cliff is a sedimentary layer that is exposed for 0.72 m. The layer is very well sorted and massive with an undulating upper contact (Fig. 5.1).

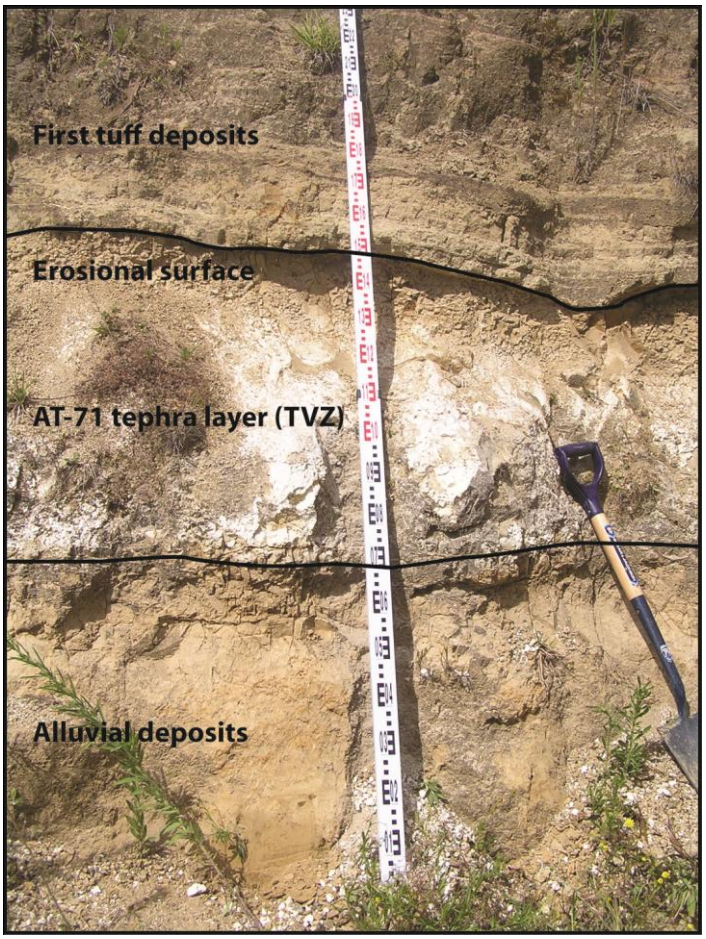

Figure 5.1: Bottom: alluvial sediments underlying the AT-71 tephra bed from the Taupo Volcanic Zone. Top: wavy bottom contact of first tuff beds suggest an erosional surface has been formed before first deposition of tuff beds.

5.3 Bombay volcanic complex

The BVC is situated in the eastern side of the SAVF (Fig. 2.3). The complex is 4.2 km NW of Pokeno and 3.4 km SSW of Bombay. The BQVC represents a complex eruptive history (Alloway *et al.* 2004).

The Bombay Quarry has been excavated into a large area of ponded basalt lava, and has uncovered columnar jointed, sheeted and massive basalt, as well as many scoria and spatter cones above and within the basalt deposit. A large section through a tuff ring has been exposed during quarrying (Fig. 5.3a). The tuff section is on the western side of the quarry and exposes a 50 m cliff of bedded tuff, topographically higher than the basalt lava flow and scoria and spatter cones (Fig.

5.3b). A tephra layer occurs at 0.74 m from the base of the tuff cliff (Fig. 5.1). The tephra layer is a normally-graded fall unit 0.48 m thick. Alloway *et al.* (2004) suggested that the tephra layer AT-71 was derived from the Taupo Volcanic Zone, between 1 and 1.2 million years ago. The tephra layer is correlated with the post-Ongatiti tephra layer AT-47 at Schnapper Rock in Beachlands. On the eastern side of the Bombay Quarry a light grey sedimentary unit has been exposed, and is comprised of unconsolidated sands. Scoria cones have been deposited in between basalt lava flows and have also been exposed by small circular failures of the quarry walls. A second large deposit of basalt lava has been identified to the north of the quarry, named Jones Block. Holcim began taking off the overburden in 2010 and have since uncovered scoria overlying thin clayey basalt flows and tuff deposits. The proposed outline for Jones Block is separate from that of Bombay Quarry. Ridge Road tuff ring is situated to the south of the Bombay Quarry tuff ring - the tuff ring rims appear to slightly overlap (Fig. 5.2).

5.4 Quarry history

The BVC is being quarried for its basalt lava aggregate by Holcim Aggregates. The quarry was previously known as Milburn Quarry before Milburn NZ Ltd was renamed to the brand of its Swiss parent company, Holcim, in 2002. Bombay Quarry obtained consents to start quarrying in 1993, and quarrying started in 1996 (Fig. 5.4) (Miller 2007). The quarry is one of the last remaining quarries still able to supply Auckland with basalt aggregate, which is mainly used for concrete and roading. The quarry begins approximately 900 m west of State Highway 1. The quarry is currently approximately 500 m wide at its widest point; however this is constantly changing as the quarrying progresses. Holcim expects Bombay Quarry to last for about 2 more years before the basalt lava is depleted.

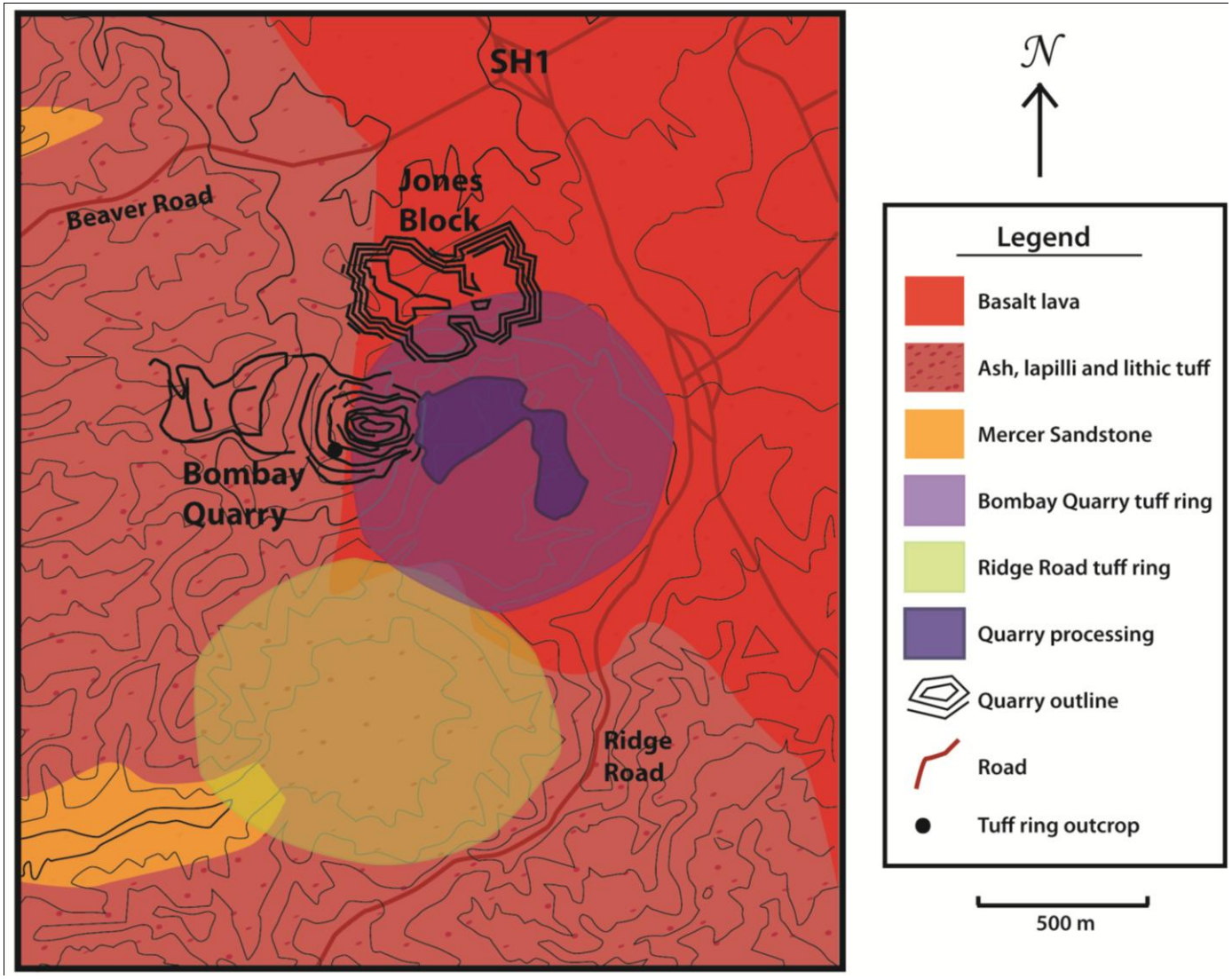

Figure 5.2: Geological map of BVC and Ridge Road tuff ring to the south (Edbrooke 2001; Holcim (New Zealand) Ltd 2007).

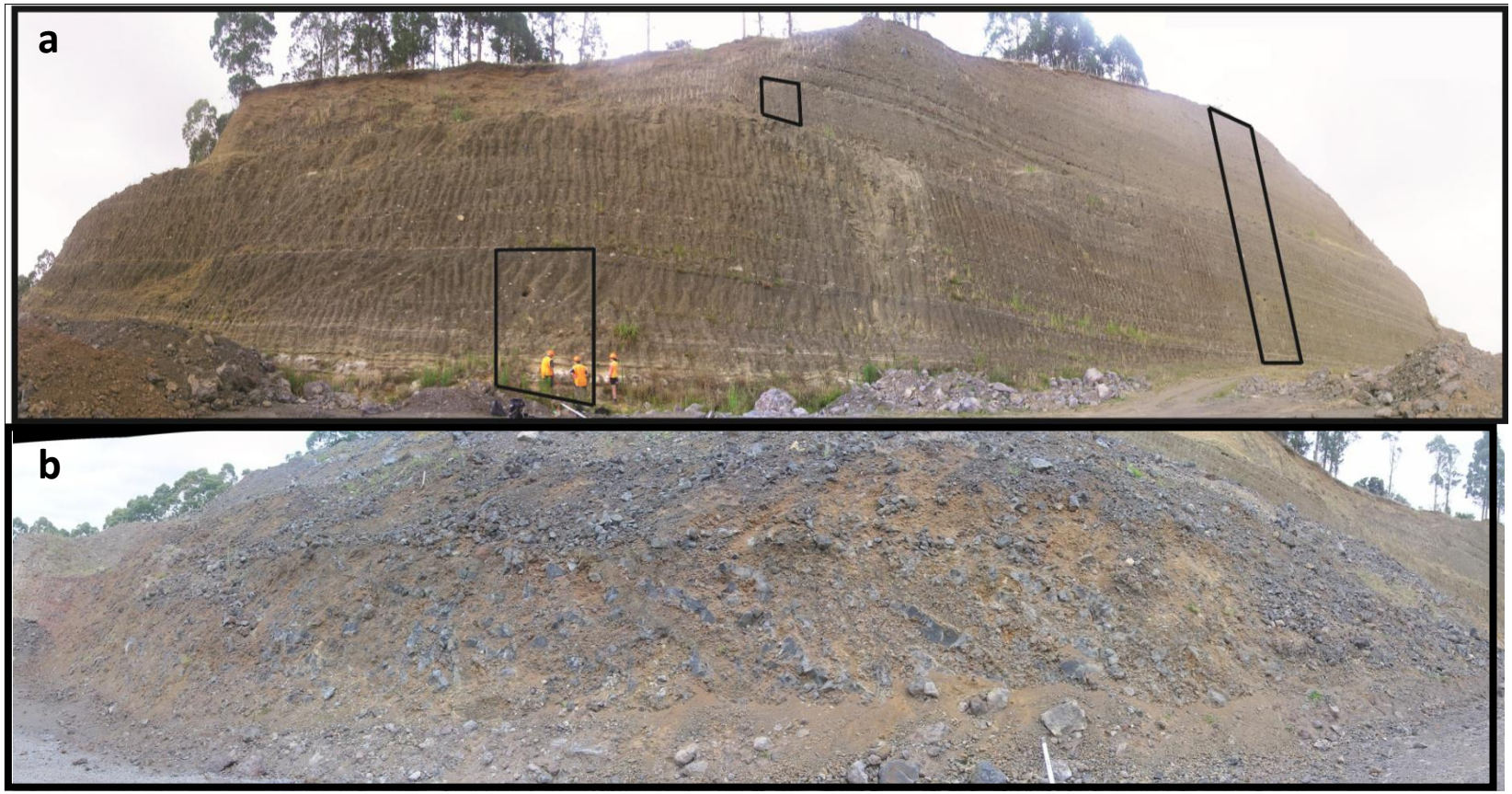

Figure 5.3: (a) 50 m high tuff cliff exposed on the western side of Bombay Quarry with areas used for stratigraphic log; (b) Spatter cone deposit with tuff cliff to right.

Holcim Aggregates have hired several companies to provide geotechnical surveys and report on the basalt sources. (Ormiston Associates Ltd 1999) has identified the underlying layers in the area of the Bombay Quarry using several logged drill cores. The layers found from top to bottom are: Upper tuff, scoriaceous basalt, rubbly basalt, clayey basalt flow, high strength basalt flow, mixed tuff/basalt breccia, lower tuff, discontinuous Tauranga Group, and Waitemata Group. (John O'Brien Associates *et al.* 1994) also used drill hole data and found the units underlying the basalt source to be Tauranga and Waitemata Groups, which had been heat-altered where direct contact with the lava had occurred (Ormiston Associates Ltd 1999).

The presence of tuff found at the base of some drill holes (John O'Brien Associates *et al.* 1994; Ormiston Associates Ltd 1999), suggests the occurrence of a phreatomagmatic eruption prior to the eruption of the basalt lava which underlies the exposed tuff ring at the surface. Ormiston Associates Ltd (1999) describes the resulting deposits to have formed a tuff cone. Due to the presence of scoria found at the base of some drill holes, John O'Brien Associates *et al.* (1994) suggests that there was an original scoria cone which is represented by the trig point between Ridge and Beaver roads. Using typical scoria cone angles, they suggest that the scoria cone was originally at least approximately 80 m higher. John O'Brien Associates *et al.* (1994) have also identified lava flows that have occurred after the eruption of the early tuff cone. They note that lava ponded/upwelled inside the tuff cone (forming the mined basalt source), which eventually flowed around the scoria cone and overflowed the sides of the tuff cone. The pre-existing topography of the underlying Tauranga and Waitemata Groups have partially affected the flow patterns of the basalt flow and have partially provided boundaries or limits to the flow (Ormiston Associates Ltd 1999). The lava that overflowed the sides of the tuff cone flowed to the west, north and southeast of the crater. The west and north flows are separate since drill logs made by John O'Brien Associates *et al.* (1994) to check for basalt and later for groundwater, showed no presence of basalt, and eventually drilled into the Waitemata Group. The scoria cone prevented the lava flows from flowing directly behind it, and the flows to the west were confined and small. The flows to the north are much thinner and spread over a larger area, in at least 3 separate flows.

John O'Brien Associates *et al.* (1994) also reports that the flow to the southeast has been overlain by a thick tuff sequence, further suggesting that the scoria cone was then destroyed by a later tuff ring explosion. Deposits of the tuff ring are visible in the exposed tuff ring rim (Fig. 5.3a), which is 60 m thick in places and overlies the remnants of the scoria cone.

The tuff ring has been breached on its south-western side by streams, and this erosion has affected the softer tuff deposits and has caused the harder volcanic materials to be elevated on ridges (GCNZ Consultants 1990; John O'Brien Associates *et al.* 1994; Manville *et al.* 2009). Due to the stream erosion the valleys on either side of the tuff ring ridge have been over-steepened and have made them susceptible to landslide failure (John O'Brien Associates *et al.* 1994).

The ponded basalt lava is around 70 m thick in its centre, and the upper 10 to 15 m is highly vesicular with clay-filled joints (GCNZ Consultants 1990). According to Ormiston Associates Ltd (1999), the highest quality basalt is at the core of the ponded mass within the first tuff cone. The high quality basalt in the centre of the resource is grey-black, fine to coarse grained, with high to extremely high strength, and is mostly free of defects such as clay or high vesicularity, with columnar jointing in some places (Ormiston Associates Ltd 1999). Around the high quality basalt is concentrically less quality basalt. The outer basalt becomes rubbly, highly vesicular and more affected by clays and weathering, with a higher number of fractures and lower rock mass strength (Ormiston Associates Ltd 1999). The outer basalt has also been mixed with tuff and lithics.

A second source of basalt has been found to the north, and a second quarry has been planned, called Jones Block (Fig. 5.5). The basalt occurs as four discrete flows, up to 40 m thick (John O'Brien Associates 1999). Holcim began combing off the overburden in 2010, and expect to reach mineable basalt in 2011. The basalt in Jones block is elevated with respect to that in the existing quarry, and the basalt is more weathered, with fractures and clay linings (John O'Brien Associates 2000).

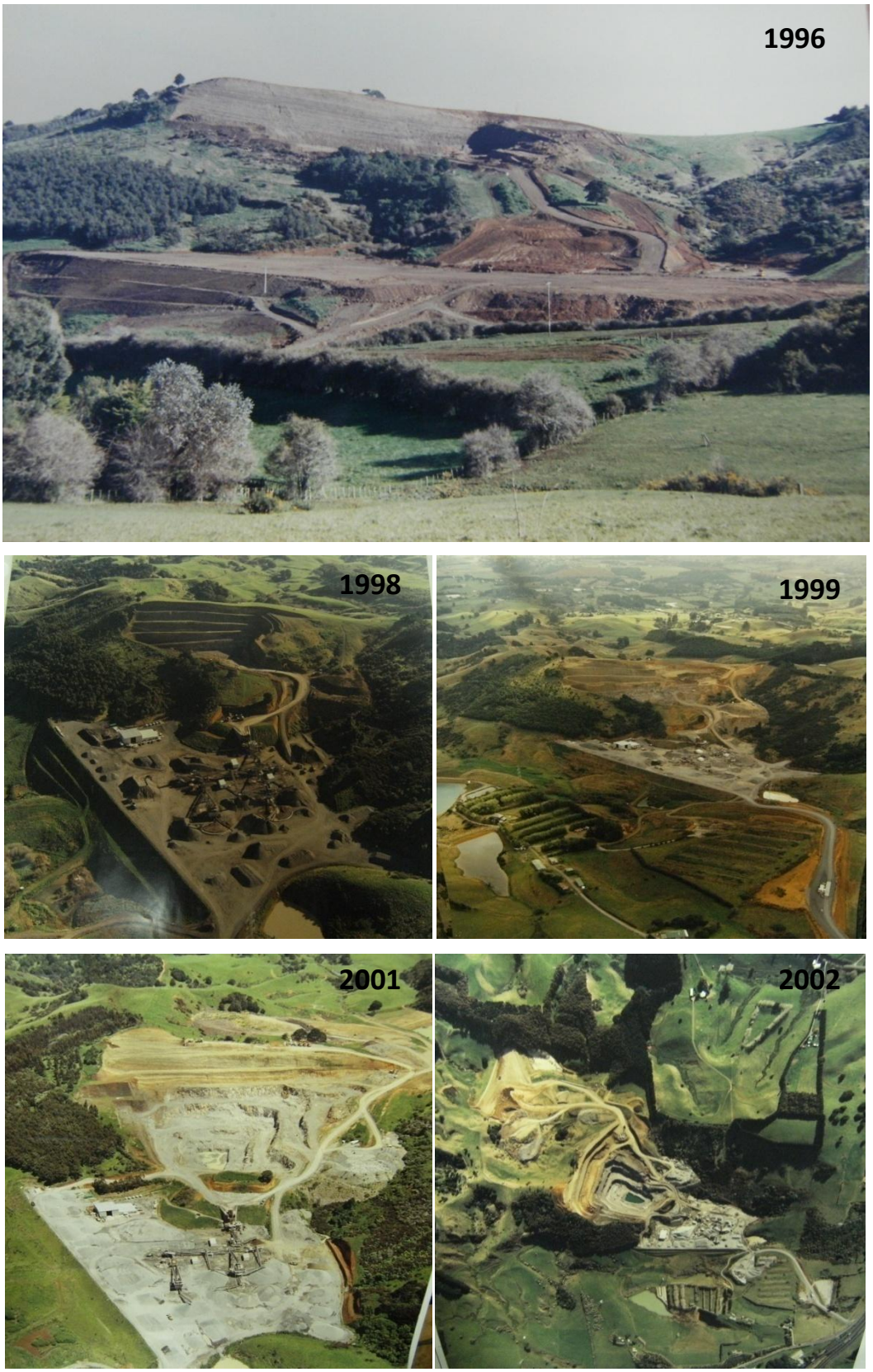

Figure 5.4: History of the excavation of Bombay Quarry from 1996 to 2002, from Holcim Aggregates (2010).

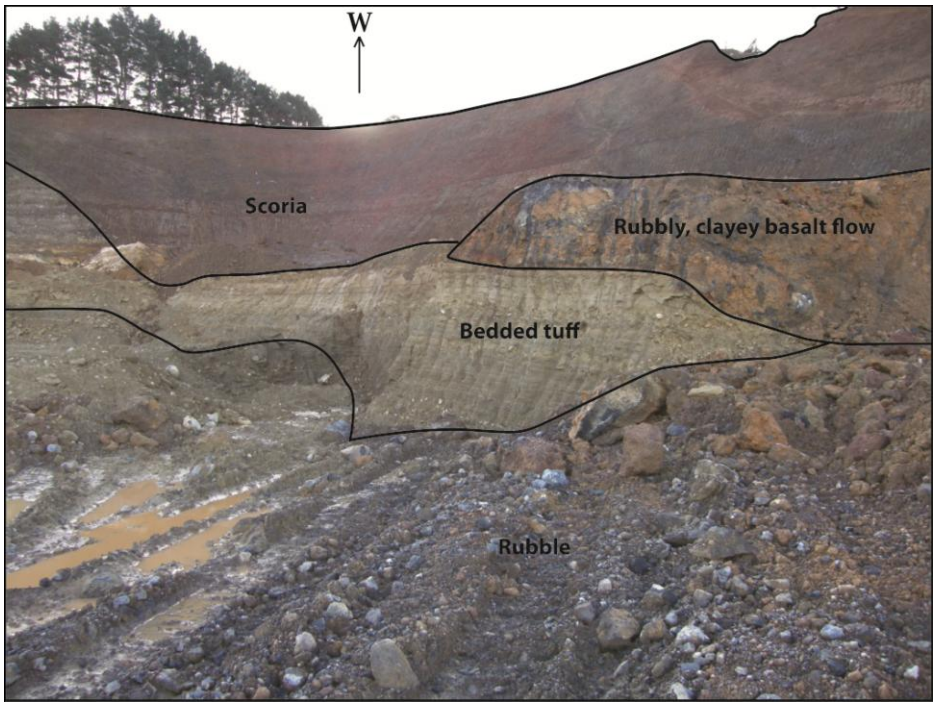

Figure 5.5: Jones Block Quarry after partial excavation of overburden, with scoria and a thin basalt flow overlying tuff deposits (pers. comm, Keith Miller 2010).

5.5 Facies and stratigraphy

5.5.1 Bombay Quarry tuff ring

The Bombay Quarry tuff ring is exposed on the southeast face of the Bombay Quarry in a 50 m high cliff, above the level of the basalt lava being mined (Fig. 5.2). The exposed tuff ring is the result of the latest phreatomagmatic eruption. The stratigraphy of the tuff ring and stratigraphic facies distribution can be seen in Fig. 5.6. Two facies have been identified in the 50 m tuff ring succession: a well sorted coarse ash to fine lapilli facies and a poorly sorted coarse lapilli facies.

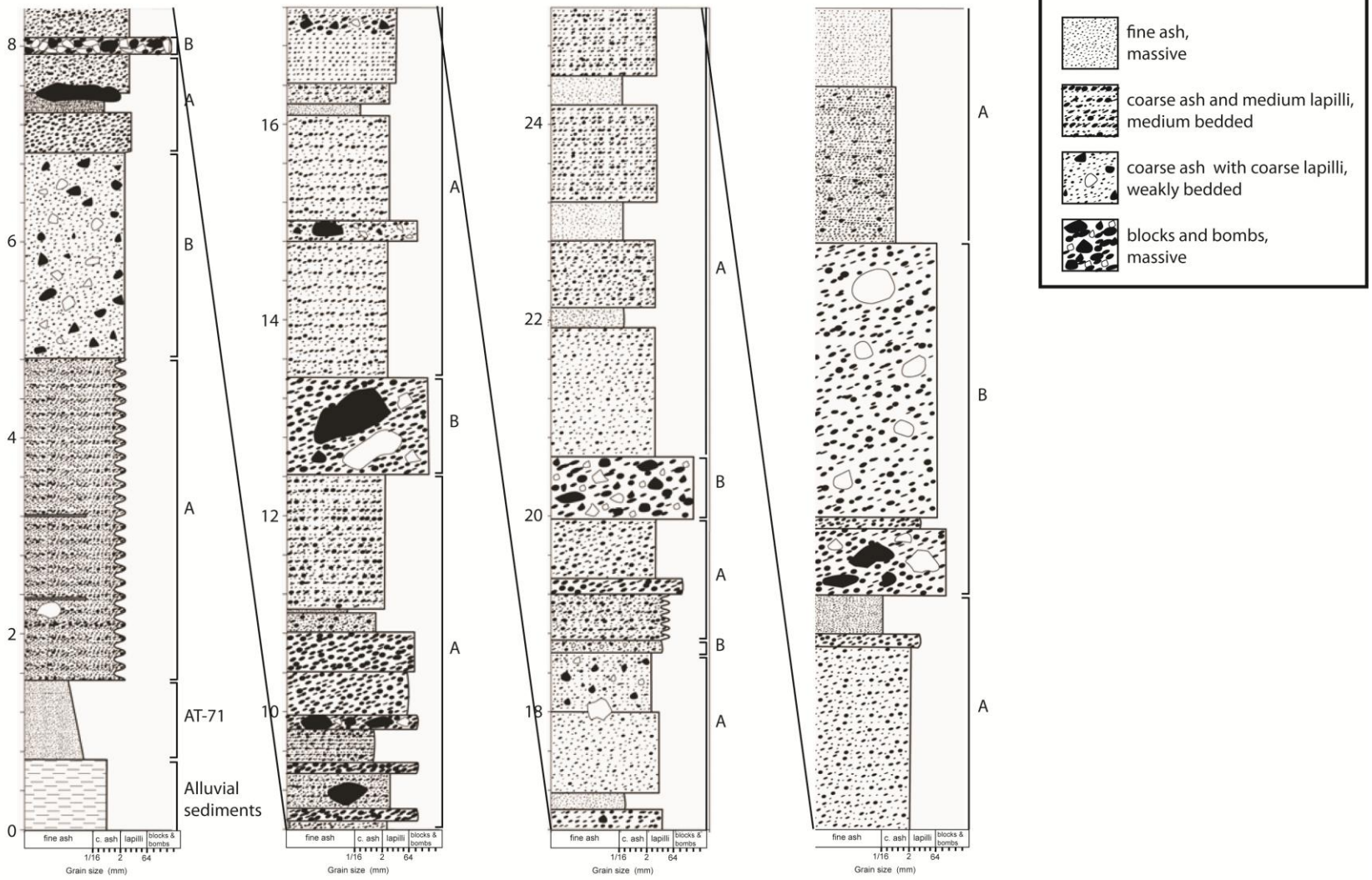

Figure 5.6: Facies and stratigraphy of the exposed 50 m cliff of Bombay Quarry tuff ring.

5.5.2 Tuff ring facies

Facies A - well sorted coarse ash to fine lapilli

Facies A is generally a medium to well sorted, medium and well bedded coarse ash to fine lapilli facies (Fig. 5.7, 5.8). Grainsize ranges from light coloured, fine ash to occasional blocks and bombs. Isolated blocks and bombs occur throughout the section. Angular dense basalt blocks occur, up to 105 mm long. Subangular vesicular ballistic basalt blocks occur up to 20 cm long, and are impacted into underlying fall deposits. Angular to rounded ballistic lithics of both siltstones and sandstones occur up to 70 cm long, and also show impact structures. Coarse lithic concentration layers 20 cm thick occur with white lithic blocks and coarse lapilli set into fine lapilli to coarse ash with medium bedding. Coarse lithic-rich lapilli occur in layers up to 40 cm thick. Medium lapilli layers are up to 40 cm thick, rich in sub-rounded lithics and some angular basalt clasts. Fine lapilli layers also occur, and are rich in scoria clasts, well sorted, and up to 40 cm thick. Coarse ash to very fine basalt and scoria lapilli layers are diffusely to well bedded and are well sorted. Dark coarse ash occurs with fine lapilli, medium bedded with approximately 2-3% white lithics. Beds of well sorted, medium coarse ash of predominantly weathered orange scoria fragments with white rims, alternate with beds of very fine and fine lapilli moderately to well sorted. Coarse ash and lapilli couples range from 4-14 mm, and are thinly bedded. Coarse ash also occurs with medium lapilli clasts and lithics, medium bedded and moderately sorted, with some laminated layers that pinch out. Fine, white ash appears massive in layers up to 20 mm thick.

Facies B - poorly sorted coarse lapilli

Facies B is generally a poorly sorted, diffusely bedded coarse lapilli facies (Fig. 5.7, 5.8). Grainsize ranges from coarse ash to blocks and bombs concentrated in layers. Blocks and bombs of subangular to angular juvenile clasts (Mc: 50 cm) and lithics (Ml: 70 cm) occur in concentrated layers up to 60 cm thick with no bedding.

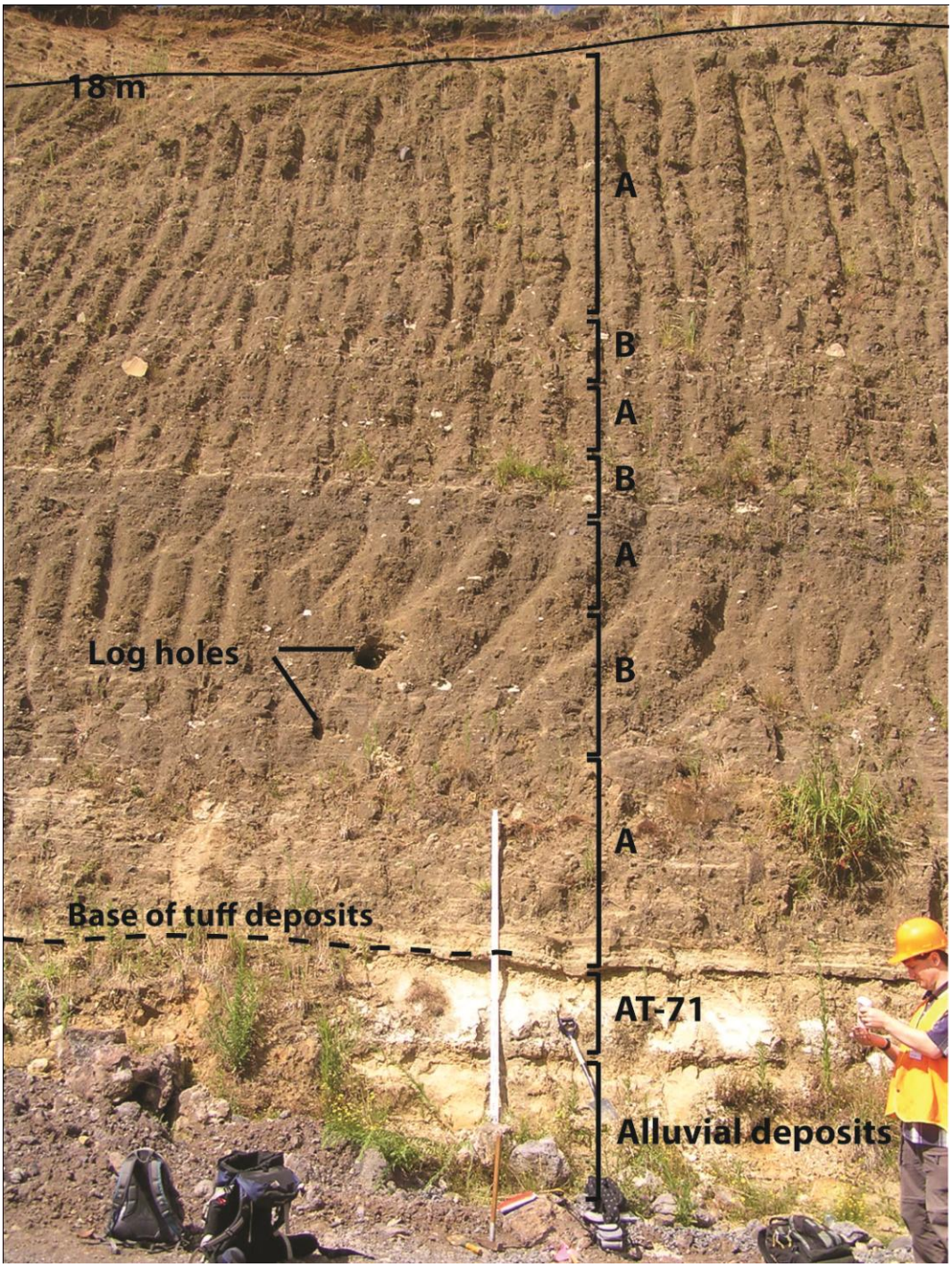

Figure 5.7: Base of tuff cliff showing alluvial deposits overlain by AT-71 tephra layer. First tuff deposits (dashed line) are shown above tephra layer. Stratigraphy of facies A and B is shown in 18 m of outcrop.

Coarse lapilli and angular blocks and bombs of lithics and juvenile clasts up to 1 m long occur in concentrated layers up to 1 m thick. Coarse lapilli also occur as 20 cm thick lithic-rich layers. Medium to coarse lapilli form medium bedded and poorly sorted layers of dark basaltic juvenile clasts and light lithics

with occasional sub-rounded basaltic bombs approximately 50 cm long, and up to 1 m. Fine lapilli occur as scoria-rich 30 cm thick layers. Dark coarse ash and very fine lapilli occur as crudely bedded, nearly massive, poorly sorted layers with coarse subangular scoria lapilli (Mc: 58 mm) and dark juvenile subangular clasts approximately 5% of unit (Mc: 60 mm).

5.5.3 Tuff ring facies stratigraphy

The stratigraphic variation of facies within the exposed tuff ring section can be seen in Fig. 5.6. Facies A occurs in packages from 1 m to 10.4 m thick. Facies B occurs in packages from 0.1 m to 9 m thick. Both facies A and B alternate in this exposed section.

5.5.4 Basalt flow, scoria and spatter facies

A panoramic photo and sketch of the Bombay Quarry (Fig. 5.8) shows Facies C and D, as well as the area of Jones Block where overburden is being combed off.

Facies C - juvenile basalt

Facies C is a juvenile basalt facies. The intact basalt was inaccessible, however basalt that had been mined from the eastern side of the quarry was accessed and analysed (Table 5.1). The structures within the basalt include columnar basalt (Fig. 5.9, 5.10) of varying sizes and development, as well as sheeted basalt (Fig. 5.9, 5.11).

Facies D - juvenile scoria and spatter

Both scoria and spatter cones were present above and between the lava flows. The scoria cones were inaccessible. Spatter cone deposits ranged in size from 5 cm to 1.62 m long (Fig. 5.12). The spatter is highly vesicular (49 – 65%) with vesicles up to 25 mm becoming larger toward the centre of each spatter deposit. The spatter sits within approximately 5 – 10% coarse ash matrix.

Figure 5.8: Panoramic photo and sketch of geological features in Bombay Quarry. Photo and sketch are facing east (north is to the left and south is to the right of the photo).

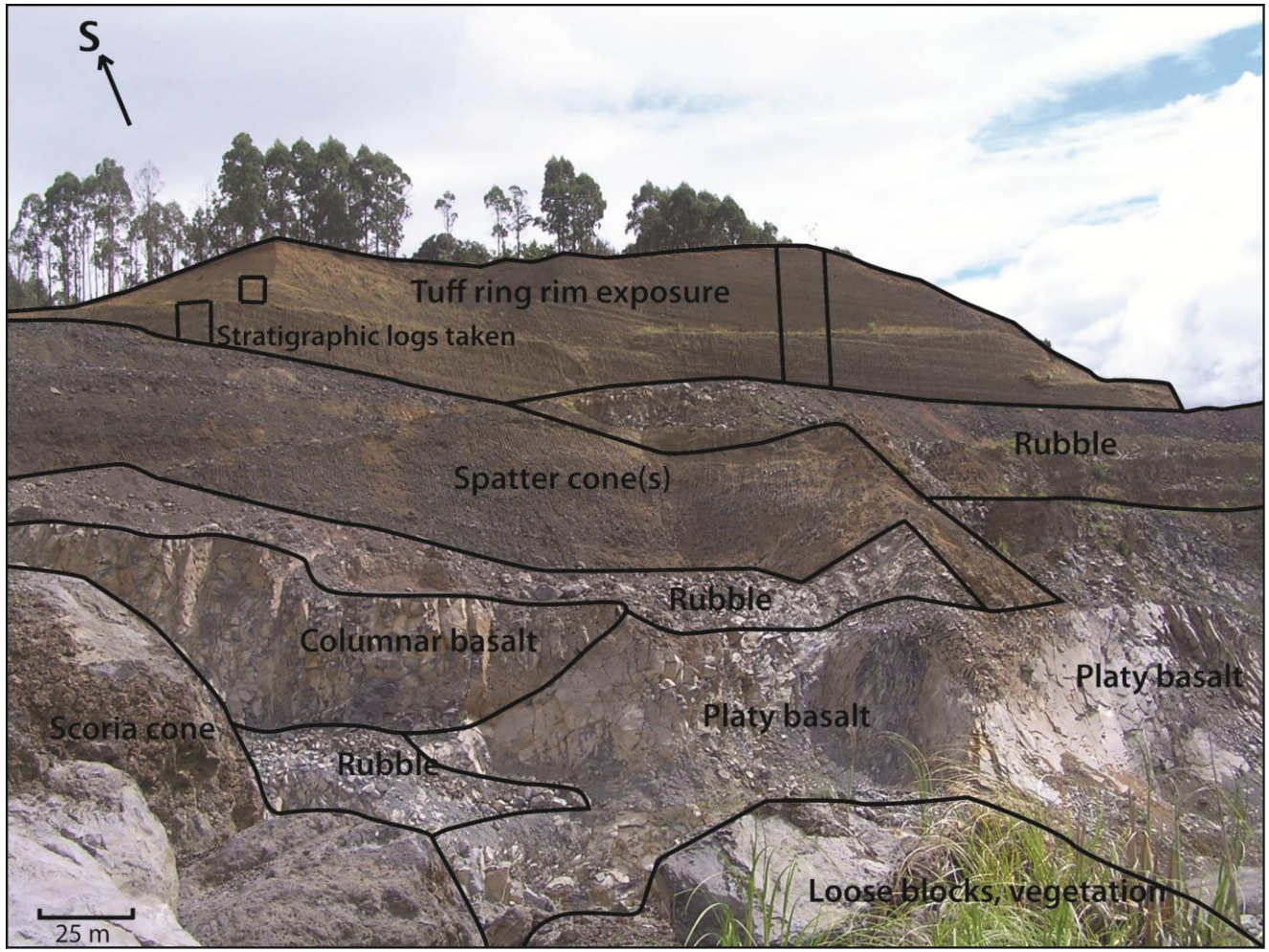

Figure 5.9: Scoria and spatter cones within basalt flows with both columnar and platy basalt types, with overlying tuff ring.

Figure 5.10: Columnar basalt from inner quarry surrounded by basalt rubble (facies C).

Figure 5.11: Sheeted basalt from inner quarry surrounded by basalt rubble (facies C).

Figure 5.12 Elongated spatter lens from a spatter cone on the western side of the quarry (Facies D)

5.5.5 Basalt geochemistry

The geochemistry of basalt from the Bombay volcanic complex has been compared with the nearby Ridge Road tuff ring (Table 3.2). The $Na_2O + K_2O$ wt% have been compared to SiO_2 wt% in order to distinguish between group A and group B basalt types. In Fig. 5.13 representative data for Bombay tuff ring and the nearby Ridge Road tuff ring were identified as group B. Fig. 5.14 compares Zr/Nb ratios with Nb (ppm), and also identifies the data as group B.

Group B represents a basanite to hawaiite group, and is derived from the upper mantle (Cook 2002). The data below suggests that magma sources from the Bombay tuff ring was generated in the upper mantle.

Table 5.1: XRF geochemical data of basalt from the Bombay Quarry. *RRTR*: Ridge Road tuff ring sample boulder from edge of tuff ring, *BQPL*: Bombay Quarry sample from ponded lava, *BQSP*: Bombay Quarry sample from spatter, *BQTR*: Bombay Quarry clast juvenile from tuff ring, BQCB: Bombay Quarry columnar basalt (sample W2011638), BQTR: Bombay Quarry basalt block from tuff ring (sample W2011590). Sample geochemical data with labels in italics are from Cook (2002).

Sample	***RRTR***	***BQPL***	***BQSP***	***BQTR***	**BQCB**	**BQTR**
	basanite	ne-hawaiite	ne-hawaiite	alkali-ol basalt		
Major elements						
SiO_2	42.77	47.64	47.46	48.19	48.35	47.94
TiO_2	2.94	2.4	2.51	2.29	2.47	2.44
Al_2O_3	12.6	14.92	14.81	15.32	15.18	14.87
Fe_2O_3	14.53	13.24	14.12	13.15	13.04	13.28
MnO	0.19	0.19	0.20	0.19	0.18	0.19
MgO	11.5	6.46	6.66	6.36	5.93	6.58
CaO	10.22	8.06	8.23	7.98	7.91	8.02
Na_2O	3.04	4.61	3.56	3.91	4.56	3.81
K_2O	1.28	1.9	1.76	2.03	2.04	1.86
P_2O_5	0.64	0.77	0.76	0.79	0.73	0.78
Total	99.71	100.18	100.06	100.21	100.38	99.76
LOI	0.10	-0.14	0.76	0.90	0.14	0.24
Trace elements						
Sc	21	15	18	16	-	-
V	288	175	215	177	169	170
Cr	326	194	228	159	151	200
Ni	240	97	158	90	77	126
Cu	67	61	57	58	64	51
Zn	104	101	131	129	94	114
Ga	23	28	26	27	27	26
As	2.6	-	-	-	-	-
Rb	20	30	27	33	32	27
Sr	666	888	883	1300	833	844
Y	25	30	30	32	22	24
Zr	231	367	350	410	385	368
Nb	43	56	58	65	59	59
Ba	214	363	288	548	260	373
La	37	53	45	52	39	44
Pb	4.1	6.6	4.1	5.5	6.0	4.9
Ce	82	97	91	94	85	86
Th	3.8	6.3	4.7	6.8	6.9	5.9
U	1.1	2.2	0.3	4.4	1.9	1.7
Group	**B**	**B**	**B**	**B**	**B**	**B**

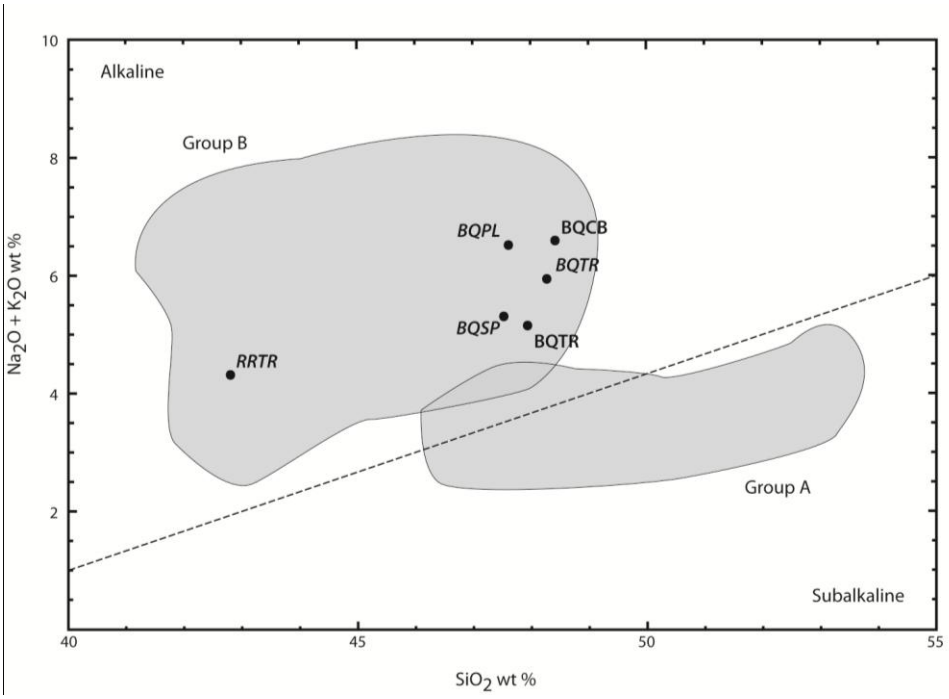

Figure 5.13: $Na_2O + K_2O$ wt% against SiO_2 wt%, with typical boundaries of Group A and B basalt from the SAVF (Cook 2002). Labels in italics are from Cook (2002).

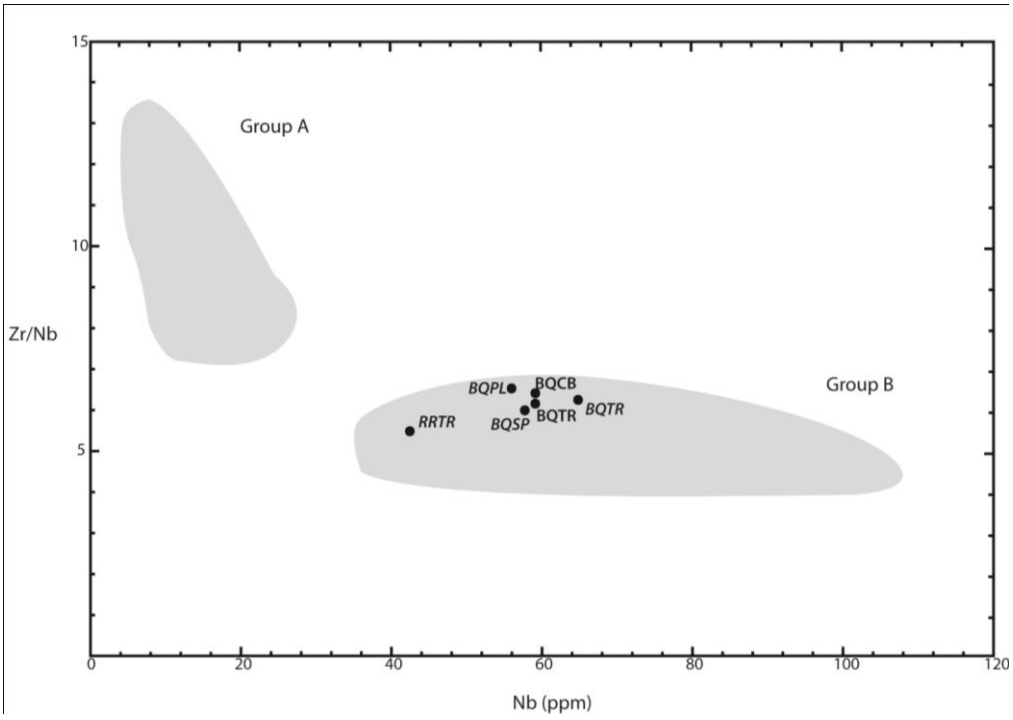

Figure 5.14: Zr/Nb ratio against Nb (ppm), with typical boundaries of Group A and B basalt from the SAVF (Cook 2002). Labels in italics are from Cook (2002).

5.6 Componentry

5.6.1 Tuff ring

Juvenile basalt clasts

Basalt clasts within the tuff deposits are angular to subangular and range in vesicularity from 30 to 55%. Two main types of porphyritic basalt clasts are present within the tuff: basalt with olivine, pyroxene and few plagioclase phenocrysts in a slightly devitrified glass and plagioclase lath hypocrystalline groundmass with titanomagnetite, and crystalline basalt with olivine and titanaugite phenocrysts in an intergranular groundmass of plagioclase, small olivines, small augites and titanomagnetite (Fig. 5.15a). Olivine phenocrysts are up to 0.35 mm and are commonly altered to red iddingsite. Some subhedral olivine phenocrysts are broken or embayed. Titanaugite phenocrysts have purple rims and occasionally have resorbed centres. Plagioclase phenocryst laths are up to 0.175 mm.

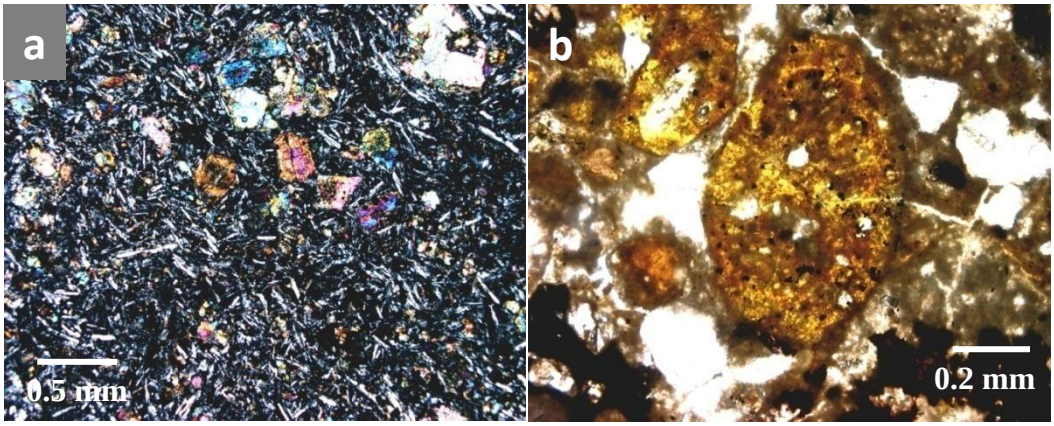

Figure 5.15: (a) hypocrystalline olivine basalt with altered subhedral olivine and subhedral pyroxene phenocrysts in a plagioclase lath and anhedral olivine intergranular groundmass, viewed under XPL (sample W2011590); (b) common anhedral orange scoria clasts with olivine and pyroxene phenocrysts, and euhedral to subhedral olivine crystals, anhedral titanomagnetite and ash size calcareous lithics (sample W2011587).

Scoria

Porphyritic scoria clasts within the tuff deposits are subrounded to rounded and orange to brown in colour (Fig. 5.15b). Phenocrysts include euhedral to subhedral olivine commonly altered to iddingsite, and occasional titanaugite. The phenocrysts are set in an intergranular groundmass of glass and plagioclase laths.

Crystals

(a) Juvenile crystals

Olivine crystals are anhedral to euhedral, sometimes embayed, up to 0.085 mm, and commonly altered to red iddingsite on rims and cores. Small plagioclase laths occur up to 0.05 mm.

(b) Xenocrysts

Quartz is the most common xenocryst within the tuff deposits occurring as anhedral grains up to 0.1 mm. Rare euhedral hypersthene xenocrysts occur up to 0.38 mm.

Lithics

Several types of lithic fragments occur within the tuff deposits. Lithics that resemble Koheroa Siltstone are fine, well sorted light grey calcareous siltstone with little to no fossils and occasional anhedral quartz grains. Lithics that resemble Mercer Sandstone are fine, well sorted light grey calcareous siltstone to sandstone with Otaian planktic and benthic foraminifera and occasional anhedral quartz grains. Rare, small fragments of non-calcareous, quartz-rich sandstone occur that may originate from a quartz-rich section of Koheroa Siltstone. Lithic fragments commonly had dark brown pyrite staining occurring sparsely throughout the lithic or as concentrated dark veins.

5.6.2 Dense basalt

The basalt deposit being mined is a dense, hypocrystalline, fine grained porphyritic olivine basalt. The basalt deposit contains olivine and pyroxene

phenocrysts within fresh glass and plagioclase lath hyalopilitic groundmass. Olivine phenocrysts are altered to iddingsite rims (Fig. 5.16) and are occasionally embayed, and common pyroxene phenocrysts are occasionally zoned.

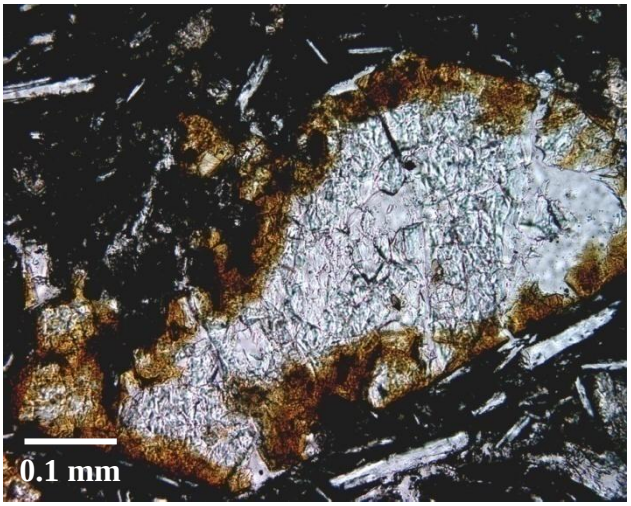

Figure 5.16: Broken olivine phenocryst with altered iddingsite rims within plagioclase and glass hyalopilitic groundmass (sample W2011602).

5.6.3 Scoria and spatter

The scoria within the multiple scoria cones has olivine phenocrysts commonly altered to iddingsite and occasionally embayed, in a glass and plagioclase lath hyalopilitic groundmass. The spatter within the multiple spatter cones has fresh olivine phenocrysts that are occasionally broken; up to 0.35 mm. Elongated purple titanaugite phenocrysts are common. Plagioclase phenocrysts also occur up to 0.175 mm. The groundmass is devitrified glass with plagioclase laths.

5.7 Stratigraphic variation

The tuff ring deposits exposed in the quarry cliff face show stratigraphic changes that reflect changes in the eruption style. Grainsize variation is shown in Fig. 5.17, and ranges from fine ash to blocks and bombs, both of which are present throughout the outcrop. Overall, the outcrop generally fines upward with

stratigraphic height. The lower third of the outcrop mainly ranges from coarse ash to blocks and bombs. The middle third of the outcrop mainly ranges from fine ash to coarse ash and is generally finer than the lower third of the outcrop. The upper third of the outcrop ranges from fine ash to blocks and bombs, and shows a trend of fining upwards. Componentry of the tuff ring deposits is illustrated in Fig. 5.17. In general, juvenile material is dominant throughout the tuff ring, however for the first 5 m exposed, juvenile material, lithic material and crystals are approximately equal in abundance. A general trend is evident of a gradual increase in juvenile material and a gradual decrease in lithics. Vesicularity changes with stratigraphic height are given in Fig. 5.17. Over the first 20 m a general increase in vesicularity is apparent, as vesicularity increases from 30 to 55%. Changes in lithic type within tuff deposits occur with height (Fig. 5.17). In the lower 10 m of the outcrop, Koheroa Siltstone lithics are dominant; however from 10 m to 20 m proportions of Mercer Sandstone and Koheroa Siltstone lithics are approximately equal. There is a general trend of Mercer Sandstone lithics increasing over the first exposed 20 m.

5.8 Discussion

5.8.1 Emplacement processes

Facies A is considered to represent a fall-dominated phase and is dominantly finer grained than facies B. Fallout has deposited well sorted, weakly bedded tuff. Alternating coarse and fine material with weak bedding may represent intermittent, non-sustained eruption pulses causing variation in the fallout rate (Houghton *et al.* 2000; Németh & White 2003). Layers of fine ash in between coarser layers possibly represent periods where deposition is primarily from fallout from the eruption cloud (Houghton *et al.* 2000). Base surges have formed laminae of coarse ash that pinch out laterally. Uncommon ballistic fallout is represented by isolated juvenile blocks and bombs and lithic blocks. A sudden vent-clearing episode is evident around 2 m where fragmentation is shallow and lithics are predominantly Mercer Sandstone, followed by a gradual deepening of fragmentation where lithic proportion of Koheroa Siltstone increases.

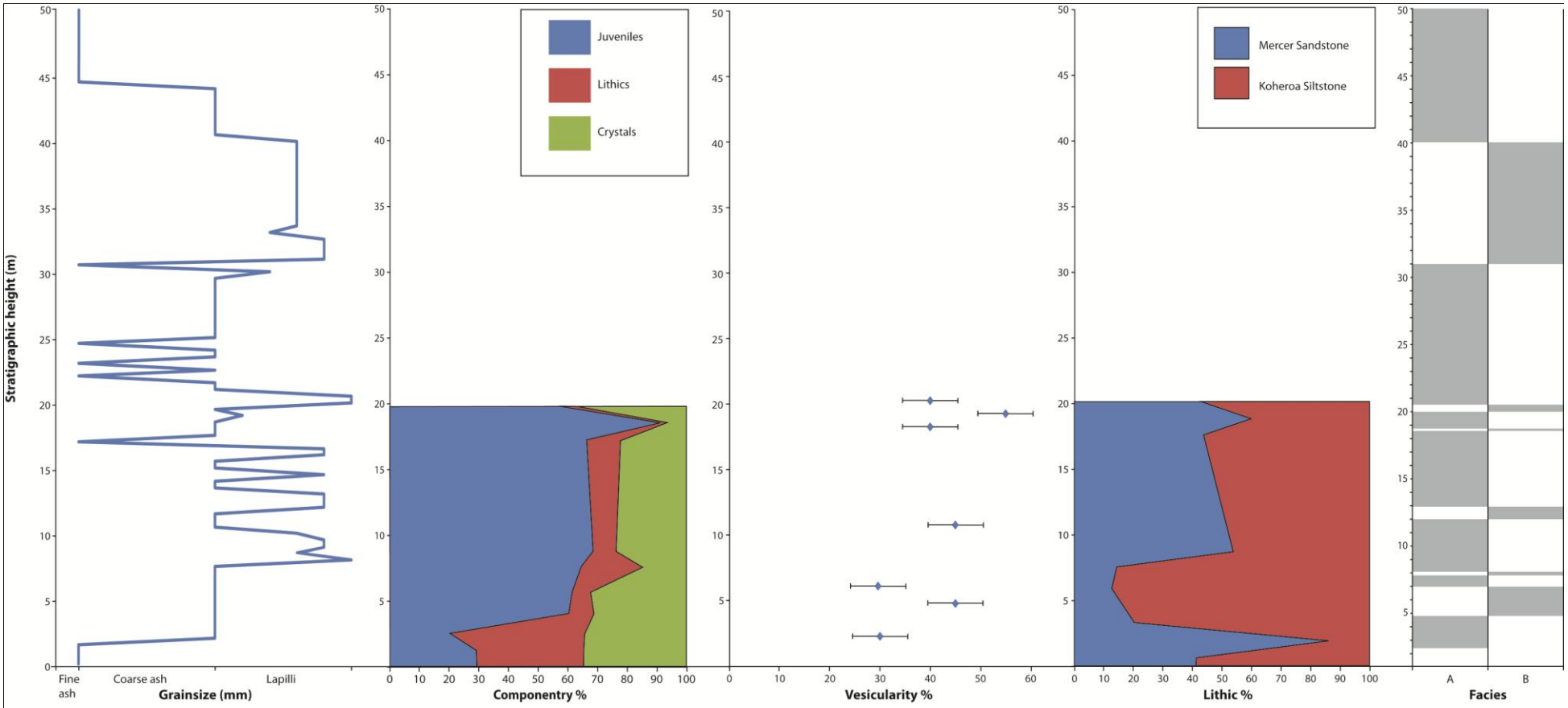

Figure 5.17: Variation with stratigraphic height throughout the 50 m exposed tuff ring succession.
Variation from left to right includes grainsize, componentry, vesicularity of juvenile clasts within tuff deposits, lithic type and facies.
Outcrop from 20 m to 50 m was inaccessible, and could not be sampled. Visual estimates were used to identify inaccessible grainsize.

This could possibly be due to changes in eruption energy or subsurface water depth. A peak in lithic content in the deposits from this facies at 3 m probably represents an increase in water content of the eruption (Houghton *et al.* 2000), followed by progressive increasing juvenile content. Changes in fragmentation depth and vent stability (Németh & White 2003) are evident with varying proportions of Mercer Sandstone and Koheroa Siltstone in this facies.

Facies B represents a fall-dominated phase and is dominantly coarser grained than facies A. Juvenile material is dominant throughout this facies, and its coarse nature represents an eruption with low water content and a low efficiency of fragmentation (Houghton *et al.* 2000). Low lithic proportions indicate a lessened interaction between magma and water content of the sedimentary rocks that make up the walls of the conduit (Houghton *et al.* 2000). Lithic type is mainly the lower Koheroa Siltstone around 6 m, representing a low fragmentation depth. At 8 m lithic type is mainly Mercer Sandstone, representing vent-clearing and fragmentation near the surface. Coarse lapilli lithic-rich layers represent vent clearing, as sedimentary rocks are fragmented by explosions (Fig. 5.7). Poorly sorted beds with weak to no bedding represent wet phases of the eruption and differing ejection angles where finer material is deposited by rapid fallout from eruption clouds at the same time as denser, coarser clasts (Houghton *et al.* 2000; Németh & White 2003).

Facies C represents a passive effusive lava flow that has ponded in the confined space of the original tuff cone. The mined centre of the ponded basalt body was massive with little to no jointing. The columnar basalt has formed on the outer edges of the ponded basalt where joints in the rock have formed as it cooled. The sheeted basalt represents either thin repetitive flows that have lined the tuff cone slopes, or perhaps the cooled shell around a lava tube-like feature.

Facies D has produced many scoria cones and spatter cones and represents many separate magmatic eruptions that occurred previously to the tuff ring eruption mentioned above, at a time where there was little to no water interaction with the rising magma (Cas 1989).

5.8.2 Eruption history

Before any eruptions occurred, the area of the BVC consisted of Waitemata Group and Tauranga Group country rock. A phreatomagmatic eruption occurred as rising magma interacted with the water-bearing sedimentary rocks or deposits. The eruption formed a tuff cone (Ormiston Associates Ltd 1999) that would have developed as rising magma interacted with a water-rich environment (Manville *et al.* 2009). A scoria cone formed on the western side of the tuff cone in a later magmatic eruption within the complex (John O'Brien Associates *et al.* 1994) at a time where the rising magma did not interact with external water. Effusive volcanism then occurred caused by a loss of gas from the magma before it was erupted. Lava ponded within the tuff cone from either a steady outpouring of lava, fire fountaining, or a mixture of both. Any spatter deposits from the fire fountaining could have agglutinated together and removed evidence of this (Cas 1989). Columnar basalt formed on the outsides of the ponded basalt as it cooled slowly on the outsides (Fig. 5.10). In some places, multiple layers of columnar jointing formed (Cas 1989). Sheeted basalt (Fig. 5.11) is also present where the basalt had formed lava tubes, or where the basalt was coating the pre-existing cooled lava.

The lava eventually overflowed the tuff cone rim, and flowed to the west, north and southeast, forming separate lava flows. This effusive eruption may have ceased due to a decrease in the discharge rate of the rising magma (Cas 1989). Spatter cones and scoria cones were then erupted by magmatic explosions during multiple Hawaiian and Strombolian eruptions (Cas 1989). Hawaiian eruptions are characteristic of basaltic volcanoes and their steady fire fountains can reach heights of over 300 m and can last from hours to days (Parfitt 2004; Houghton & Gonnermann 2008). Spatter cones would have been formed from eruptions nearby to the vent(s) as they represent shorter ballistic trajectories caused by lower initial gas contents and lower explosivities in comparison with those of scoria cones (Sumner *et al.* 2005), forming massive, agglutinated deposits. Scoria cones would have been erupted further away from the vent due to longer trajectories and higher explosivity (Sumner *et al.* 2005), forming massive deposits. Some spatter and scoria deposits were then overlain by lava flows (Fig. 5.8).

Figure 5.18: Spatter cone directly underlying alluvial deposits and AT-71 tephra layer, with overlying exposed tuff ring deposits (pers. comm. David Lowe 2010, photo from 2007).

Enough time passed after this to allow the sedimentation of Quaternary alluvial deposits and a tephra layer 1 - 1.2 million years ago above the magmatic deposits (Fig. 5.1, 5.18). A phreatomagmatic eruption occurred as rising magma interacted with a water source. The phreatomagmatic eruption was fall-dominated with few surges. The eruption began with pulsing jets and ballistic fallout (facies A). A vent clearing phase followed where lithic material surrounding the growing vent was ripped up and deposited (facies B). The eruption alternated between these two phases (Fig. 5.7). The late stages of the eruption were characterised by pulsing jets of fine material and few ballistics (facies A). Comparing juvenile and lithic proportions can provide an estimated water/magma ratio, which can be used to estimate the efficiency of the eruption. The estimated water/magma ratio of the Bombay Quarry tuff ring ranged from 0.2 to 0.3, suggesting that the eruption was highly efficient (Wohletz & Sheridan 1983). The eruption may have ceased due to either a decrease in the rate of supply of the rising magma, or a decrease in the external water available.

A second group of eruptions have occurred just north of the Bombay Quarry. This area is called Jones Block (Fig. 5.2), and also represents a complex eruptive history where a large basalt deposit occurs beneath the surface. This basalt deposit could have formed within a pre-existing tuff ring or cone, as the basalt deposit at Bombay Quarry did. This has been overlain by a tuff deposit, and then thin lava flows and scoria cones (Fig. 5.5) (John O'Brien Associates 1999). The time scale for both the BQVC and the centre represented by Jones Block to form both the phreatomagmatic and effusive types of volcanism present would have been long, over weeks to years (Houghton *et al.* 1999). All basaltic volcanic products sampled from Bombay Quarry (nepheline hawaiites and alkali olivine-basalts) and the nearby Ridge Road tuff ring (basanites) can be categorised as Group B basalts (Cook 2002).

It has been assumed that the source vent of the basalt lava that ponded inside the original tuff ring was in the same place as the vent for both known phreatomagmatic eruptions (tuff cone and tuff ring). However it is possible that the source vent of the ponded lava was from a distal source, perhaps the nearby (3 km) Bombay lava shield. In this case a lava flow would have travelled the distance from the Bombay lava shield to the Bombay Quarry tuff cone and proceeded to pond there.

Chapter Six: Discussion

6.1 Introduction

The eruptions of the Kellyville volcanic complex (KVC), Onewhero tuff ring and Bombay volcanic complex (BVC) have been compared in order to further understand the eruption styles and processes of the South Auckland volcanic field. The eruptions have been summarised in order to determine their controlling factors.

6.2 Eruptive styles and processes

Kellyville volcanic complex

The KVC began with an early phreatomagmatic eruption caused by the interaction of basaltic magma with a large volume of external water, resulting in a tuff ring. A later magmatic phase of the complex occurred, with Hawaiian eruptions creating two intra-tuff ring scoria cones (cf. Paulick *et al.* 2009). The entire eruption sequence occurred 1.48 million years ago, probably over weeks to years. The underlying country rock geology consists of the Mercer Sandstone and Koheroa Siltstone of the Waitemata Group.

The early stages of the tuff ring eruption involved fluctuating eruption intensities causing pulses in dominant rapid eruption cloud fallout and occasional base surges (cf. Németh & White 2003), as well as changes in the direction of the eruption column. Pauses in the eruption intensity and tephra output occurred intermittently (cf. Houghton *et al.* 2000). The vent stability varied and vent-clearing stages occurred intermittently, as magma interacted explosively with the subsurface water within the country rock (cf. Németh & White 2003; Nemeth *et al.* 2008). Isolated lithic blocks and juvenile clast block and bomb ballistics were common. Highly efficient magma-water interactions caused a high level of fragmentation. Fragmentation mostly occurred close to the surface (cf. Lorenz 2003) in the Mercer Sandstone at depths less than 26 m, with occasional deepening in the Koheroa Siltstone to depths up to about 50 m. The middle stages

in the development of the tuff ring eruption continued on in much the same manner, but with less vent clearing and more common base surges occurring. “Drier” (more magmatic) pulsating stages of the eruption were increased. The later stages of the eruption had steady magma-water interaction and very high levels of fragmentation due to its high water content. Intermittent lowering of fragmentation depth to about 50 m within the Koheroa Siltstone occurred. Pulsating explosions of fallout and alternating fallout and base surge deposition occurred (cf. Németh & White 2003). There was a general increase in lithic content towards the end of the eruption, suggesting an increase in magma-water interaction (cf. Németh & White 2003).

Overall, stratigraphic variations from bottom to top in the Kellyville tuff ring are characterised by a general decrease in grainsize, a general increase in lithic and external water content, eruption energy and fragmentation (cf. Houghton *et al.* 1999), decreasing dominant juvenile proportions and increasing lithic proportions (cf. Nemeth *et al.* 2008). Both fallout and surge processes occurred. The ancestral Waipa/Waikato River could have been a possible source of surface water for the eruption, but there are no lithics present that are typical of alluvial deposits, which does not support the river as a source of external water. The shallow Mercer Sandstone is the dominant lithic type throughout the eruption deposits and the most likely aquifer due to its high porosity and transmissivity (20 to 60 m^2d) (Greig 1989).

Onewhero tuff ring

The Onewhero tuff ring was created by a phreatomagmatic eruption caused by the interaction of basaltic magma with a large volume of external water, probably over weeks to years, 0.88 million years ago. Nearby, a lava flow has formed from a vent on the outskirts of the tuff ring. The underlying geology consists of the Te Kuiti Group. The Waimai Limestone of the Aotea Formation is overlain by the Carter Siltstone of the Te Akatea Formation.

The early stages of the tuff ring eruption had inefficient levels of fragmentation due to low water content and low energy levels. Pulsating intensity formed fallout from eruption clouds and base surges (cf. Németh & White 2003). Fragmentation depth was shallow, and may have occurred within the Carter

Siltstone of the Te Akatea Formation at depths of less than about 30 m, with possible occasional deepening into the underlying Aotea Formation to depths of about 35 m (cf. Waterhouse 1978; Lorenz 2003). Vent clearing events were uncommon, as were peaks in lithic content of the eruption and associated fragmentation of lithic material. The late stages of the tuff ring eruption had stages of higher fragmentation due to high lithic content, alternating with drier eruption stages where the magma was less fragmented. Steady fallout was dominant, as well as stages of pulsating eruption intensity. The eruption vent varied between stable and unstable stages.

Overall, eruptions in the Onewhero tuff ring represent a general constant grainsize (cf. Houghton *et al.* 1999), as well as constant dominant juvenile proportion and a slight increase in lithic proportion towards the end of the eruption. Both fallout and surge processes occurred. The Carter Siltstone member of the Te Akatea Formation is the dominant lithic type; however it has a low porosity and permeability and so is unlikely to be the main source of subsurface water supply for the eruption. Onewhero has the largest diameter of any tuff ring in the SAVF as well as a maximum height of 87 m above the tuff ring floor, and therefore must have had the largest magma volume, as the deposits are much more extensive due to the tuff ring's large diameter and height. This suggests that the water supply must have been large also, in order to produce a sustained tuff ring eruption. Lithic proportion remained steady, suggesting that the fragmentation was constant. This means that a large, readily available steady supply of external water was available for interaction with the magma. As mentioned before, the country rock is unsuitable for holding such large amounts of water. This suggests that a river or stream and the associated alluvial sediments could have been the water source. The quartz, hypersthene and plagioclase lithic crystals found in the tuff ring deposits are typical of floodplain alluvial sediments of a river that has drained the pre-Onewhero eruption volcanic deposits of the Taupo Volcanic Zone, for example the Mangakino-derived ignimbrites by the Waipa River. The Waikato Heads Fault to the north of the Onewhero tuff ring has had approximately 60 m of Pleistocene movement (cf. Rodgers & Grant-Mackie 1978). The Waikato Heads Fault is a branch of the Waikato Fault, which has had a total of 0.7 km uplift to the east and 2.7 km uplift to the west in the Pleistocene alone (Hochstein & Nunns

1976). The elevation of the tuff ring floor is approximately 100 m a.s.l., suggesting that it was originally at the height of the flood plain of the ancestral Waipa/Waikato River at the time it was erupting, and has since been uplifted in the southern block of the SAVF. The ancestral Waipa/Waikato River and its associated water-rich alluvial sediments would have supplied a steady, large volume of water that interacted with the steadily rising magma to produce the tuff ring.

Bombay volcanic complex

The BVC consists of an early tuff cone formed with a large scoria cone on its western rim. Basalt then ponded in the cone and overflowed its edges as numerous scoria cones and spatter cones were formed above and in between the basalt layers. Alluvial deposits were then sedimented followed by a tephra layer 1.71 million years ago in shallow water. A later tuff ring (described here) was then erupted and deposited on top of the complex. The underlying geology consists of the Mercer Sandstone of the Waitemata Group overlain by Quaternary alluvial sediments.

The deposits of the later tuff ring eruption are relatively constant and alternate between two sets of conditions. Fallout dominated eruption pulses with some base surges have high water content. Vent clearing episodes occur. Fragmentation may have occurred in both Mercer Sandstone and Koheroa Siltstone, perhaps around depths of 25 to 30 m. A general increase in juvenile content and decrease in lithic content occurs towards the end of the eruption. This alternates with a fallout dominated phase of low water content explosive activity, with occasional peaks in lithic content. The vent is unstable in this phase, and juvenile material is dominant. The eruption has low levels of fragmentation with less interaction between magma and lithic material.

Overall, eruptions in the Bombay Quarry tuff ring represent a relatively steady eruption with a general decrease in grainsize and a general decrease in water content, eruption energy and fragmentation. Fallout processes were dominant. Fragmentation depth was generally intermediate. Juvenile material was dominant and lithic type was generally evenly distributed between Mercer Sandstone and Koheroa Siltstone. Mercer Sandstone is the most likely aquifer for

the subsurface water source of the tuff ring eruption due to its high porosity and transmissivity (Greig 1989).

6.3 Summary

The eruption features of the Kellyville and Onewhero tuff rings can be compared. Their underlying geology is different, and while deposits of Kellyville tuff ring decrease in grain size with stratigraphic height, Onewhero tuff ring deposits stay constant in this regard. The water/magma ratio of the tuff rings increases, along with associated fragmentation efficiency and energy. The deposits of Kellyville tuff ring decrease in juvenile content with stratigraphic height, while the juvenile content of Onewhero tuff ring is relatively constant. The deposits of both tuff rings increase in proportion of lithic material in the later stages, similar to that described in the Pula maar by Nemeth *et al*. (2008), and both have been deposited by fallout and surge processes, with fragmentation at shallow depths. Kellyville had two later magmatic phases associated with the tuff ring.

The eruption features of the Bombay Quarry tuff ring are markedly different to those of Kellyville and Onewhero tuff rings. The underlying country rock geology of the Bombay Quarry is similar to that of Kellyville tuff ring, and the grain size of the Bombay Quarry tuff ring deposits decreased similar to that of Kellyville. However water content of the eruption decreases along with eruption energy and fragmentation, and juvenile content increases with decreasing lithic content. Fallout processes dominate and fragmentation is at intermediate depths.

The main control on eruption style and energy of the Kellyville tuff ring is the increase in interaction between the magma and the subsurface water readily available within the porous Mercer Sandstone country rock at generally shallow depths less than 26 m. With the increasing water and lithic proportions throughout the eruption, grainsize decreased (cf. Houghton *et al.* 1999). This indicated either an increase in fragmentation or a decrease in magma ascent rate and eruption energy. The latter option may be more viable due to the decrease in juvenile proportions within the eruption deposits. The water/magma ratio of the Kellyville

tuff ring eruption increased over the course of the eruption. In the early stages of the eruption the water/magma ratio was approximately 0.2 (Fig. 6.1a), and towards the middle it increased to approximately 0.3 (Fig. 6.1b) where efficiency of the eruption is highest (cf. Wohletz & Sheridan 1983). The water/magma ratio near the end of the eruption increased to about 1 (Fig. 6.1c), where surges were dominant. This also suggests that the decrease in grainsize was due to a decrease in magma ascent and eruption energy, as the fragmentation became less efficient over the eruption.

The main control on eruption style and energy of the Onewhero tuff ring is the constant magma ascent rate and therefore juvenile content, and its increasing vesicularity, as well as the constant large supply of water most likely from the ancestral Waipa/Waikato River. The water/magma ratio of the Onewhero tuff ring stayed relatively steady through the eruption, at an approximate ratio of 0.2 (Fig. 6.1a) (cf. Wohletz & Sheridan 1983), producing surge-dominated beds towards the end of the eruption.

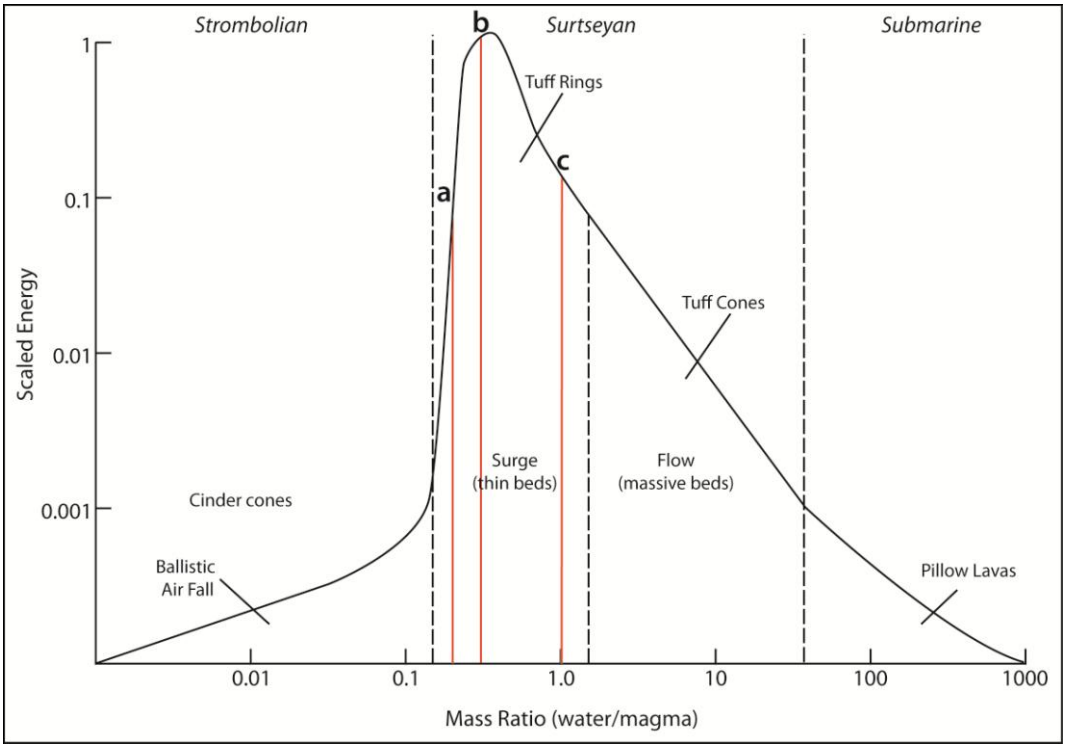

Figure 6.1: Water/magma ratios versus explosive energy (figure adapted from Wohletz & McQueen 1984): (a) mass ratio of 0.2; (b) mass ratio of 0.3; (c) mass ratio of 1.

The main control on eruption style and energy of the Bombay Quarry tuff ring is represented by the decrease in grainsize. The decrease in grainsize as the eruption progressed is due to either a decrease in ascent rate and eruption energy, causing the eruption products to decrease in size; or an increase in ascent rate and increase in eruption fragmentation. Through the course of the eruption, magma and juvenile content increases and lithic and water content decreases, causing the fragmentation of the eruption to become increasingly efficient, as ideal water/magma ratios of 0.2 to 0.3 are reached (Fig. 6.1a,b) (cf. Wohletz & Sheridan 1983; Risso *et al.* 2008). Fallout is the dominant process due to a highly efficient eruption and steady eruption column.

The nature of the monogenetic SAVF and the how volcanism has developed within it is characterised by several factors, including the distribution of faults, as well as the interaction of differing magma supplies and ascent rates with water from subsurface sedimentary rocks and the ancestral Waipa/Waikato River. The eruption progression of the tuff rings studied in this thesis offers further insight into the structure and processes of tuff ring eruptions in general, and their controlling factors. Gaining an improved understanding of the SAVF, which represents the entire history of a monogenetic basaltic volcanic field, can assist in the progression of knowledge of the controlling factors of other similar fields; whether they are young and still active or have long ago ceased activity.

References

Alloway, B., Westgate, J., Pillans, B., Pearce, N., Newnham, R., Byrami, M. & Aarburg, S. 2004, 'Stratigraphy, age and correlation of middle Pleistocene silicic tephras in the Auckland region, New Zealand: a prolific distal record of Taupo Volcanic Zone volcanism', *New Zealand Journal of Geology and Geophysics*, vol. 47, pp. 447-479.

Barnes, P. M., Lamarche, G., Bialas, J., Henrys, S., Pecher, I., Netzeband, G. L., Greinert, J., Mountjoy, J. J., Pedley, K. & Crutchley, G. 2010, 'Tectonic and geological framework for gas hydrates and cold seeps on the Hikurangi subduction margin, New Zealand', *Marine Geology*, vol. 272, pp. 26-48.

Battey, M. H. 1949, 'The geology of the Tuakau-Mercer area, Auckland', *Transactions of the Royal Society, New Zealand*, no. 77, pp. 429-55.

Briggs, R. M., Okada, T., Itaya, T., Shibuya, H. & Smith, I. E. M. 1994, 'K-ar ages, paleomagnetism, and geochemistry of the South Auckland volcanic field, North Island, New Zealand', *New Zealand Journal of Geology and Geophysics*, vol. 37, pp. 143-153.

Briggs, R. M., Pittari, A. & Rosenberg, M. D. 2010, 'Controls on volcanism in the South Auckland volcanic field', *GeoNZ 2010*, Auckland, pp. 45.

Cas, R. A. F. 1989, 'Physical Volcanology', in R. W. Johnson (ed.), *Intraplate Volcanism*, Cambridge University Press, Cambridge, pp. 55-87.

Cas, R. A. F. & Wright, J. V. 1987, *Volcanic successions- modern and ancient*, Allen and Unwin, London.

Cassidy, J., France, S. J. & Locke, C. A. 2007, 'Gravity and magnetic investigation of maar volcanoes, Auckland volcanic field, New Zealand', *Journal of Volcanology and Geothermal Research*, vol. 159, pp. 153-163.

Cimarelli, C., Di Traglia, F. & Taddeucci, J. 2010, 'Basaltic scoria textures from a zoned conduit as precursors to violent Strombolian activity', *Geology*, vol. 38, no. 5, pp. 439-442.

Colchester, D. M. 1968, *Geology of the Kellyville Tuff Ring- Mercer*, Victoria University, Wellington.

Connor, C. B. & Conway, F. M. 2000, 'Basaltic Volcanic Fields', in H. Sigurdsson (ed.), *Encyclopedia of Volcanoes*, Academic Press, California, pp. 331-343.

Cook, C. 2002, Petrogenesis and evolution of alkalic basaltic magmas in a continental intraplate setting: the South Auckland volcanic field, New Zealand, Thesis, University of Waikato.

Cook, C., Briggs, R. M., Smith, I. E. M. & Maas, R. 2005, 'Petrology and geochemistry of intraplate basalts in the South Auckland volcanic field, New Zealand: Evidence for two coeval magma suites from distinct sources', *Journal of Petrology*, vol. 46, no. 3, pp. 473-503.

Edbrooke, S. W. 2001, *Geology of the Auckland Area*, Institute of Geological and Nuclear Sciences Limited, Lower Hutt, New Zealand.

Fisher, R. V. & Schmincke, H.-U. 1984, *Pyroclastic rocks*, Springer-Verlag, Berlin.

Francis, P. & Oppenheimer, C. 2004, *Volcanoes*, Oxford University Press, New York.

GCNZ Consultants 1990, *Hydrogeology of a proposed quarry site at Bombay-South Auckland*, Auckland.

Greig, D. A. 1989, *A study of the Kaawa Formation aquifer system in the Manukau Lowlands*, Technical Publication No. 85, Auckland Regional Water Board, Auckland.

Hadfield, J. C. 1988, Aspects of Kaawa Formation hydrogeology: A preliminary evaluation of a steady state finite element groundwater model, Thesis, University of Waikato.

Heming, R. F. 1980, 'Patterns of Quaternary basaltic volcanism in the northern North Island, New Zealand', *New Zealand journal of geology and geophysics*, vol. 23, pp. 335-344.

Hochstein, M. P. & Nunns, A. G. 1976, 'Gravity measurements across the Waikato Fault, North Island, New Zealand', *New Zealand journal of geology and geophysics*, vol. 19, pp. 347-358.

Houghton, B. F. & Gonnermann, H. M. 2008, 'Basaltic explosive volcanism: Constraints from deposits and models', *Chemie der Erde*, vol. 68, pp. 117-140.

Houghton, B. F. & Nairn, I. 1991, 'The 1976-1982 Strombolian and phreatomagmatic eruptions of White Island, New Zealand: eruptive and depositional mechanisms at a 'wet' volcano', *Bulletin of Volcanology*, vol. 54, pp. 25-49.

Houghton, B. F., Wilson, C. J. N. & Pyle, D. M. 2000, 'Pyroclastic fall deposits', in H. Sigurdsson (ed.), *Encyclopedia of Volcanoes*, Academic Press, California, pp. 555-570.

Houghton, B. F., Wilson, C. J. N. & Smith, I. E. M. 1999, 'Shallow-seated controls on styles of explosive basaltic volcanism: a case study from New Zealand', *Journal of Volcanology and Geothermal Research*, vol. 91, pp. 97-120.

Ilanko, T. 2010, Eruption and emplacement processes of the Barriball Road tuff ring, South Auckland, Thesis, University of Waikato.

John O'Brien Associates 1999, *Bombay Quarry resource geology update*, Auckland.

John O'Brien Associates 2000, *Report on scout drilling at Bombay boreholes B1-B11*, Auckland.

John O'Brien Associates, Boffa Miskell Partners & John Thacker and Associates 1994, *Management Plan and Emergency Procedures Bombay Quarry*, Milburn New Zealand Ltd, Auckland.

Johnson, R. W. & Wellman, P. 1989, 'Framework for volcanism', in R. W. Johnson (ed.), *Intraplate volcanism*, Cambridge University Press, Cambridge, pp. 1-53.

Jukic, M. F. 1995, A geological and geophysical subsurface investigation of the South Auckland volcanic field, Thesis, The University of Auckland.

Kear, D. 1961, 'Stratigraphy of Pokeno District, Auckland', *New Zealand journal of geology and geophysics*, vol. 4, no. 1, pp. 148-164.

Kear, D. 1996, *North Island volcanism, and inferred New Zealand tectonic development during the late Cenozoic* David Kear, Whakatane, New Zealand.

Kear, D. & Schofield, J. C. 1978, *Geology of the Ngaruawahia subdivision*, New Zealand, Dept. of Scientific and Industrial Research, Wellington.

Kermode, L. O. 1992, *Inventory of Quaternary volcanoes and volcanic features of Northland, Auckland, South Auckland and Taranaki* Geological Society of New Zealand, Lower Hutt, New Zealand

Kokelaar, P. 1986, 'Magma-water interactions in subaqueous and emergent basaltic volcanism', *Bulletin of Volcanology*, vol. 48, pp. 275-289.

Lorenz, V. 2003, 'Maar-diatreme volcanoes, their formation, and their setting in hard-rock or soft-rock environments', *GeoLines*, vol. 15, pp. 72-83.

Manville, V., Németh, K. & Kano, K. 2009, 'Source to sink: A review of three decades of progress in the understanding of volcaniclastic processes, deposits, and hazards', *Sedimentary Geology*, vol. 220, pp. 136-161.

Miller, K. 2007, *Jones Block resource consent*, Holcim NZ Ltd, Auckland.

Nemeth, K., Goth, K., Martin, U., Csillag, G. & Suhr, P. 2008, 'Reconstructing paleoenvironment, eruption mechanism and paleomorphology of the Pliocene Pula maar, (Hungary)', *Journal of Volcanology and Geothermal Research*, vol. 177, pp. 441-456.

Németh, K. & White, J. D. L. 2003, 'Reconstructing eruption processes of a Miocene monogenetic volcanic field from vent remnants: Waipiata volcanic field, South Island, New Zealand', *Journal of Volcanology and Geothermal Research*, vol. 124, pp. 1-21.

Németh, K., White, J. D. L., Reay, A. & Martin, U. 2003, 'Compositional variation during monogenetic volcano growth and its implications for magma supply to continental volcanic fields', *Journal of the Geological Society, London*, vol. 160, pp. 523-530.

Neri, A., Papale, P. & Macedonio, G. 1998, 'The role of magma composition and water content in explosive eruptions: 2. Pyroclastic dispersion dynamics', *Journal of Volcanology and Geothermal Research*, vol. 87, pp. 95-115.

Ormiston Associates Ltd 1999, *Review of basalt resource at Bombay Quarry*, Auckland.

Parfitt, E. A. 2004, 'A discussion of the mechanisms of explosive basaltic eruptions', *Journal of Volcanology and Geothermal Research*, vol. 134, pp. 77-107.

Paulick, H., Ewen, C., Blanchard, H. & Zöller, L. 2009, 'The Middle-Pleistocene (~300 ka) Rodderberg maar-scoria cone volcanic complex (Bonn,

Germany): eruptive history, geochemistry, and thermoluminescence dating', *International Journal of Earth Sciences*, vol. 98, pp. 1879-1899.

Rafferty, W. J. 1977, The volcanic geology and petrology of South Auckland, Thesis, University of Auckland.

Rafferty, W. J. & Heming, R. F. 1979, 'Quaternary alkalic and sub-alkalic volcanism in South Auckland, New Zealand', *Contributions to Mineralogy and Petrology*, vol. 71, pp. 139-150.

Risso, C., Németh, K., Combina, A. M., Nullo, F. & Drosina, M. 2008, 'The role of phreatomagmatism is a Plio-Pleistocene high-density scoria cone field: Llancanelo volcanic field (Mendoza), Argentina', *Journal of Volcanology and Geothermal Research*, vol. 169, pp. 61-86.

Rosenberg, M. D. 1991, The nature and mechanisms of phreatomagmatic volcanism in the South Auckland volcanic field, Thesis, University of Waikato.

Schofield, J. C. 1958, 'Notes on the volcanism and structure in Franklin County', *New Zealand Journal of Geology and Geophysics*, vol. 1, pp. 541-559.

Schofield, J. C. 1967, *Geological map of New Zealand, Sheet 3*, DSIR NZ.

Smith, I. E. M., Okada, T., Itaya, T. & Black, P. M. 1993, 'Age relationships and tectonic implications of late Cenozoic basaltic volcanism in Northland, New Zealand', *New Zealand journal of geology and geophysics*, vol. 36, no. 3, pp. 385-393.

Sohn, Y. K. 1996, 'Hydrovolcanic processes forming basaltic tuff rings and cones of Cheju Island, Korea', *Geological Society of America Bulletin*, vol. 108, pp. 1199-1211.

Stipp, J. J. 1968, The geochronology and petrogenesis of the Cenozoic volcanics of North Island, New Zealand, Thesis, Australian National University.

Sumner, J. M., Blake, S., Matela, R. J. & Wolff, J. A. 2005, 'Spatter', *Journal of Volcanology and Geothermal Research*, vol. 142, pp. 49-65.

Waterhouse, B. C. 1978, *Onewhero*, Department of Scientific and Industrial Research, Wellington.

Waterhouse, B. C. 1980, *Mercer Diatomite*, N. Z. Geological Survey

Waterhouse, B. C. & White, P. J. 1994, *Geology of the Raglan Kawhia area*, Institute of Geological and Nuclear Sciences, Lower Hutt, New Zealand.

Weaver, S. D. & Smith, I. E. M. 1989, 'New Zealand Intraplate Volcanism', in R. W. Johnson (ed.), *Intraplate Volcanism*, Cambridge University Press, Cambridge, pp. 157-187.

Wohletz, K. H. & McQueen, R. G. 1984, 'Experimental studies of hydromagmatic volcanism', in G. S. committee (ed.), *Explosive volcanism: inception, evolution and hazards*, National Academy Press, Washington, pp. 158-169.

Wohletz, K. H. & Sheridan, M. F. 1983, 'Hydrovolcanic Explosions II. Evolution of basaltic tuff rings and tuff cones', *American Journal of Science*, vol. 283, pp. 385-413.

Zanon, V., Pacheco, J. & Pimentel, A. 2009, 'Growth and evolution of an emergent tuff cone: Considerations from structural geology, geomorphology and facies analysis of Sao Roque volcano, Sao Miguel (Azores)', *Journal of Volcanology and Geothermal Research*, vol. 180, pp. 277-291.

Appendix One

Appendix One

Sample data for all samples taken from Kellyville volcanic complex, Onewhero tuff ring and Bombay volcanic complex are available below.

Table A1.1: Sample information of all samples taken from Kellyville, Onewhero and Bombay.

Collection no.	Field no.	Field area	Site description	Locality	Collection date	NZTopo50 Easting	NZTopo50 Northing	Sample type	Thin section	Archived
W2011500	1	Kellyville tuff ring	Road outcrop	4	3/11/2009	1782858	5973298	Lithics	X	
W2011501	2	Kellyville tuff ring	Road outcrop	4	3/11/2009	1782858	5873298	Lithics	X	
W2011502	3	Kellyville tuff ring	Road outcrop	4	3/11/2009	1782858	5873298	Basalt Juvenile	X	
W2011503	4	Kellyville tuff ring	Road outcrop	4	3/11/2009	1782858	5873298	Lithics	X	
W2011504	5	Kellyville tuff ring	Road outcrop	4	3/11/2009	1782858	5873298	Basalt Juvenile	X	
W2011505	6	Kellyville tuff ring	Road outcrop	4	3/11/2009	1782858	5873298	Tuff	X	X
W2011506	7	Kellyville tuff ring	Road outcrop	4	3/11/2009	1782858	5873298	Tuff	X	
W2011507	8	Kellyville tuff ring	Road outcrop	4	3/11/2009	1782862	5873305	Tuff	X	
W2011508	9	Kellyville tuff ring	Road outcrop	4	3/11/2009	1782862	5873305	Tuff	X	X
W2011509	10	Kellyville tuff ring	Road outcrop	4	3/11/2009	1782862	5873305	Lithics	X	
W2011510	11	Kellyville tuff ring	Road outcrop	4	3/11/2009	1782862	5873305	Lithics	X	
W2011511	12	Kellyville tuff ring	Road outcrop	4	3/11/2009	1782862	5873305	Tuff	X	
W2011512	13	Kellyville tuff ring	Road outcrop	4	3/11/2009	1782878	5873323	Basalt Juvenile	X	X
W2011513	14	Kellyville tuff ring	Road outcrop	4	3/11/2009	1782878	5873323	Ash	X	
W2011514	15	Kellyville tuff ring	Road outcrop	4	3/11/2009	1782878	5873323	Ash	X	
W2011515	16	Kellyville tuff ring	Road outcrop	4	3/11/2009	1782904	5873356	Tuff	X	
W2011516	17	Kellyville tuff ring	Road outcrop	4	3/11/2009	1782904	5873356	Lithics	X	
W2011517	18	Kellyville tuff ring	Road outcrop	4	3/11/2009	1782904	5873356	Lithics	X	X
W2011518	19	Kellyville tuff ring	Road outcrop	4	3/11/2009	1782878	5873323	Tuff	X	

W2011519	20	Onewhero tuff ring	Large cliff	2	4/11/2009	1769585	5868580	Ash	X	
W2011520	21	Onewhero tuff ring	Large cliff	2	4/11/2009	1769585	5868580	Tuff	X	X
W2011521	22	Onewhero tuff ring	Large cliff	2	4/11/2009	1769585	5868580	Tuff	X	
W2011522	23	Onewhero tuff ring	Large cliff	2	4/11/2009	1769585	5868580	Tuff	X	
W2011523	24	Onewhero tuff ring	Large cliff	2	4/11/2009	1769585	5868580	Tuff	X	X
W2011524	25	Onewhero tuff ring	Large cliff	2	4/11/2009	1769585	5868580	Tuff	X	X
W2011525	28	Kellyville tuff ring	Road outcrop	4	3/11/2009	1782904	5873356	Lithics	X	
W2011526	29	Kellyville tuff ring	Road outcrop	4	3/11/2009	1782904	5873356	Basalt Juvenile	X	
W2011527	30	Kellyville tuff ring	Road outcrop	4	3/11/2009	1782904	5873356	Tuff	X	
W2011528	31	Kellyville tuff ring	Road outcrop	4	3/11/2009	1782904	5873356	Ash	X	
W2011529	32	Kellyville tuff ring	Road outcrop	4	3/11/2009	1782904	5873356	Ash	X	X
W2011530	33	Kellyville tuff ring	Road outcrop	4	3/11/2009	1782955	5873420	Tuff	X	
W2011531	34	Kellyville tuff ring	Road outcrop	4	3/11/2009	1782955	5873420	Tuff	X	
W2011532	35	Kellyville tuff ring	Diatomite outcrop	7	3/11/2009	1782425	5872786	Diatomite		
W2011533	36	Kellyville tuff ring	Diatomite outcrop	7	3/11/2009	1782425	5872786	Diatomite		
W2011534	37	Kellyville tuff ring	Diatomite outcrop	7	3/11/2009	1782425	5872786	Diatomite	X	
W2011535	38	Kellyville tuff ring	Diatomite outcrop	7	3/11/2009	1782425	5872786	Diatomite		
W2011536	39	Kellyville tuff ring	Diatomite outcrop	7	3/11/2009	1782425	5872786	Diatomite	X	X
W2011537	40	Kellyville tuff ring	Diatomite outcrop	7	3/11/2009	1782425	5872786	Diatomite		X
W2011538	41	Kellyville tuff ring	Glass Hill	6	3/11/2009	1782249	5872612	Scoria	X	X
W2011539	42	Kellyville tuff ring	Glass Hill	6	19/01/2010	1782217	5872558	Scoria		X
W2011540	43	Kellyville tuff ring	Glass Hill	6	19/01/2010	1782217	5872558	Scoria	X	
W2011541	44	Kellyville tuff ring	Glass Hill	6	19/01/2010	1782246	5872537	Scoria	X	
W2011542	45	Kellyville tuff ring	Glass Hill	6	19/01/2010	1782199	5872645	Scoria	X	X
W2011543	46	Kellyville tuff ring	Northern rim breach	8	19/01/2010	1781698	5873479	Lithics	X	X
W2011544	47	Kellyville tuff ring	Southern rim breach	9	19/01/2010	1781636	5872117	Lithics	X	X
W2011545	48	Kellyville tuff ring	South eastern rim	3	20/01/2010	1782818	5871911	Tuff	X	
W2011546	49	Kellyville tuff ring	South eastern rim	3	20/01/2010	1782818	5871911	Tuff	X	
W2011547	50	Kellyville tuff ring	South eastern rim	3	20/01/2010	1782818	5871911	Tuff	X	

W2011548	51	Kellyville tuff ring	South eastern rim	3	20/01/2010	1782818	5871911	Ash	X	
W2011549	52	Kellyville tuff ring	South eastern rim	3	20/01/2010	1782821	5871921	Ash and tuff		
W2011550	53	Kellyville tuff ring	South eastern rim	3	20/01/2010	1782821	5871921	Tuff		
W2011551	54	Kellyville tuff ring	School Hill	5	20/01/2010	1782643	5872641	Scoria		X
W2011552	55	Kellyville tuff ring	School Hill	5	20/01/2010	1782671	5872634	Basalt Juvenile	X	X
W2011553	56	Kellyville tuff ring	Glass Hill	6	20/01/2010	1782246	5872537	Scoria	X	
W2011554	57	Kellyville tuff ring	Glass Hill	6	20/01/2010	1782246	5872537	Scoria		
W2011555	58	Kellyville tuff ring	Glass Hill	6	20/01/2010	1782246	5872537	Scoria		
W2011556	59	Kellyville tuff ring	Glass Hill	6	20/01/2010	1782246	5872537	Scoria		
W2011557	60	Onewhero tuff ring	Opposite large cliff	3	26/01/2010	1769512	5868594	Tuff	X	
W2011558	61	Onewhero tuff ring	Opposite large cliff	3	26/01/2010	1769512	5868594	Tuff	X	
W2011559	62	Onewhero tuff ring	Opposite large cliff	3	26/01/2010	1769512	5868594	Tuff	X	
W2011560	63	Onewhero tuff ring	Opposite large cliff	3	26/01/2010	1769512	5868594	Tuff	X	X
W2011561	64	Onewhero tuff ring	Opposite large cliff	3	26/01/2010	1769512	5868594	Tuff		
W2011562	65	Onewhero tuff ring	Opposite large cliff	3	26/01/2010	1769512	5868594	Tuff		
W2011563	BQ1	Bombay Quarry	Tuff cliff	1	12/02/2010	1776298	5879119	Lithics/ash	X	
W2011564	BQ2	Bombay Quarry	Tuff cliff	1	12/02/2010	1776298	5879119	Ash	X	
W2011565	BQ3	Bombay Quarry	Tuff cliff	1	12/02/2010	1776298	5879119	Tuff	X	
W2011566	BQ4	Bombay Quarry	Tuff cliff	1	12/02/2010	1776298	5879119	Tuff	X	
W2011567	BQ5	Bombay Quarry	Tuff cliff	1	12/02/2010	1776298	5879119	Ash	X	
W2011568	BQ6	Bombay Quarry	Tuff cliff	1	12/02/2010	1776298	5879119	Basalt Juvenile	X	
W2011569	BQ7	Bombay Quarry	Tuff cliff	1	12/02/2010	1776298	5879119	Lithics	X	
W2011570	BQ8	Bombay Quarry	Tuff cliff	1	12/02/2010	1776298	5879119	Tuff	X	
W2011571	BQ9	Bombay Quarry	Tuff cliff	1	12/02/2010	1776298	5879119	Scoria	X	X
W2011572	BQ10	Bombay Quarry	Tuff cliff	1	12/02/2010	1776298	5879119	Tuff	X	
W2011573	BQ11	Bombay Quarry	Tuff cliff	1	12/02/2010	1776298	5879119	Lithics	X	
W2011574	BQ12	Bombay Quarry	Tuff cliff	1	12/02/2010	1776298	5879119	Lithics	X	
W2011575	BQ13	Bombay Quarry	Tuff cliff	1	12/02/2010	1776298	5879119	Lithics	X	
W2011576	BQ14	Bombay Quarry	Tuff cliff	1	12/02/2010	1776298	5879119	Scoria	X	

W2011577	KB1	Kellyville tuff ring	Under road log	2	24/02/2010	1782858	5873347	Lithic	X	
W2011578	KB2	Kellyville tuff ring	Under road log	2	24/02/2010	1782858	5873347	Tuff		
W2011579	KB3	Kellyville tuff ring	Under road log	2	24/02/2010	1782858	5873347	Tuff	X	
W2011580	KB4	Kellyville tuff ring	Under road log	2	24/02/2010	1782858	5873347	Tuff		
W2011581	KB5	Kellyville tuff ring	Under road log	2	24/02/2010	1782858	5873347	Tuff	X	
W2011582	KB6	Kellyville tuff ring	Under road log	2	24/02/2010	1782858	5873347	ash		X
W2011583	KB7	Kellyville tuff ring	Under road log	2	24/02/2010	1782858	5873347	Tuff		
W2011584	KB8	Kellyville tuff ring	Under road log	2	24/02/2010	1782858	5873347	Tuff	X	
W2011585	KB9	Kellyville tuff ring	Under road log	2	24/02/2010	1782858	5873347	Tuff	X	
W2011586	KB10	Kellyville tuff ring	Under road log	2	24/02/2010	1782858	5873347	Tuff	X	
W2011587	BQA1	Bombay Quarry	Tuff cliff	1	24/02/2010	1776298	5879119	Tuff	X	
W2011588	BQA2	Bombay Quarry	Tuff cliff	1	24/02/2010	1776298	5879119	Tuff	X	
W2011589	BQA3	Bombay Quarry	Tuff cliff	1	24/02/2010	1776298	5879119	Tuff		
W2011590	BQA4	Bombay Quarry	Tuff cliff	1	24/02/2010	1776298	5879119	Tuff	X	X
W2011591	BQA5	Bombay Quarry	Tuff cliff	1	24/02/2010	1776298	5879119	Tuff		
W2011592	BQA6	Bombay Quarry	Tuff cliff	1	24/02/2010	1776298	5879119	Tuff		
W2011593	BQA7	Bombay Quarry	Tuff cliff	1	24/02/2010	1776298	5879119	Tuff		
W2011594	BQA8	Bombay Quarry	Tuff cliff	1	24/02/2010	1776298	5879119	Tuff		
W2011595	BQA9	Bombay Quarry	Tuff cliff	1	24/02/2010	1776298	5879119	Basalt Juvenile	X	
W2011596	BQA10	Bombay Quarry	Tuff cliff	1	24/02/2010	1776286	5879295	Tuff	X	
W2011597	BQA11	Bombay Quarry	Tuff cliff	1	24/02/2010	1776286	5879295	Tuff	X	
W2011598	BQA12	Bombay Quarry	Tuff cliff	1	24/02/2010	1776286	5879295	Tuff	X	
W2011599	BQA13	Bombay Quarry	Tuff cliff	1	24/02/2010	1776286	5879295	Tuff	X	
W2011600	BQA14	Bombay Quarry	Tuff cliff	1	24/02/2010	1776286	5879295	Tuff	X	
W2011601	BQA15	Bombay Quarry	Spatter cone	1	24/02/2010	1776387	5879338	Scoria	X	X
W2011602	BQA16	Bombay Quarry	Spatter cone	1	24/02/2010	1776387	5879338	Scoria	X	X
W2011603	ONEA1	Onewhero tuff ring	Small outcrop	1	23/02/2010	1769452	5868795	Tuff	X	
W2011604	ONEA2	Onewhero tuff ring	Small outcrop	1	23/02/2010	1769452	5868795	Tuff	X	
W2011605	ONEA3	Onewhero tuff ring	Small outcrop	1	23/02/2010	1769452	5868795	Tuff	X	

W2011606	ONEA4	Onewhero tuff ring	Small outcrop	1	23/02/2010	1769452	5868795	Tuff	X	
W2011607	A	Kellyville tuff ring	Large road log	4	17/02/2010	1782985	5873344	Tuff		
W2011608	B	Kellyville tuff ring	Large road log	4	17/02/2010	1782985	5873344	Tuff	X	
W2011609	C	Kellyville tuff ring	Large road log	4	17/02/2010	1782914	5873365	Tuff	X	
W2011610	E	Kellyville tuff ring	Middle outcrop	1	17/02/2010	1782655	5873451	Ash		
W2011611	F	Kellyville tuff ring	Middle outcrop	1	17/02/2010	1782655	5873451	Tuff	X	
W2011612	G	Kellyville tuff ring	Middle outcrop	1	17/02/2010	1782655	5873451	Lithics	X	
W2011613	H	Kellyville tuff ring	Middle outcrop	1	17/02/2010	1782655	5873451	Ash	X	
W2011614	I	Kellyville tuff ring	Middle outcrop	1	17/02/2010	1782655	5873451	Tuff	X	
W2011615	J	Kellyville tuff ring	Middle outcrop	1	17/02/2010	1782655	5873451	Lithics	X	X
W2011616	K	Kellyville tuff ring	Middle outcrop	1	17/02/2010	1782655	5873451	Lithics	X	
W2011617	L	Kellyville tuff ring	Middle outcrop	1	17/02/2010	1782655	5873451	Lithics	X	
W2011618	M	Kellyville tuff ring	Middle outcrop	1	17/02/2010	1782655	5873451	Tuff	X	
W2011619	N	Kellyville tuff ring	Middle outcrop	1	17/02/2010	1782655	5873451	Lithics	X	
W2011620	X	Kellyville tuff ring	School Hill	5	17/02/2010	1782662	5872641	Scoria	X	X
W2011621	Y	Kellyville tuff ring	School Hill	5	17/02/2010	1782662	5872641	Scoria	X	X
W2011622	Z	Kellyville tuff ring	School Hill	5	17/02/2010	1782662	5872641	Scoria	X	X
W2011623	WF01	Onewhero tuff ring	Waterfall	4	23/02/2010	1770200	5869110	Lithics	X	X
W2011624	WF02	Onewhero tuff ring	Waterfall	4	23/02/2010	1770200	5869110	Lithics	X	X
W2011625	WF03	Onewhero tuff ring	Waterfall	4	23/02/2010	1770200	5869110	Lithics	X	
W2011626	WF04	Onewhero tuff ring	Waterfall	4	23/02/2010	1770200	5869110	Basalt flow	X	X
W2011627	66	Onewhero tuff ring	Opposite large cliff	3	26/01/2010	1769660	5868400	Tuff		
W2011628	67	Onewhero tuff ring	Opposite large cliff	3	26/01/2010	1769660	5868400	Tuff		X
W2011629	68	Onewhero tuff ring	Opposite large cliff	3	11/05/2010	1769512	5868594	Tuff		
W2011630	69	Onewhero tuff ring	Opposite large cliff	3	11/05/2010	1769512	5868594	Tuff		
W2011631	70a	Onewhero tuff ring	Opposite large cliff	3	11/05/2010	1769512	5868594	Tuff		
W2011632	70b	Onewhero tuff ring	Opposite large cliff	3	11/05/2010	1769512	5868594	Tuff		
W2011633	70c	Onewhero tuff ring	Opposite large cliff	3	11/05/2010	1769512	5868594	Tuff		
W2011634	71	Onewhero tuff ring	Waterfall	4	11/05/2010	1770200	5869110	Basalt	X	

W2011635	72	Onewhero tuff ring	Opposite large cliff	3	11/05/2010	1769512	5868594	Tuff		
W2011636	73	Onewhero tuff ring	Opposite large cliff	3	11/05/2010	1769512	5868594	Tuff		
W2011637	74	Onewhero tuff ring	Waterfall	4	11/05/2010	1770200	5869110	lithics		
W2011638	75	Bombay Quarry	Columnar basalt	-	11/05/2010	2686654	6440779	Basalt	X	X
W2011639	76	Bombay Quarry	Columnar basalt	-	11/05/2010	2686654	6440779	Basalt	X	
W2011640	77	Bombay Quarry	Spatter cone	1	11/05/2010	2686654	6440779	Scoria		X
W2011641	78	Bombay Quarry	Tuff cliff	1	11/05/2010	2686654	6440779	lithics		

Appendix Two

Appendix 2

All stratigraphic logs taken at Kellyville volcanic complex, Onewhero tuff ring and Bombay volcanic complex are available below, and samples taken have been noted on each log.

VOLCANOLOGICAL STRATIGRAPHIC LOG SHEET

Location: Bombay Quarry | Locality: Tuff cliff (1) | Date taken: 12/02/2010

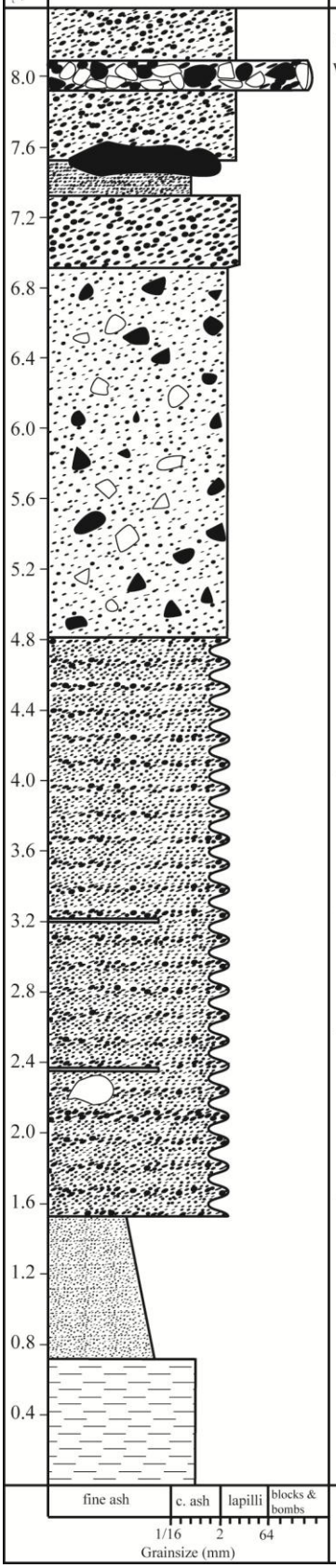

Sample no.	Field notes
W2011589	Dark coarse ash to fine lapilli.
W2011573-6 W2011641	Bomb layer, 20-30cm thick, white lithics and basalt clasts, subangular to angular.
W2011587	Dark coarse ash to fine lapilli with approx 2-3% white lithics.
W2011572	White very fine coarse ash to very coarse ash layer approx 20cm thick, uniform fall deposit, laminated, medium sorted, laminae pinch out, large white lithic very angular sunk into ash, approx 60-70cm long.
W2011571	Dark fine scoria lapilli, very well sorted, 30-40cm thick.
W2011588	Dark coarse ash to very fien lapilli, diffusely bedded, nearly massive, poorly sorted, with scoria clasts bomb size subangular, max. 58mm, with large angular white lithics approx. 15-20% of unit, max. 55mm, with large dark clasts subangular approx 5% of unit, max. 60mm.
W2011569	Alternating beds of coarse ash, well sorted, with beds of fine to very fine lapilli, moderately sorted, medium bedding.
W2011566	
W2011567	
W2011570	Alternating beds of medium coarse ash, well sorted, predominantly weathered scoria fragments- orange with white rims, with beds of very fine and fine lapilli moderately to well sorted, coarse ash and lapilli bed couples range from 4mm to 14mm, thinly bedded.
W2011568	2.1m: fine scoria lapilli, 30mm thick, well sorted. 2.4m: fine ash layer 20mm thick. 3.2m: white fine ash fall 15mm thick. 2.2-2.3m: dense angular basalt block 105mm.
W2011565	Coarse ash, white, tephra AT-71 1-1.2 Ma (ITPFT), visible from hand specimens: quartz, plagioclase, mafics. Very well sorted, massive, appears more clay rich at top, darker.
W2011564	Fine sands, becomes crumbly/frittery at top, soft, darker colour at top. Iron pans present at top and part way through unit, very well sorted, massive.
W2011563	

VOLCANOLOGICAL STRATIGRAPHIC LOG SHEET

Location: Bombay Quarry | Locality: Tuff cliff (1) | Date taken: 12/02/2010

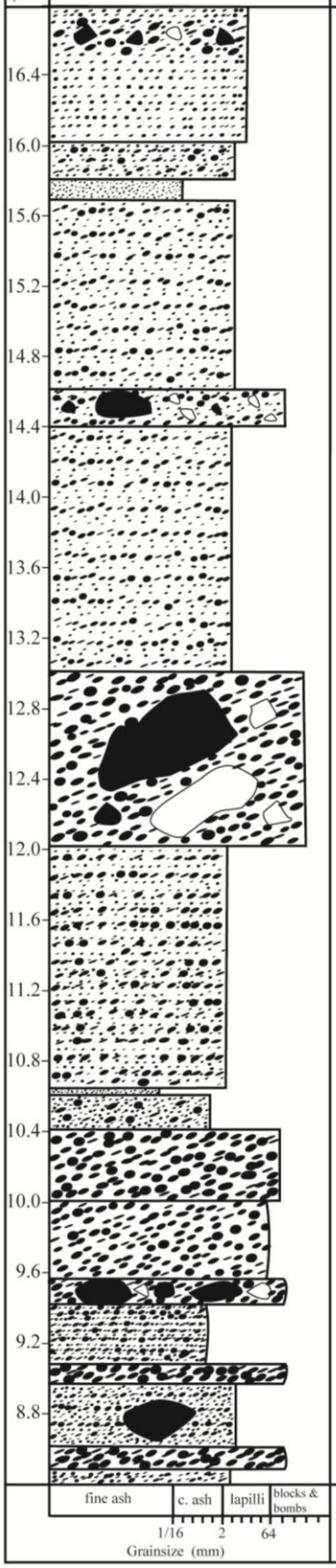

Sample no.	Field notes
	Very coarse lapilli with blocks and bombs, white subangular lithics concentration layer approx 10% of unit, 1m thick, 16.6-16.7m, set into fine lapilli, medium bedding, well sorted.
	Coarse ash to fine lapilli, medium bedding, well sorted, lapilli lithics and clasts.
	Light, fine ash, massive, 15cm thick.
	Coarse ash to fine lapilli, medium bedding, well sorted, lapilli lithics and clasts.
	Very coarse lapilli clasts and lithics with some white lithic blocks, concentrated layer 14.4-14.6m, set into fine lapilli to coarse ash with medium bedding.
	Coarse ash to fine lapilli, medium bedding, well sorted, lapilli lithics and clasts.
	Very coarse lapilli and block and bomb layer, 1m thick, lithics and clasts both subangular, lithics max. 70cm, clasts max. 50cm.
W2011595	Coarse ash with medium lapilli clasts and lithics, midium bedding, moderately sorted.
W2011594	
	Light, fine ash, massive, 5cm thick.
W2011593	Coarse ash with medium to coarse lapilli lithics and clasts.
	White coarse lapilli lithic layer, 40cm thick.
W2011591	Very coarse to medium lapilli, basalt and scoria with some lithics, moderately to well sorted.
W2011590	White lapilli layer, lithics up to 30-40cm, subrounded, some angular basalts.
W2011592	Medium coarse ash surge layer, well bedded, well sorted, with very fine lapilli basalt and scoria.
	Very coarse white lapilli lithic layer 15-20cm thick.
	Dark coarse ash to fine lapilli with very large light brown lithic rounded, approx 40-50cm diameter, well bedded.
	Very coarse lapilli lithic layer 15cm thick.

VOLCANOLOGICAL STRATIGRAPHIC LOG SHEET

Location: Bombay Quarry | Locality: Tuff cliff (1) | Date taken: 12/02/2010

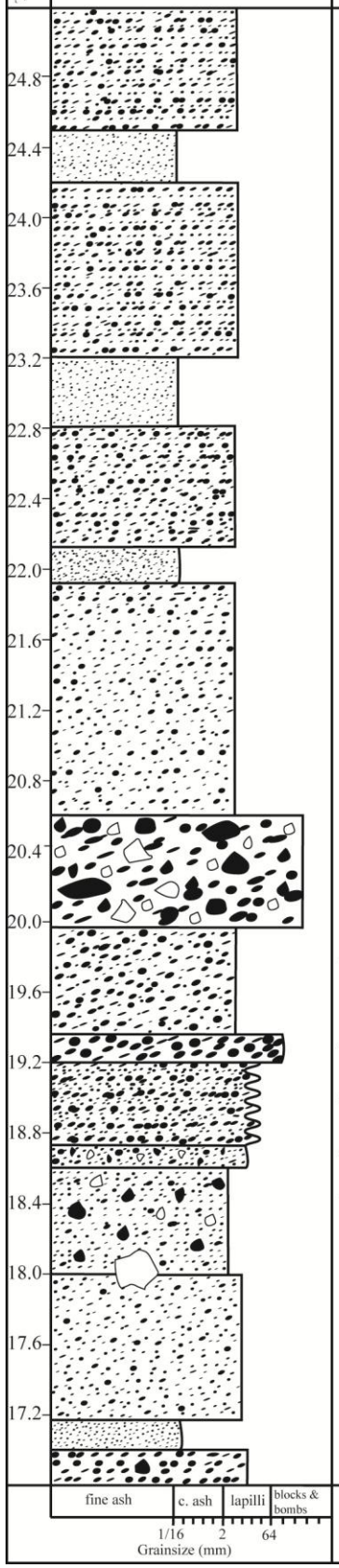

Sample no.	Field notes
	Coarse ash to very fine lapilli, well sorted, well bedded.
	Fine ash, light, very well sorted, 30cm thick, massive.
	Coarse ash to very fine lapilli, well bedded, well sorted.
	Fine ash layer, light colour, 40cm thick, massive, very well sorted.
	Coarse ash to very fine lapilli, diffuse bedding, well sorted.
	Fine ash layer, light colour, massive, very well sorted.
	Coarse ash to very fine lapilli, diffuse bedding, well sorted.
	Blocks and bombs- clasts and lithics, 60cm thick layer, massive.
W2011600	Very coarse ash with fine and medium lapilli, angular to sub-angular clasts, some very fine lapilli lithics, medium bedding.
W2011598	Light coarse lapilli lithics 20cm thick layer.
W2011599	Very coarse ash and fine lapilli, angular clasts and lithics, well sorted, medium bedding.
W2011596	Coarse ash to fine lapilli, massive, with dark very coarse lapilli mainly clasts, few lapilli, poorly sorted, slightly vesicular clasts max. 42mm, lithics max. 32mm.
W2011597	Light coarse ash with very fine lapilli, lithics and clasts with scoria, well sorted, with blocks and bombs- many coarse white lithics and some dark basalt clasts. Very large subangular basalt block, slightly vesicular 20cm long, sunk into ash from above.
	Coarse ash to very fine lapilli, diffusely bedded, well sorted.
	Fine ash layer, light colour, 15cm thick, massive, very well sorted.

VOLCANOLOGICAL STRATIGRAPHIC LOG SHEET

Location: Bombay Quarry | Locality: Tuff cliff (1) | Date taken: 12/02/2010

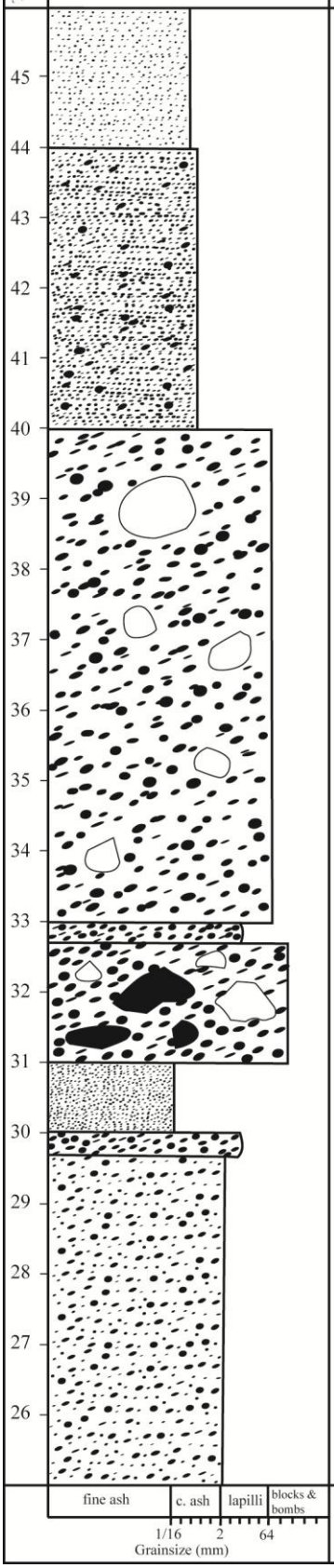

Sample no.	Field notes
	Up to 50m (top of tuff cliff outcrop): fine ash to finer coarse ash, medium bedded, little to no clasts, with 3-4m of sands/soils on top.
	Finer coarse ash, well bedded, few medium lapilli lithics and clasts.
	Medium to coarse lapilli- dark basaltic clasts and light coloured lithics, with some very large basalt sub-rounded bombs approx 50cm length, and one very large basalt subrounded bomb approx 1m long. Medium bedded, poorly sorted.
	Dark fine lapilli, scoria, 30cm thick.
	Coarse lapilli to blocks and bombs, very large clasts and lithics, both angular, both approx max. 1m length.
	Fine to coarser fine ash, well bedded, very well sorted.
	Dark fine lapilli, scoria, 30cm thick.
	Coarse ash to very fine lapilli, medium bedded, well sorted.

VOLCANOLOGICAL STRATIGRAPHIC LOG SHEET

Location: Kellyville tuff ring | Locality: Under road log (2) | Date taken: 24/02/2010

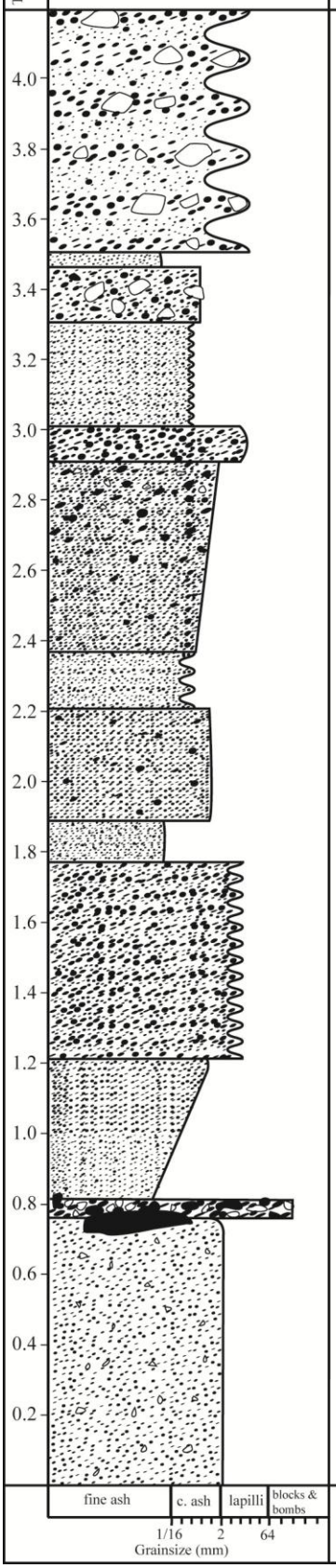

Sample no.	Field notes
	Up to top of outcrop (4.5m): coarser fine ash with fine lapilli, moderately sorted, bedded with fine to medium lapilli layers with very large basalt blocks. Well bedded, lapilli layers very poorly sorted.
W2011586	
W2011585	Fine ash layer with coarse ash lapilli, well sorted, weak bedding. Coarse ash with medium bedding, with fine and medium lapilli and very large basaltic blocks and bombs, very poorly sorted.
	Alternating beds of fine and coarse ash, beds approx 5mm thick, with coarse ash lapilli, well bedded, well sorted.
W2011584	
W2011583	Very fine lapilli with medium lapilli, well bedded, well sorted.
W2011582	Light, coarse ash with fine lapilli, predominantly clasts, well bedded, moderately sorted, coarsening upwards to coarse ash with large lapilli clasts and lithics, scoriaceous clasts max. 16.5mm, lithics max. 8.75mm.
	Coarse ash alternating with fine ash beds, well bedded, moderately sorted.
	Light, coarse ash with fine to medium lapilli, moderately sorted, well bedded.
	Very light fine ash with coarse ash lapilli lithics and clasts- red weathered scoria lapilli, finely bedded, very well sorted.
	Well bedded coarse ash and very fine lapilli lithics and clasts, alternating with fine lapilli.
W2011581	
W2011580	Fine ash with coarse ash lapilli, clasts and lithics, red weathered scoria lapilli, well sorted, well bedded. Coarsening up to coarse ash bedded with coarse ash lapilli layers, well bedded, alternating coarse ash layers approx 10mm, coarse ash lapilli layers approx 30mm.
W2011579	Coarse lapilli to blocka nd bomb layer, clasts max. 27.5mm, lithic max. 47.5mm, no bedding, very poorly sorted, very large
W2011577	sedimentary lithic embedded into lower layer 30cm long.
	Very coarse ash with fine lapilli lithics and clasts, angular clasts max. 7.8mm, subrounded lithics max.7.6mm, moderately to well sorted, medium bedded.
W2011578	

VOLCANOLOGICAL STRATIGRAPHIC LOG SHEET

Location: Kellyville tuff ring | Locality: Road log (4) | Date taken: 3/11/2009

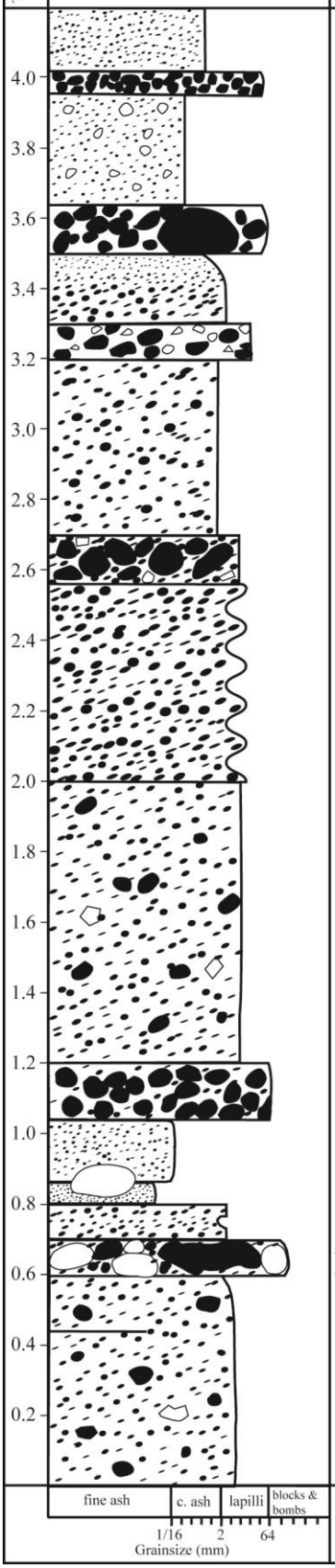

Sample no.	Field notes
	Coarse lapilli lithic layer max. 21mm.
W2011511	Fine to coarse ash, very thinly planar bedding, moderately sorted, approx 2% lithics, some juvenile basalt max. 18mm.
W2011510	Very coarse lapilli lithics max. 60mm, 240mm sst lithic rounded.
	Fine lapilli- scoria and lithics, fines up to fine ash.
W2011509	Very coarse lapilli lithics max. 60mm, coarse juvenile basalt clasts max 27mm.
	Very fine lapilli to very coarse ash, medium bedded.
W2011508	
W2011507	Medium to fine lapilli lithic layer, subrounded-rounded clasts max. 95mm, 15% vesicular basalt clasts, lithics show cracking and zoning, white.
	Alternating coarse to fine lapilli, medium bedding 10-30cm, well sorted, mixed scoria and lithics.
	Fine to medium lapilli, predominantly scoria, well sorted, massive, occasional large lithics- some vesicular or dense and angular basalts and (most) white unkown lithics max. 50.5mm.
W2011506	
W2011504	Very coarse lithic lapilli max. 63mm.
W2011505	Thinly bedded fine to coarse ash, very light brown, 180mm basalt bomb med. vesicular at 0.86m.
	Fine ash, very light brown, small coarse ash scoria fragments.
	Very fine lapilli and coarse ash with 2-4cm bedding.
W2011500-1 W2011503	Clast-supported block and bomb layer with fine to coarse lapilli lithics. Large white lithics eg glauconitic sst 330mm, well rounded large basalt clasts max. 117mm.
	Fine lapilli fining upwards to very fine lapilli. lithics max. 70mm, large angular basalt block 85mm. Light grey fine ash layer at 0.44m
W2011502	

VOLCANOLOGICAL STRATIGRAPHIC LOG SHEET

Location: Kellyville tuff ring | Locality: Road log (4) | Date taken: 3/11/2009

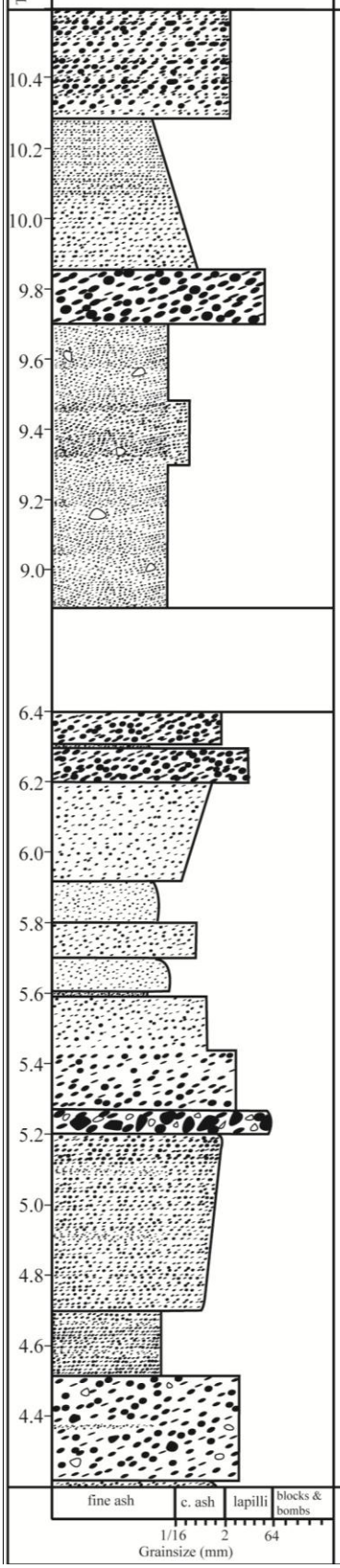

Sample no.	Field notes
W2011607	Very fine lapilli, planar laminated, alternaitng coarse ash to very fine lapilli.
	Coarse ash fining upwards to fine ash, finely laminated at top.
W2011515	
	Medium to coarse lapilli, max. 24mm.
	Cross-bedded, laminated coarse to fine ash with occasional ballistic lapilli- dark grey, slightly vesicularm max. 30mm.
W2011608	
	2.5m gap, outcrop not exposed.
	Massive fine lapilli fining upwards to very fine lapilli, well sorted, white cement. fine ash layer 5mm thick at 6.3m.
W2011514	Diffusely bedded coarse ash, coarsening upwards.
	Fine ash, white, massive.
	Coarse ash, massive.
	Fine lapilli, fining upwards to coarse ash and then to fine ash, diffusely bedded. Fine white ash layer 1cm thick at 5.6m.
W2011513	
W2011512	Very coarse lapilli lithics max. 46mm, basalt clasts max. 23mm.
	Coarse ash, coarsening upwards, laminated.
	Coarse ash, very thinly bedded.
	Fine lapilli, massive, with 5-10% basalt and coarse lapilli lithics max. 23mm.
	with intermittent fine ash beds, fall, approx 6-9% of section.

VOLCANOLOGICAL STRATIGRAPHIC LOG SHEET

Location: Kellyville tuff ring | Locality: Road log (4) | Date taken: 3/11/2009

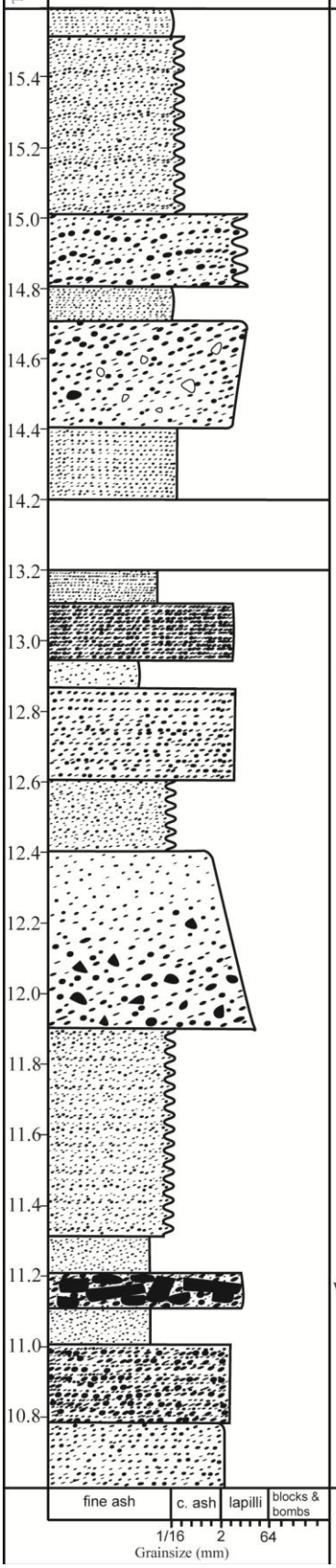

Sample no.	Field notes
	Coarse to fine ash, wavy, laminated beds.
	Coarse ash to fine lapilli, semi-planar laminated with broad waves in bedding.
	Fine ash, laminated.
W2011518	Very fine lapilli reverse grading upwards to fine lapilli. One silty sst lithic, max. basalt clasts 12.6mm.
	Fine to coarse ash, laminated.
	1m gap, outcrop not exposed.
	Fine ash, laminated, light colour.
	Very fine lapilli, laminated.
W2011609	Fine ash with some coarse ash, massive.
	Very fine lapilli, planar laminated beds with very thin to thin bedding.
	Fine to coarse ash laminated beds.
	Fine lapilli, diffusely bedded, massive with very coarse lapilli lithics max. 27.8mm, grading upwards to coarse ash diffusely bedded.
	Well laminated beds approx 10-15mm thick, alternating fine to coarse ash.
	Fine ash, massive, light colour.
W2011516-7	Fine to medium lapilli, lithics: sst, lst, blocks max. 181mm, layer shows ballistic direction.
	Fine ash, massive, light colour.
	Alternating coarse ash to fine lapilli, planar laminated.

VOLCANOLOGICAL STRATIGRAPHIC LOG SHEET

Location: Kellyville tuff ring | Locality: Road log (4) | Date taken: 3/11/2009

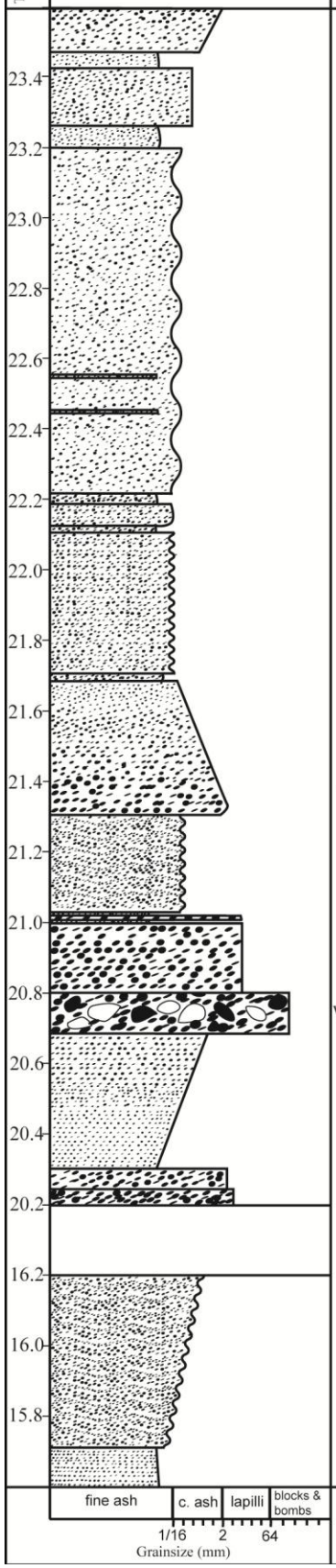

Sample no.	Field notes
	Fine ash layer 30mm thick.
	Coarse to medium ash, wavy beds.
	Fine ash layer 45mm thick.
	Alternating surge beds with ash fall layers. ash:surge - 12cm:100cm. Two fine ash layers.
W2011529	Predominantly coarse ash, with fine ash- thin to very thin beds. Two fine ash layers.
	Ash layer, 20mm thick, cemented.
	Very fine lapilli, cemented, grading upwards to laminated, fine to coarse ash- slightly cross bedded.
W2011528	Alternating fine to coarse ash, slightly cross bedded, low-angle.
	Fine lapilli with two fine ash layers over 2.5cm approx 5mm thick each.
W2011525-7	Block and bomb layer, smallest is medium lapilli, max. basalt juveniles 93mm, max. lithics 74mm.
	Fine ash coarsening upwards to coarse ash, laminated.
	Very fine lapilli, massive, well sorted.
	Fine lapilli, massive, well sorted.
	3.8m gap, outcrop not exposed.
	Coarse ash and fine ash layer couples- fine ash layer contributes approx 20-50%. Beds are wavy, laminated, coarsening upwards overall.
	Fine ash, laminated, planar bedded, white to very light brown.

VOLCANOLOGICAL STRATIGRAPHIC LOG SHEET

Location: Kellyville tuff ring | Locality: Road log (4) | Date taken: 3/11/2009

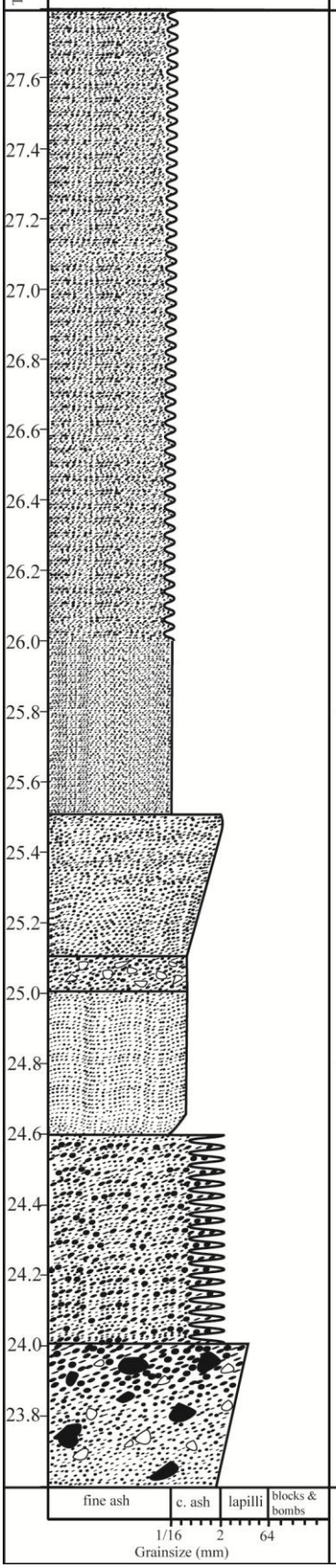

Sample no.	Field notes
	Fine to coarse ash beds with occasional fine lapilli beds, very well bedded, laminated, very continuous.
	Well cemented fine ash to very fine coarse ash layer, accretionary lapilli zone?? up to 10 mm thick.
W2011531	
	Coarse, lensoidal ash, cross bedded and wavy beds up to10mm thick, coarsening upwards to coarse ash beds 7-25mm thick, cross beds, pinching out.
	Coarse ash with very fine lapilli clasts- basalt max. 47.2mm.
	Very fine to fine coarse ash, very laminated, wavy.
W2011530	
	Alternating beds of very fine coarse ash up to fine lapilli, wavy beds, cross beds and laminated, very thin beds.
	Coarse ash coarsening upwards to fine lapilli to medium lapilli, abrupt upper contact, isolated basalt clasts max.43.4mm, sst lithics subangular to rounded max. 90mm.

VOLCANOLOGICAL STRATIGRAPHIC LOG SHEET

Location: Kellyville tuff ring | Locality: Road log (4) | Date taken: 3/11/2009

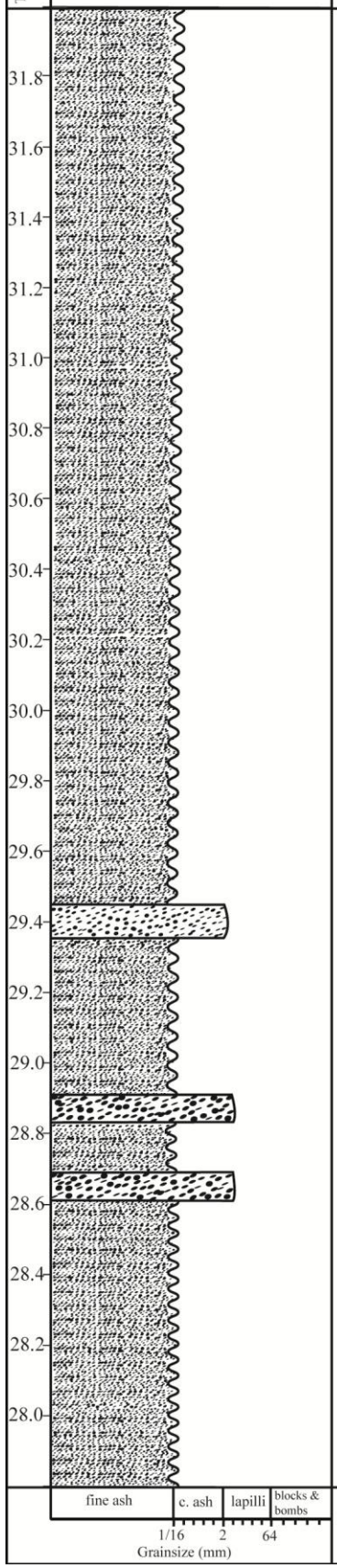

Sample no.	Field notes
	Alternating beds of fine ash and coarse ash, well bedded, laminated, continuous, some beds of medium coarse ash approx. 10mm. Some beds pinch out, others are continuous accross the outcrop, despite being thin.
	Very fine lapilli layer 10cm thick.
	Fine lapilli layer, 7cm thick.
	Fine lapilli layer, 8cm thick.
	Alternating beds of fine ash and coarse ash, well bedded, laminated, continuous, some beds of medium coarse ash approx. 10mm. Some beds pinch out, others are continuous accross the outcrop, despite being thin.

VOLCANOLOGICAL STRATIGRAPHIC LOG SHEET

Location: Kellyville tuff ring | Locality: Road log (4) | Date taken: 3/11/2009

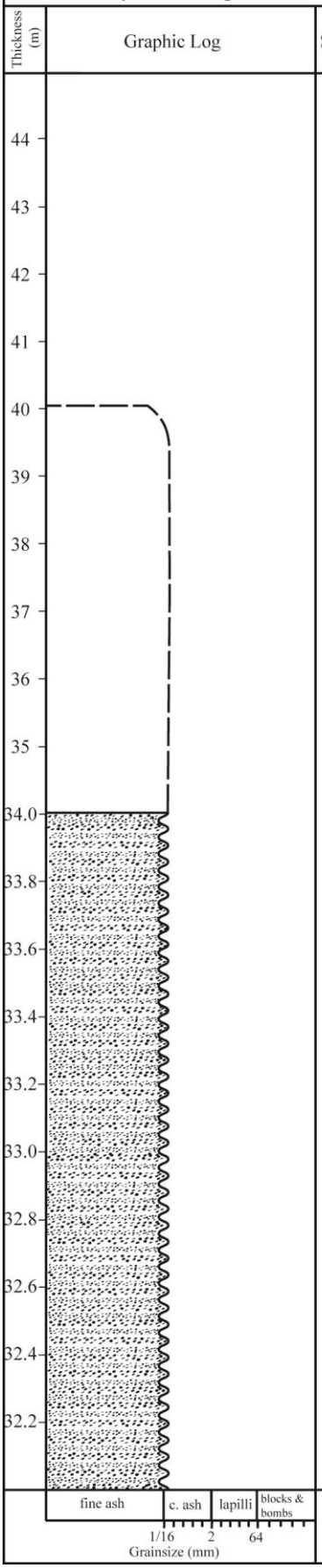

Sample no.	Field notes
	Outcrop unaccessible; appears similar to below, very continuous.
	Scale changes.
	Alternating fine and coarse ash, well bedded, laminated, some beds of medium coarse ash approx 10mm. very continuous.

VOLCANOLOGICAL STRATIGRAPHIC LOG SHEET

Location: Kellyville tuff ring Locality: South eastern rim (3) Date taken: 20/01/2010

Thickness (m)	Graphic Log	Sample no.	Field notes
2.0	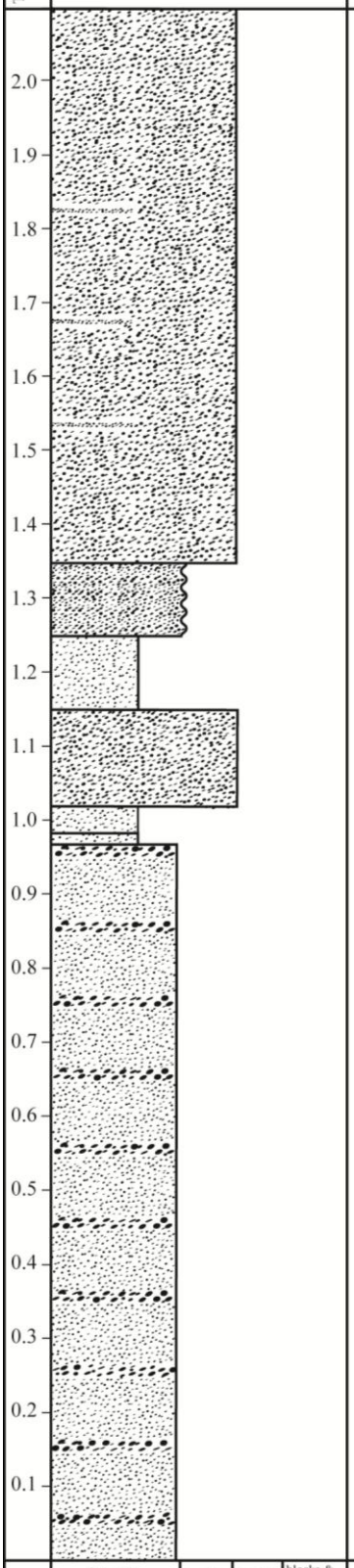		Coarse ash, dark orange, with coarse ash lapilli- lithics and clasts, approx 20% of unit, with three thin white ash layers, massive, max. 3cm thick, sharp contacts, no grading.
1.9		W2011545	
1.8			
1.7			
1.6			
1.5			
1.4			
1.3			Fine ash, white, with alternating coarse ash surge beds, pinching out, 4cm thick average.
1.2		W2011546	Very fine ash, light, massive, very well sorted.
1.1		W2011547	Coarse ash, dark orange, with coarse ash lapilli- white lithics and clasts approx 20%.
1.0			Very fine ash, light, massive, very well sorted. Very fine ash, dark brown, massive, very well sorted.
0.9			Fine ash, massive, white, with thin beds of coarse ash to fine lapilli.
0.8			
0.7		W2011548	
0.6			
0.5			
0.4			
0.3			
0.2			
0.1			

fine ash | c. ash | lapilli | blocks & bombs

1/16 2 64

Grainsize (mm)

VOLCANOLOGICAL STRATIGRAPHIC LOG SHEET

Location: Kellyville tuff ring Locality: South eastern rim (3) Date taken: 20/01/2010

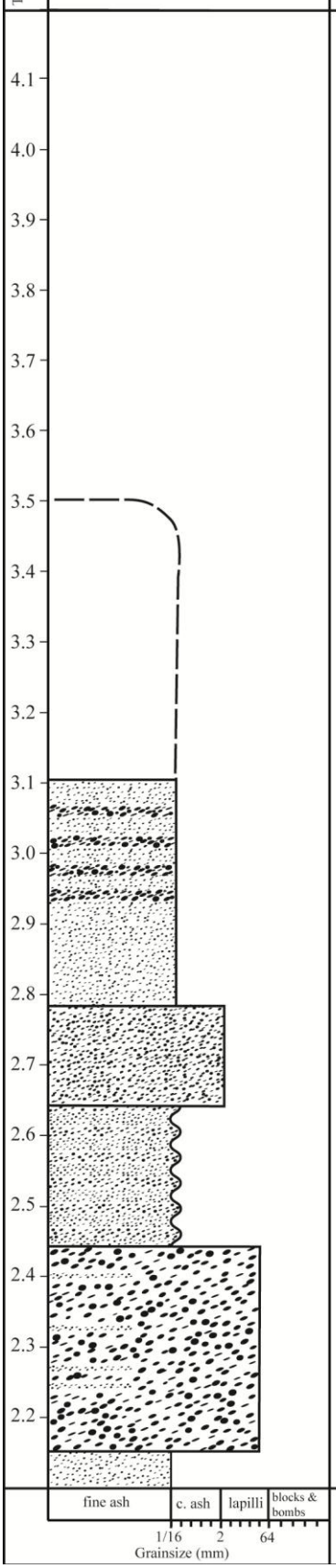

Sample no.	Field notes
	Outcrop covered in vegetation.
	Fine ash, white, alternating with coarse ash to fine lapilli layers, clasts and lithics.
W2011549	
	Fine white ash, massive, with two dark fine ash layers approx 1cm thick, seperated by fine white ash.
	Coarse ash, orange, clasts and lithics.
W2011550	
	Fine white ash alternating with coarse ash, lithic dominated.
	Fine to medium lapilli, dark orange, clast rich, no bedding, with 4 very fine ash layers each approx 0.5cm thick.
	Fine ash, white, massive.

VOLCANOLOGICAL STRATIGRAPHIC LOG SHEET

Location: Kellyville tuff ring Locality: School Hill scoria cone (5) Date taken: 17/02/2010

Thickness (m)	Graphic Log	Sample no.	Field notes
4.0			
3.8			
3.6			
3.4			
3.2			
3.0			
2.8			
2.6			Top of outcrop/cutting covered by vegetation and soil. Actual scoria hill goes higher to approx 5m at top.
2.4			Predominantly fine lapilli size scoria, with few coarsest lapilli max. 42.5mm, and few blocks max. 117.5mm.
2.2		W2011622	
2.0			
1.8			Light to medium grey and red-brown scoria, angular, range of sizes, fine and medium lapilli max. 5.4mm, to coarsest lapilli max. 43mm, and angular scoria blocks max. 117mm. massive.
1.6			
1.4			
1.2		W2011621	
1.0			
0.8			Red-brown scoria, massive, no flow patterns, welded, highly vesicular, approx 50-60% vesicular, little to no clast outline, vesicles are well sorted in size, max. vesicle size 3mm.
0.6			
0.4		W2011620	
0.2			

fine ash | c. ash | lapilli | blocks & bombs

1/16 2 64

Grainsize (mm)

VOLCANOLOGICAL STRATIGRAPHIC LOG SHEET

Location: Kellyville tuff ring | Locality: Middle outcrop (1) | Date taken: 17/02/2010

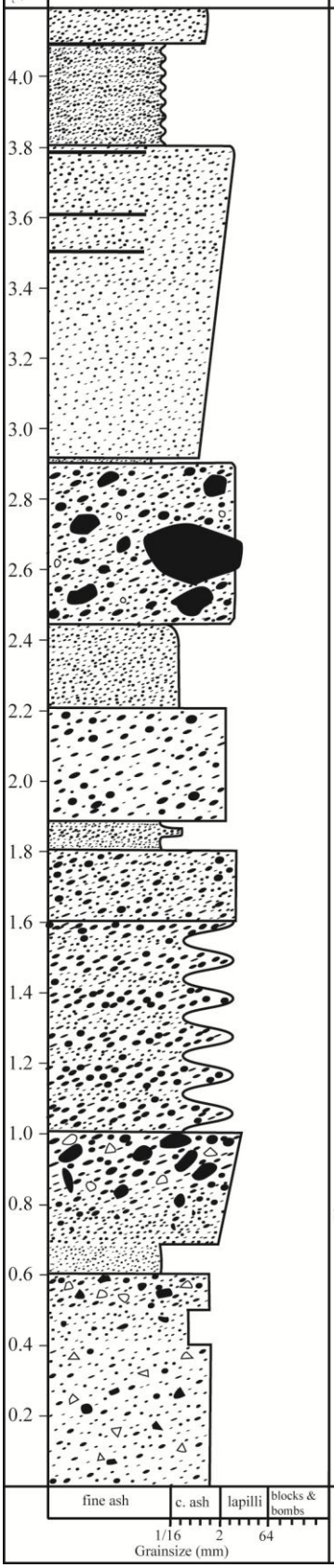

Sample no.	Field notes
	Medium brown coarse ash, very well sorted, massive.
	White ash layer, 1cm thick, fine ash, massive.
	Fine to coarse ash, thinly bedded, wavy beds, well sorted.
	Coarse white ash, well sorted, medium bedded, coarsening upwards to very coarse ash. Massive fine ash beds occur at 2.9m (1cm thick), 3.5m (1 cm thick), 3.6m (0.5cm thick), and 3.77-3.79m (2cm thick).
W2011616	
W2011615 W2011619	Very coarse ash to very fine lapilli, very poorly sorted with fine up to coarsest lapilli and blocks and bombs, max. lithics 70mm subangular, max. clasts 14mm subrounded. Very large white lithic, subangular, 240mm long and 150mm wide.
W2011614	Fine coarse ash, light colour, massive, very well sorted.
	Very coarse ash to very fine lapilli with coarse lapilli lithics and clasts, massive, poorly sorted, clasts max. 12mm, lithics max. 4.5mm.
	4cm fine ash, under 3cm coarse ash, under 2cm fine ash, well bedded, well sorted.
	Very coarse ash to very fine lapilli with fine to medium lapilli clasts and lithics, clasts max. 6.6mm, lithics max. 6.2mm, medium to poorly sorted, diffusely bedded.
W2011613	Alternating beds of light, finer coarse ash, medium bedded with approx 5% fine lapilli, lithics and clasts, angular, beds 35-50mm thick; and beds of fine lapilli, moderately to poorly sorted, medium well bedded, clasts max. 5.25mm, lithics max. 4.25mm, beds 40-70mm thick.
	Coarse ash, medium bedded, with approx 10% fine lapilli lithics coarsening upwards to very fine lapilli with coarse lapilli and blocks and bombs, clasts max. 29mm, lithics max. 61mm.
W2011611,2	
W2011610	Fine white ash, massive.
	Coarse ash with very fine basaltic lapilli and some lithics, medium lapilli clasts max. 9.2mm, some angular scoria, lithics coarse lapilli max. 21.8mm, angular, moderate to poor sorting, massive. With light, finer coarse ash layer with dark very fine lapilli clasts, massive.

VOLCANOLOGICAL STRATIGRAPHIC LOG SHEET

Location: Kellyville tuff ring | Locality: Middle outcrop (1) | Date taken: 17/02/2010

Thickness (m)	Graphic Log	Sample no.	Field notes
8.2			
8.0			
7.8			
7.6			
7.4			
7.2			
7.0			
6.8			
6.6			
6.4			
6.2			
6.0			Colluvium at top of section.
5.8			
5.6			
5.4			Coarse ash to very fine lapilli, medium bedded, orange-brown colour, moderately well sorted, very fine lapilli lithics and clasts. Layers up to 150mm thick of fine to very coarse lapilli up to blocks and bombs. Basaltic clasts max. 8.5mm, light coloured lithics max. 28mm, lithic bombs max. 60mm.
5.2			
5.0			
4.8		W2011618	
4.6			
4.4		W2011617	

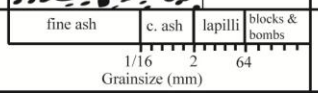

VOLCANOLOGICAL STRATIGRAPHIC LOG SHEET

Location: Onewhero tuff ring Locality: Cliff section near stream (2) Date taken: 4/11/2009

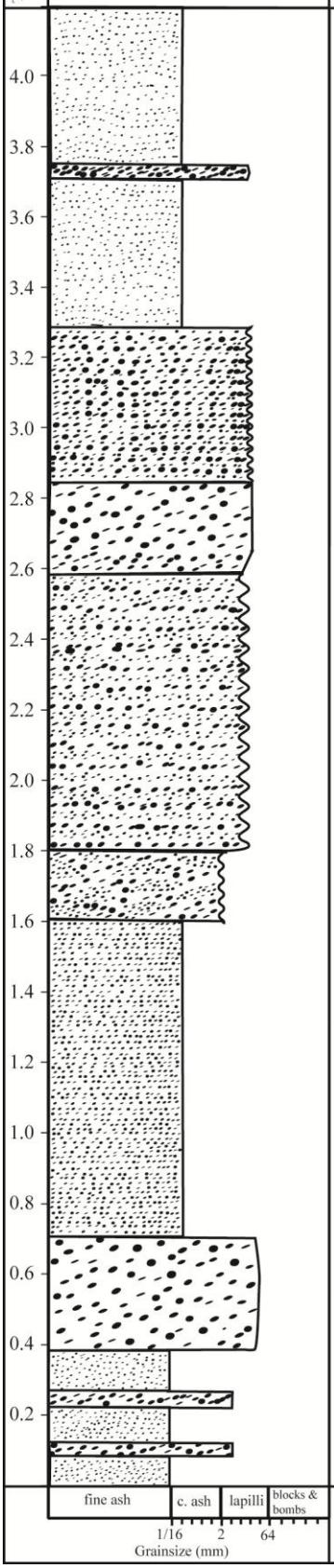

Sample no.	Field notes
	Fine ash, wavy bedding, very well sorted, bedding low angle, wavelength 1.2m, amplitude 25-50mm (varies).
W2011522	
	Very fine lapilli, well sorted, no bedding, 30cm thick.
	Fine ash, wavy bedding, very well sorted, bedding low angle, wavelength 1.2m, amplitude 25-50mm (varies).
W2011521	
	Laminated coarse ash and very fien lapilli approx 50-50. layers very well sorted.
	Fine lapilli, bottom is reverse graded, finely bedded.
	Coarse ash, laminated, with very fine lapilli layers 5-7cm thick.
	Coarse ash and very fine lapilli beds, cross bedded.
	Finer coarse ash, laminated, very well sorted.
W2011519	
W2011520	Fine to medium lapilli, diffusely bedded, with grey slightly vesicular basalt clasts max. 10.6mm.
	Fine ash, well bedded, laminated, with 2-4cm thick very fine lapilli beds orange, grey and red in colour, with basaltic juvenile clasts and white siltstone lithics. Coarse beds are wavy bedded.

VOLCANOLOGICAL STRATIGRAPHIC LOG SHEET

Location: Onewhero tuff ring Locality: Cliff section near stream (2) Date taken: 4/11/2009

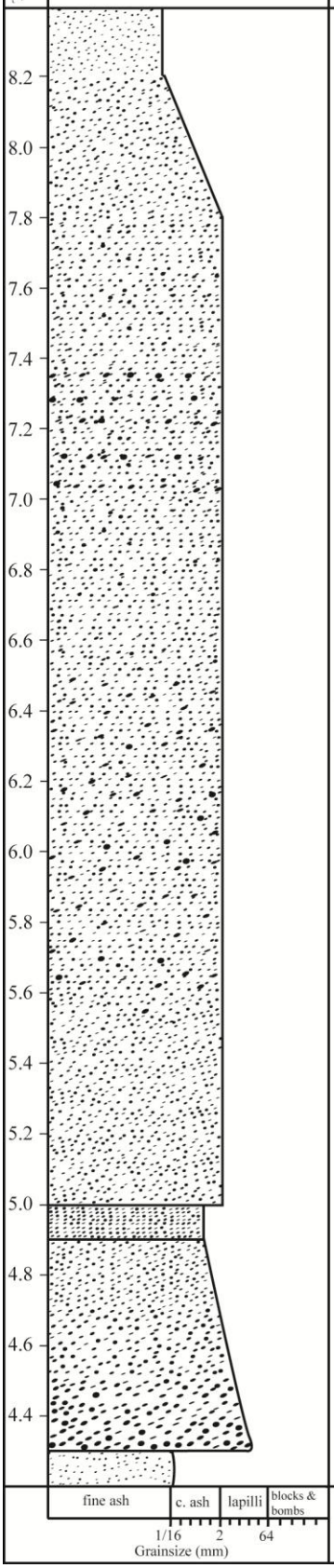

Sample no.	Field notes
	Coarse ash with alternating fine lapilli beds, medium bedded, fining upwards to coarse ash with some very fine lapilli, diffusely bedded, fining upwards to coarse ash, massive, well sorted, fining upwards to fine ash, massive, well sorted.
	Coarse ash with basaltic lapilli clasts approx 25%, subangular, max. 4.8mm (fine lapilli), ash very well sorted, fining upwards to coarse ash with very fine lapilli clasts.
W2011524	
	Coarse ash, finely cross bedded, pinching out, very well sorted.
	Coarse ash, laminated, very well sorted.
	Fine lapilli to coarse ash, normally graded, medium well bedded, small scale waves between 4.4 and 4.6m, visible in hand specimen only.
W2011523	

VOLCANOLOGICAL STRATIGRAPHIC LOG SHEET

Location: Onewhero tuff ring Locality: Cliff section near stream (2) Date taken: 4/11/2009

Thickness (m)	Graphic Log	Sample no.	Field notes
12.4			
12.2			
12.0			
11.8			
11.6			
11.4			
11.2			
11.0			
10.8			
10.6			Cliff outcrop jutts out and is inaccessible. Cliff extends to about 25-30m high, cliff face is obscured by layer of altered material.
0.4			
10.2			
10.0			Fine ash, massive, well sorted, no bedding, from approx 8.2m until at least 10m.
9.8			
9.6			
9.4			
9.2			
9.0			
8.8			
8.6			

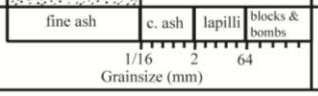

VOLCANOLOGICAL STRATIGRAPHIC LOG SHEET

Location: Onewhero tuff ring Locality: Opposite cliff section (3) Date taken: 26/01/2010

Thickness (m)	Graphic Log	Sample no.	Field notes
4.0	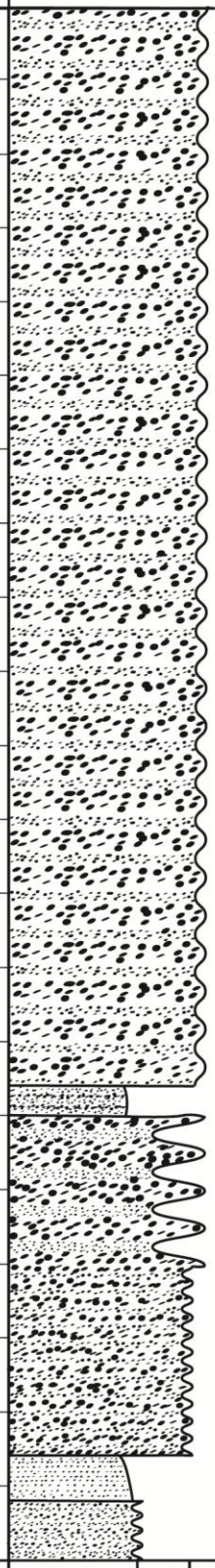		Very coarse ash with lapilli max. 4.8mm clasts, well bedded with some very well sorted fine ash beds 4-10mm thick, as well as fine lapilli beds 70mm thick. Moderately sorted.
3.8			
3.6			
3.4			
3.2			
3.0			
2.8			
2.6			
2.4			
2.2			
2.0			
1.8			
1.6			
1.4		W2011559	
1.2			Dark very fine ash with coarse ash lapilli, black, <1mm, well sorted.
1.0			Coarse ash with very fine lapilli, beds 4-5cm thick, grading upwards to fine ash bedded with dark fine lapilli, max. 5mm, beds 5-10cm thick, with a fine ash layer above, with no lapilli.
0.8			
0.6			
0.4		W2011558	
0.2		W2011557	Fine white ash, very thinly bedded/laminated, non-indurated.
			Alternating beds of fine ash and coarse ash, thinly bedded, dark coarse ash well sorted, indurated.

fine ash | c. ash | lapilli | blocks & bombs

1/16 2 64

Grainsize (mm)

VOLCANOLOGICAL STRATIGRAPHIC LOG SHEET

Location: Onewhero tuff ring Locality: Opposite cliff section (3) Date taken: 26/01/2010

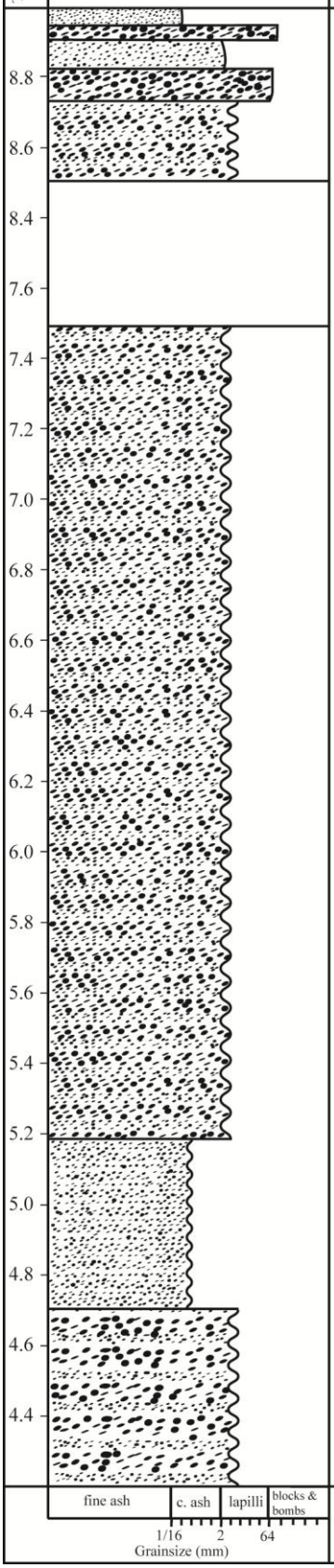

Sample no.	Field notes
	Fine to medium lapilli layer, surge deposit.
	Medium coarse ash, massive, well sorted.
	Fine to medium lapilli layer, surge deposit.
	Very coarse ash with fine lapilli, well bedded with fine ash beds well sorted, and fine lapilli beds moderately sorted.
	Outcrop covered with vegetation.
	Very coarse ash with fine lapilli, well bedded with fine ash beds well sorted, and fine lapilli beds moderately sorted.
W2011627	
	Very fine coarse ash with coarser ash beds and clasts and lithics. Black very fine lapilli clasts max. 2.8mm, white fine lapilli lithics max. 4.6mm.
W2011560	

VOLCANOLOGICAL STRATIGRAPHIC LOG SHEET

Location: Onewhero tuff ring Locality: Opposite cliff section (3) Date taken: 26/01/2010

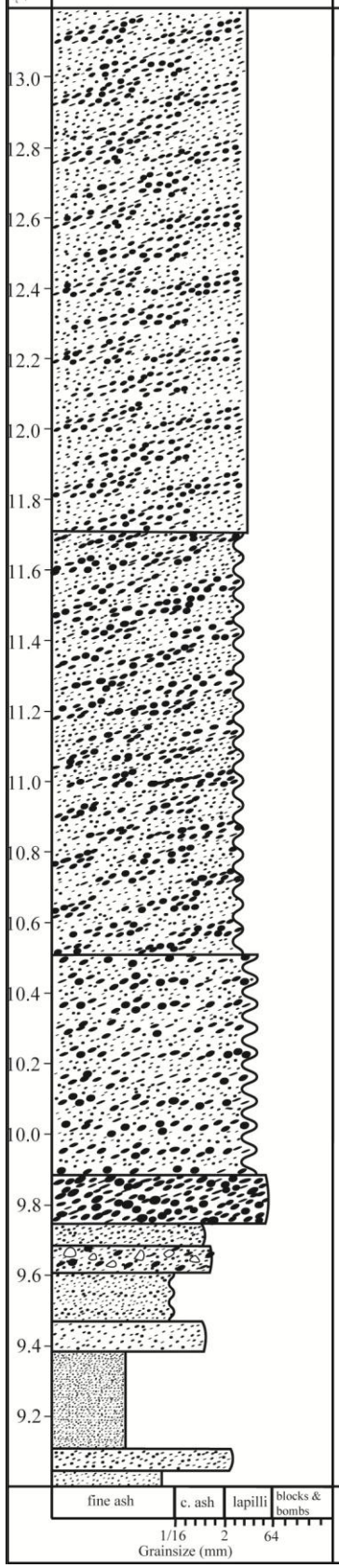

Sample no.	Field notes
	Coarse ash and very fine lapilli layers, well sorted, lapilli 1-2mm, indurated, cross bedded.
W2011562	Coarse ash and fine lapilli layers, well bedded, thin beds, indurated, cross bedded, angling/pinching out away from vent, highly energetic phase of eruption, surge dominated.
	Well bedded coarse ash with medium lapilli layers. Lapilli clasts max. 9mm, lapilli lithics light coloured max. 8.4mm.
W2011561	
	Medium lapilli, poorly sorted, max. 9.8mm.
	Coarse ash, moderately sorted, approx 10% dark clasts <1mm. Coarse ash with medium lapilli, indurated, poorly sorted, lapilli clasts max. 9.4mm, approx 50% lithics, angular. Alternating coarse and fine ash, well sorted.
	Coarse ash medium brown, well sorted. Very fine ash, light colour, very well sorted, very finely layered.
	Coarse ash surge deposit, medium brown. Fine ash, massive, light colour.

VOLCANOLOGICAL STRATIGRAPHIC LOG SHEET

Location: Onewhero tuff ring Locality: Opposite cliff section (3) Date taken: 26/01/2010

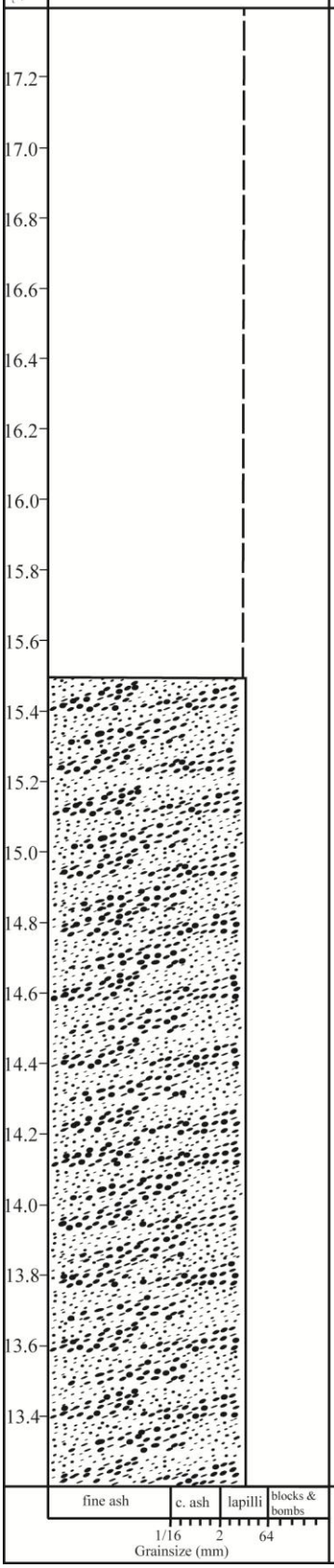

Sample no.	Field notes
	Outcrop not visible, exposure continues to approximately 20-25m.
	Coarse ash and very fine lapilli layers, developing finer ash layers between, becoming well bedded upwards.
W2011628	

VOLCANOLOGICAL STRATIGRAPHIC LOG SHEET

Location: Onewhero tuff ring Locality: Maoa's Waterfall (4) Date taken: 23/02/2010

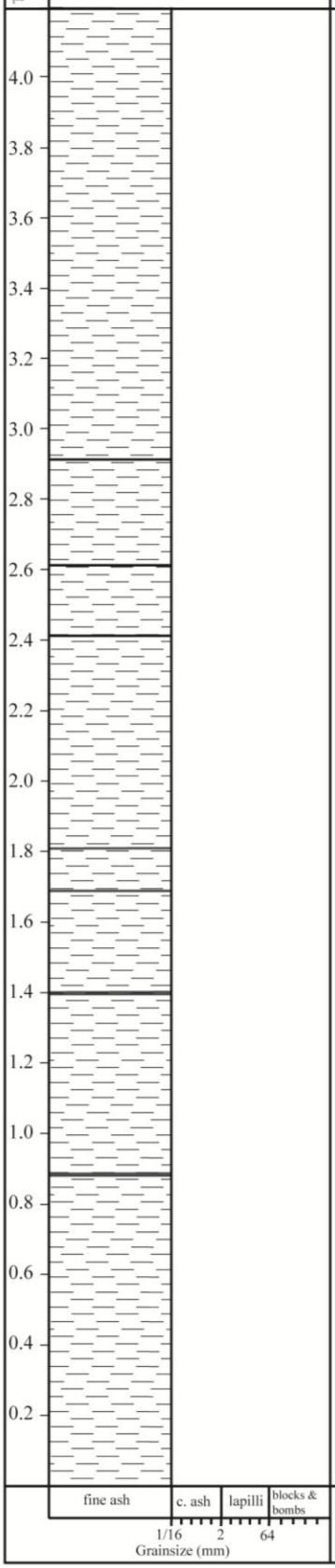

Sample no.	Field notes
	Unit extends up to at least 5m, beyond this is obscured by vegetation and colluvium.
	Siltstone finer than below, less weathered, (more) massive, no visible iron pans.
W2011625	
W2011624	Iron pan, 20cm thick, dark orange-brown.
	Thin iron pans, dark orange-brown.
	Iron pan 2cm thick, dark orange-brown.
	Medium grey layer, concentration (?) 1cm thick.
W2011623	Light grey, sedimentary rock, siltstone or very fine sandstone, possibly glauconitic, very finely bedded but diffusely to massive. highly weathered face. Outcrop extends up to 2.9m, goes further down than shown, bottom of log is approximately 20cm above water level on middle "step" of waterfall, water runs over this unit for as far as visible (low angle).

VOLCANOLOGICAL STRATIGRAPHIC LOG SHEET

Location: Onewhero tuff ring Locality: Small cliff section (1) Date taken: 23/02/2010

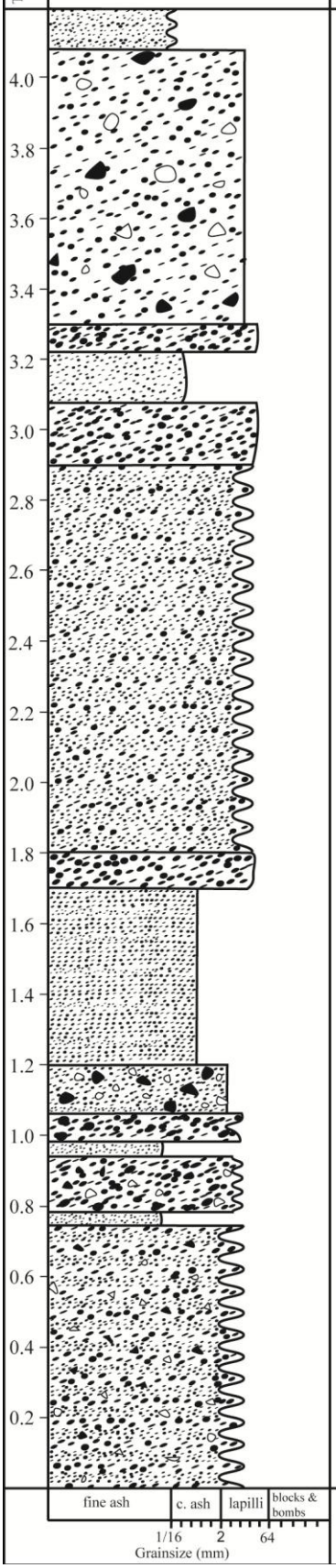

Sample no.	Field notes
	Coarse ash to fine lapilli with large coarse blocks and bombs, poorly sorted, medium bedding, clasts subrounded, lithics subangular.
	Fine to medium lapilli, dark, well sorted.
	Very fine coarse ash, light brown.
	Fine to medium lapilli, dark, well sorted.
	Coarse ash approx 60%, with alternating darker fine lapilli beds approx 40%, well bedded, coarse ash well sorted, fine lapilli moderately sorted.
W2011606	Medium lapilli, moderately sorted, clasts and lithics.
	Coarse ash , medium bedded with light fine ash layers approx 40%, massive.
W2011605	
	Very coarse ash with medium to fine lapilli, poorly sorted, subrounded clasts max. 20mm, rounded lithics max. 27.5mm.
	Fine lapilli with medium to coarse lapilli, moderately sorted with upper fine ash layer.
	Fine light ash, massive.
W2011604	Fine lapilli with medium to coarse lapilli, moderately sorted, lithics max. 13.5mm, clasts max. 10mm.
	Fine light ash, massive.
	Coarse ash, medium bedded with fine and medium lapilli, very poorly sorted, clasts very angular, max. 15mm, lithics subangular max. 14.5mm.
W2011603	

VOLCANOLOGICAL STRATIGRAPHIC LOG SHEET

Location: Onewhero tuff ring Locality: Small cliff section (1) Date taken: 23/02/2010

Thickness (m)	Graphic Log	Sample no.	Field notes
8.2	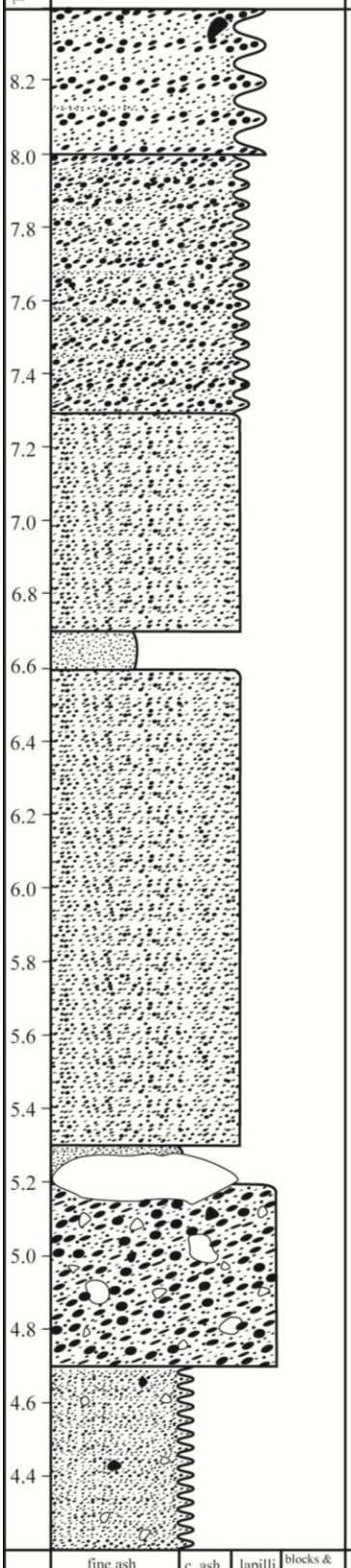		
8.0			Alternating coarse ash and fine lapilli with fine ash thin layers, well bedded.
7.8			
7.6			
7.4			
7.2			Coarse ash to very fine lapilli, medium bedding, medium to well sorted, dark colour.
7.0			
6.8			
6.6			Fine ash, light colour, weak bedding/massive. Coarse ash to very fine lapilli, medium bedding, medium to well sorted.
6.4			
6.2			
6.0			
5.8			
5.6			
5.4			
5.2			Fine ash, light colour, massive, continuous, with dark, angular block clast sinking into ash. Lapilli rich layer, coarse ash with 60-70% coarse lapilli, mainly clasts, very few lithics, mainly coarse lapilli with few blocks/bombs clasts, weak/no bedding.
5.0			
4.8			
4.6			Alternating fine and coarse ash layers with approx 5% coarse lapilli, clasts and lithics, subrounded.
4.4			

VOLCANOLOGICAL STRATIGRAPHIC LOG SHEET

Location: Onewhero tuff ring Locality: Small cliff section (1) Date taken: 23/02/2010

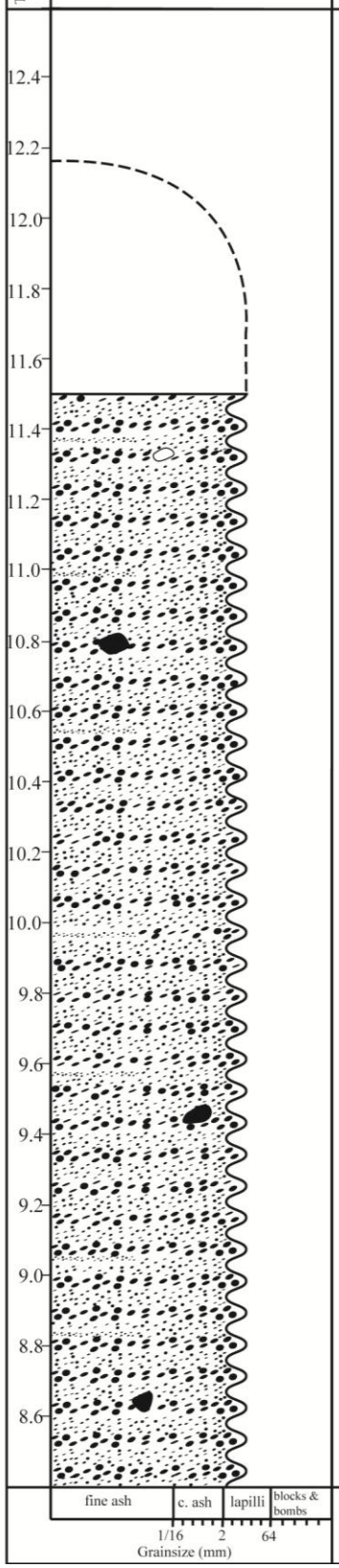

Sample no.	Field notes
	Soil and colluvium covering outcrop.
	Alternating coarse ash and medium lapilli with thin fine ash layers, lapilli rich, some blocks and bombs, mostly lithics, some clasts, medium bedding.

Appendix Three

Appendix Three

Raw data of vesicularity and density measurements of clasts are available below. Results are summarised in Table A3.13.

Table A3.1: Raw vesicularity and density data for sample W2011538.

Sample:	41	Glass Hill, Kellyville				
Phi size:	-4 ϕ					
DRE density:	3					
Clast no.	Dry weight (g)	Wet weight (g)	Ballast weight (g)	# wax sheets	Density	Vesicularity
1	8.13	11.88	8.61	2	1.69	43.54
2	19.16	31.91	23.43	3	1.81	39.69
3	16.37	31.40	23.43	3	1.97	34.34
4	13.44	14.69	8.61	3	1.85	38.38
5	27.74	38.42	23.43	3	2.19	26.96
6	12.51	11.86	8.61	2	1.36	54.67
7	4.76	10.52	8.61	2	1.71	43.13
8	12.95	29.56	23.43	3	1.92	35.86
9	10.03	13.09	8.61	2.5	1.83	38.93
10	20.07	32.07	23.43	3.5	1.77	40.93

Table A3.2: Raw vesicularity and density data for sample W2011539.

Sample:	42	Glass Hill, Kellyville				
Phi size:	-4 ϕ					
DRE density:	3					
Clast no.	Dry weight (g)	Wet weight (g)	Ballast weight (g)	# wax sheets	Density	Vesicularity
1	15.23	31.67	23.43	2	2.20	26.74
2	16.13	30.13	23.43	5	1.74	42.06
3	14.51	30.78	23.43	3	2.05	31.59
4	6.19	11.22	8.61	2.5	1.77	41.13
5	25.21	35.43	23.43	3.5	1.92	35.88
6	17.39	32.06	23.43	4	2.01	32.91
7	6.95	11.61	8.61	2	1.79	40.45
8	15.41	31.39	23.43	3	2.09	30.21
9	18.91	32.82	23.43	4	2.01	32.94
10	36.82	43.10	23.43	4	2.16	27.93

Table A3.3: Raw vesicularity and density data for sample W2011542.

Sample:	45	Glass Hill, Kellyville				
Phi size:	-4 ϕ					
DRE density:	3					
Clast no.	Dry weight (g)	Wet weight (g)	Ballast weight (g)	# wax sheets	Density	Vesicularity
1	10.66	26.46	23.43	3	1.41	52.87
2	7.91	25.25	23.43	3	1.32	56.06
3	12.80	26.37	23.43	3	1.31	56.33
4	9.57	11.02	8.61	3	1.35	54.88
5	13.28	27.43	23.43	4	1.45	51.67
6	8.12	11.47	8.61	3	1.57	47.65
7	6.03	10.09	8.61	2	1.34	55.23
8	5.43	9.86	8.61	2	1.32	56.07
9	6.92	23.91	23.43	4	1.09	63.50
10	7.86	9.53	8.61	5	1.16	61.41

Table A3.4: Raw vesicularity and density data for sample W2011551.

Sample:	54	New Scoria Hill, Kellyville				
Phi size:	-4 ϕ					
DRE density:	3					
Clast no.	Dry weight (g)	Wet weight (g)	Ballast weight (g)	# wax sheets	Density	Vesicularity
1	8.39	21.32	23.43	3	0.81	73.13
2	9.99	23.65	23.43	2	1.03	65.71
3	6.88	9.37	8.61	2	1.14	62.16
4	6.36	8.06	8.61	2	0.93	69.05
5	7.36	8.95	8.61	2	1.06	64.75
6	8.02	9.09	8.61	2	1.07	64.26
7	8.68	24.05	23.43	2	1.09	63.83
8	5.05	8.17	8.61	2	0.93	69.00
9	11.56	24.68	23.43	3	1.13	62.30

Table A3.5: Raw vesicularity and density data for sample W2011552.

Sample:	55	New Scoria Hill, Kellyville basalt flow at base				
Phi size:	-4 ϕ					
DRE density:	3					
Clast no.	Dry weight (g)	Wet weight (g)	Ballast weight (g)	# wax sheets	Density	Vesicularity
1	13.85	15.14	8.61	3	1.92	36.15
2	7.68	12.64	8.61	2	2.14	28.69
3	11.58	28.94	23.43	3	1.94	35.45
4	7.48	12.26	8.61	2	1.98	33.86
5	7.18	12.20	8.61	2	2.03	32.20
6	8.13	11.77	8.61	3	1.67	44.47
7	21.27	34.09	23.43	3	2.02	32.60
8	20.04	33.37	23.43	3	2.00	33.27
9	24.23	35.58	23.43	4	2.03	32.47
10	21.03	19.03	8.61	4	2.00	33.17

Table A3.6: Raw vesicularity and density data for sample W2011571.

Sample:	BQ9	Bombay Quarry clast				
Phi size:	-4 ϕ					
DRE density:	3					
Clast no.	Dry weight (g)	Wet weight (g)	Ballast weight (g)	# wax sheets	Density	Vesicularity
1	14.43	28.54	23.43	3	1.56	47.89
2	20.65	34.78	23.43	3	2.24	25.26
3	18.68	33.55	23.43	3	2.21	26.49
4	22.34	36.19	23.43	3	2.35	21.53
5	20.32	30.79	23.43	3	1.58	47.37
6	9.90	12.98	8.61	3	1.82	39.34
7	10.00	13.37	8.61	2	1.93	35.65
8	19.75	34.41	23.43	3	2.28	24.16
9	17.70	17.90	8.61	5	2.14	28.57
10	7.99	11.83	8.61	3	1.71	43.09

Table A3.7: Raw vesicularity and density data for sample W2011601.

Sample:	BQA15	Spatter, Bombay Quarry				
Phi size:	-4 ϕ					
DRE density:	3					
Clast no.	Dry weight (g)	Wet weight (g)	Ballast weight (g)	# wax sheets	Density	Vesicularity
1	3.39	9.46	8.61	1.5	1.36	54.71
2	3.83	9.47	8.61	2.5	1.32	55.90
3	11.94	26.48	23.43	3	1.36	54.77
4	5.65	10.03	8.61	2	1.35	54.84
5	10.78	26.30	23.43	2	1.37	54.23
6	3.09	9.32	8.61	1.5	1.32	55.89
7	7.77	25.39	23.43	2.5	1.35	54.84
8	2.44	9.11	8.61	1	1.28	57.42
9	6.99	10.37	8.61	1.5	1.35	55.06

Table A3.8: Raw vesicularity and density data for sample W2011602.

Sample:	BQA16	Spatter, Bombay Quarry				
Phi size:	-4 ϕ					
DRE density:	3					
Clast no.	Dry weight (g)	Wet weight (g)	Ballast weight (g)	# wax sheets	Density	Vesicularity
1	14.90	27.52	23.43	3	1.39	53.67
2	9.80	26.08	23.43	3	1.39	53.73
3	6.00	10.12	8.61	3	1.36	54.55
4	4.04	9.57	8.61	2	1.34	55.41
5	14.39	27.11	23.43	3	1.35	54.83
6	5.07	9.76	8.61	3	1.32	55.87
7	12.14	26.51	23.43	4	1.36	54.74
8	5.14	9.90	8.61	2	1.36	54.79
9	12.01	27.66	23.43	3	1.56	47.94
10	7.45	25.55	23.43	3	1.42	52.61

Table A3.9: Raw vesicularity and density data for sample W2011620.

Sample:	X	New Scoria Hill, Kellyville				
Phi size:	-4 ϕ					
DRE density:	3					
Clast no.	Dry weight (g)	Wet weight (g)	Ballast weight (g)	# wax sheets	Density	Vesicularity
1	5.01	22.43	23.43	1.5	0.84	72.00
2	6.17	22.14	23.43	2	0.83	72.21
3	8.06	21.75	23.43	2	0.83	72.25
4	7.18	21.44	23.43	2	0.79	73.73
5	7.56	21.45	23.43	3	0.80	73.33
6	9.51	20.04	23.43	2	0.74	75.31
7	10.47	21.28	23.43	2.5	0.83	72.18
8	3.89	7.18	8.61	1.5	0.74	75.42
9	3.16	22.45	23.43	2	0.77	74.18
10	4.96	22.34	23.43	2	0.83	72.40

Table A3.10: Raw vesicularity and density data for sample W2011621.

Sample:	Y	New Scoria Hill, Kellyville				
Phi size:	-4 ϕ					
DRE density:	3					
Clast no.	Dry weight (g)	Wet weight (g)	Ballast weight (g)	# wax sheets	Density	Vesicularity
1	18.20	29.87	23.43	3	1.56	48.01
2	21.94	27.47	23.43	3	1.23	58.94
3	5.48	6.97	8.61	2	0.78	74.13
4	3.84	8.27	8.61	1	0.93	69.16
5	5.19	8.19	8.61	1	0.93	69.00
6	8.51	24.40	23.43	2	1.14	62.08
7	9.83	21.30	23.43	2	0.83	72.46
8	7.98	9.25	8.61	2	1.10	63.46
9	4.61	8.00	8.61	1.5	0.89	70.31
10	7.91	24.82	23.43	1.5	1.22	59.28

Table A3.11: Raw vesicularity and density data for sample W2011622.

Sample:	Z	New Scoria Hill, Kellyville				
Phi size:	-4 ϕ					
DRE density:	3					
Clast no.	Dry weight (g)	Wet weight (g)	Ballast weight (g)	# wax sheets	Density	Vesicularity
1	19.42	24.60	23.43	1	1.07	64.47
2	9.02	9.82	8.61	3	1.17	61.05
3	5.42	8.96	8.61	3	1.09	63.72
4	13.35	25.17	23.43	2	1.16	61.47
5	9.14	22.62	23.43	3	0.93	69.10
6	17.49	24.12	23.43	3	1.05	65.11
7	10.82	25.73	23.43	4	1.29	57.06
8	14.92	22.43	23.43	2	0.94	68.64
9	13.38	24.86	23.43	2	1.13	62.49
10	10.96	24.61	23.43	2	1.13	62.41

Table A3.12: Raw vesicularity and density data for sample W2011640.

Sample:	77	Spatter cone, Bombay Quarry				
Phi size:	-4 ϕ					
DRE density:	3					
Clast no.	Dry weight (g)	Wet weight (g)	Ballast weight (g)	# wax sheets	Density	Vesicularity
1	7.54	21.83	23.43	2	0.83	72.32
2	6.64	23.12	23.43	2	0.96	67.88
3	11.70	24.34	23.43	2	1.09	63.65
4	9.03	24.44	23.43	2	1.13	62.19
5	12.35	24.32	23.43	2	1.08	63.89
6	7.09	9.14	8.61	2	1.09	63.64
7	11.21	24.41	23.43	2	1.10	63.26
8	6.69	6.66	8.61	2	0.78	74.01
9	9.70	10.20	8.61	2	1.20	59.83
10	17.49	23.91	23.43	3	1.03	65.54

Table A3.13: Summary of vesicularity and density data.

Collection number	Mean dry weight (g)	Mean density	Maximum density	Minimum density	Standard deviation	Mean vesicularity	Maximum vesicularity	Minimum vesicularity	Standard deviation
W2011538	14.52	1.81	2.19	1.36	0.21	39.64	54.67	26.96	7.15
W2011539	17.28	1.97	2.2	1.74	0.17	34.18	42.06	26.74	5.5
W2011542	8.86	1.33	1.57	1.09	0.14	55.57	63.5	47.65	4.52
W2011551	7.23	0.92	1.14	0.81	0.11	59.42	73.13	62.16	3.66
W2011552	14.25	1.97	2.14	1.67	0.12	34.23	44.47	28.69	4.12
W2011571	15.38	1.81	2.35	1.56	0.3	29.63	47.89	21.53	10.04
W2011601	5.59	1.21	1.37	1.28	0.03	49.77	57.42	54.23	0.97
W2011602	9.09	1.39	1.56	1.32	0.07	53.81	55.87	47.94	2.26
W2011620	6.6	0.8	0.84	0.74	0.04	73.3	75.42	72	1.31
W2011621	9.35	1.06	1.56	0.78	0.24	64.68	74.13	48.01	7.95
W2011622	12.39	1.09	1.29	0.93	0.11	63.55	69.1	57.06	3.58
W2011640	9.94	1.03	1.2	0.78	0.13	65.62	74.01	59.83	4.5